

Prague Medical REPORT

(Sborník lékařský)

Multidisciplinary Biomedical Journal
of the First Faculty of Medicine,
Charles University

Vol. 124 (2023) No. 3

Reviews

Therapeutic Drug Monitoring of Protein Kinase Inhibitors in the Treatment of Non-small Cell Lung Cancer / Staša J., Gregorová J., Slanař O., Šíma M. page 199

Effects of Cannabidiol in Inflammation: A Review of Pre-clinical and Clinical Findings / Sklenárová M., Šíma M., Slanař O. page 216

Primary Scientific Studies

Effect of Convalescent Plasma Therapy on Mortality and Viral Load in Severely Ill Patients with COVID-19 / Moravec J., Müller M., Turek P., Moravec M., Nejtek T., Zazula R. page 230

The Predictive Value of Serum Aldosterone Level for Coronary Artery Calcium Score in Patients with Chronic Kidney Disease: A Single-center Study / Semenov V. V., Bosdriesz J. R., Kuryata O. page 242

The Role of Demographic and Clinical Characteristics in Distinguishing Testicular Torsion from Torsion of the Appendix Testis: A Single-center Retrospective Study / Zvizdic Z., Aganovic A., Milisic E., Jonuzi A., Zvizdic D., Vranic S. page 255

Rehabilitation of Dentofacial Asymmetry Secondary to Unilateral Temporomandibular Joint Ankylosis with Dual Distraction and Fixed Orthodontics – Stability at Three-year Follow-up / Singh H., Mishra S., Srivastava D., Sharma P., Chandra L., Kapoor P., Maurya R. K. page 265

Case Reports

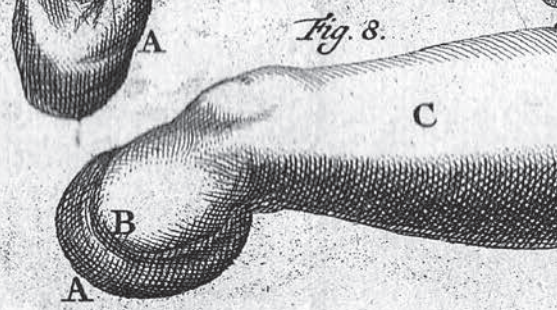
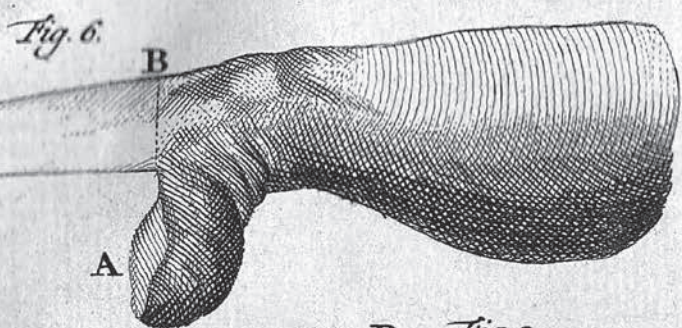
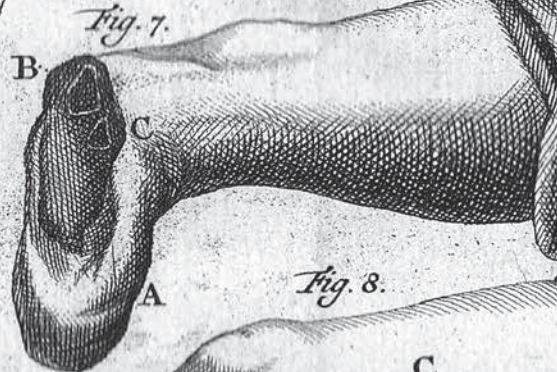
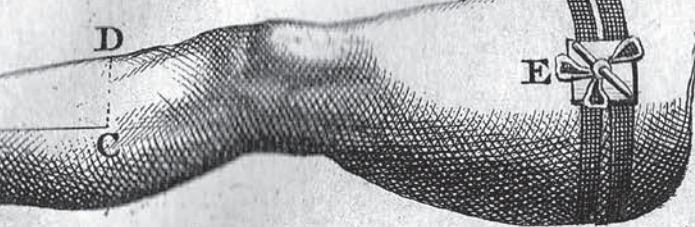
Vaping Associated Acute Eosinophilic Pneumonia: A Clinical and Radiologic Mimicker of COVID-19 / Bonnier A., Nida A., Chong W. H., Saha S., Saha B. K. page 283

Osteomyelitis and Thrombosis in a Newborn with Group A Streptococcus Infection / Mitsiakos G., Gialamprinou D., Tsakalidis C., Babatseva E., Lithoxopoulou M., Diamanti E. page 293

Successful Treatment of Detachment of the Incision after Al-Ghorab Procedure: A Case Report and Review of Literature / Ergül R. B., Ramazanoğlu M. A., Sambel M., Akşit S., Dursun M., Kadioğlu A. page 301

Use of a Questionnaire for Evaluation of Surgical Treatment of Masseter Muscle Hypertrophy: A Case Report / Bin L. R., Pavelski M. D., Fernandes A. C. F., Garbin E. Á. Jr. page 308

Instructions to Authors page 320



Prague Medical Report (Prague Med Rep) is indexed and abstracted by Index-medicus, MEDLINE, PubMed, EuroPub, CNKI, DOAJ, EBSCO, and Scopus.

Abstracts and full-texts of published papers can be retrieved from the World Wide Web (<https://pmr.lf1.cuni.cz>).

Therapeutic Drug Monitoring of Protein Kinase Inhibitors in the Treatment of Non-small Cell Lung Cancer

Judita Staša^{1,2}, Jana Gregorová², Ondřej Slanař¹, Martin Šíma¹

¹Institute of Pharmacology, First Faculty of Medicine, Charles University and General University Hospital in Prague, Prague, Czech Republic;

²Department of Clinical Pharmacy, Bulovka University Hospital, Prague, Czech Republic

Received March 15, 2023; Accepted August 27, 2023.

Key words: Oral targeted therapy – Personalised medicine – Anticancer drugs – Individualized dosing – Trough plasma levels – Concentration-guided dosing

Abstract: Targeted therapy with protein kinase inhibitors (PKIs) represents one of the important treatment options for non-small cell lung cancer (NSCLC). It has contributed to improve patients' survival and quality of life significantly. These anticancer drugs are administrated orally in flat-fixed doses despite the well-known large interpatient pharmacokinetic variability and the possible need for dose individualization. To optimize and individualize dosing of PKIs, and thereby increasing the effectiveness and safety of the treatment, therapeutic drug monitoring (TDM) is the most frequently mentioned method. Unlike other areas of medicine, TDM has been rather exceptional in oncological practise since there is a little evidence or no data for concentration-effect relationships of PKIs. Therefore, the aim of this review is to summarize the pharmacokinetic characteristics of PKIs and provide the evidence supporting the use of TDM for personalised treatment of patients with NSCLC.

This study was supported by the Charles University Project Cooperatio (research area PHAR).

Mailing Address: PharmDr. Judita Staša, Department of Clinical Pharmacy, Bulovka University Hospital, Budínova 67/1, 180 01 Prague 8, Czech Republic; Mobile Phone: +420 737 286 062; e-mail: judita.stasa@bulovka.cz

<https://doi.org/10.14712/23362936.2023.16>

© 2023 The Authors. This is an open-access article distributed under the terms of the Creative Commons Attribution License (<http://creativecommons.org/licenses/by/4.0>).

Introduction

Twenty years ago, in addition to conventional chemotherapy, targeted molecules began to be used in lung cancer treatment, which significantly contributed to prolonged and improved lives of patients (Huang et al., 2020). Nevertheless, lung cancer remains the leading cause of cancer-related death in both sexes worldwide (Siegel et al., 2022).

Protein kinase inhibitors (PKIs) are one of the widely represented drugs for targeted anticancer treatment. In the pharmacotherapy of lung cancer, PKIs are used in patients with non-small cell lung cancer (NSCLC), that represents about 80% of all cases of lung cancer (Kastelijin et al., 2019). PKIs are enzyme inhibitors that disrupt the signalling pathway in the cell by blocking the action of one or more of the specific kinases, mostly tyrosine kinases. Such an inhibition affects the proliferation and survival of the tumour cells (Arora and Scholar, 2005). Targeted PKI treatment is indicated for patients in whom the presence of driving mutations, especially activating mutations of EGFR (epidermal growth factor receptor) and ALK (anaplastic lymphoma kinase), is identified (Kastelijin et al., 2019). More than 50 tyrosine kinase inhibitors are currently approved for the treatment of various malignancies, and the number is expected to increase (Cohen et al., 2021).

These small molecule inhibitors show high inter-individual variability in some pharmacokinetic parameters, which translates into significantly different drug concentrations in blood (de Wit et al., 2015; Petit-Jean et al., 2015; Fahmy et al., 2021). For instance, with gefitinib, the first tyrosine kinase inhibitor used in the treatment of NSCLC, up to 16-fold interindividual variability of exposure with repeated administration, is reported (Zhao et al., 2011). Regardless, the “one-dose-fits-all” approach to PKI dosing still dominates. Consequently, some patients are at risk of treatment failure in the case of underdosing or increased toxicity in the case of overdose leading to treatment-limiting side effects (Lankheet et al., 2014; Menz et al., 2021). Additionally, due to oral administration of PKIs, high demanding patients’ adherence may also contribute to significant differences in the therapeutic response of these drugs in individuals (Greer et al., 2016).

In context of personalized cancer therapy, therapeutic drug monitoring (TDM) appears to be a valuable tool to tailor the treatment of the individual patients. TDM may help to adapt PKIs dosage regimen to a specific patient based on the measured concentrations of drugs in the blood at designed intervals (Kang and Lee, 2009). This method offers the possibility to reduce toxicity while maintaining efficacy (Kang and Lee, 2009; Groenland et al., 2019). Unlike the common practice of determining the levels of certain groups of drugs, such as antibiotics, antiepileptics, immunosuppressants, TDM is performed exceptionally for oncology drugs (Clarke et al., 2021). For now, one of the limitations is the lack of information about relationship among plasma concentration, efficacy and toxicity of most PKIs (Mueller-Schoell et al., 2021). However, positive results with individualized imatinib

Table 1 – Basic characteristic of EMA- and FDA-approved small protein kinase inhibitors in NSCLC therapy (by January 2023)

PKIs	Target kinases	Type of kinase inhibitor	Recommend dose regimen (mg)	Fasted or Fed state
Afatinib	EGFR, HER2	Tyrosine	40 od	Fasted 3 h before or 1 h after meal
Alectinib	ALK	Tyrosine	600 bid	Fed
Brigatinib	ALK	Tyrosine	90 od for the first 7 d 180 od from 8 th d	NI
Capmatinib	MET	Tyrosine	400 bid	NI
Ceritinib	ALK, ROS1	Tyrosine	450 od	Fed
Crizotinib	ALK, ROS1, MET	Tyrosine	250 bid	NI
Dabrafenib*	BRAF V600E	Serine/ Threonine	150 bid	Fasted 1 h before or 2 h after meal
Dacomitinib	EGFR, HER2	Tyrosine	45 od	NI
Entrectinib	ROS1, TRK, ALK	Tyrosine	600 od	NI
Erlotinib	EGFR	Tyrosine	150 od	Fasted 1 h before or 2 h after meal
Gefitinib	EGFR	Tyrosine	250 od	NI
Larotrectinib	TRK	Tyrosine	100 bid	NI
Lorlatinib	ALK, ROS1	Tyrosine	100 od	NI
Mobocertinib	EGFR	Tyrosine	160 od	NI
Osimertinib	EGFR T790M	Tyrosine	80 od	NI
Pralsetinib	RET	Tyrosine	400 od	Fasted 2 h before or 1 h after meal
Selpercatinib	RET	Tyrosine	< 50 kg 120 bid > 50 kg 160 bid	NI
Tepotinib	MET	Tyrosine	450 od	Fed
Trametinib*	MEK1/2	Serine/ Threonine	2 od	Fasted 1 h before or 2 h after meal

PKIs are listed alphabetically; source: EPAR – www.ema.europa.eu; NDA – www.fda.gov

*used in combination with dabrafenib or trametinib in NSCLC therapy; ALK – anaplastic lymphoma kinase; bid – twice daily; BRAF – v-raf murine sarcoma viral oncogene homolog B1; d – day; EGFR – epidermal growth factor receptor; EMA – European Medicines Agency; FDA – US Food and Drug Administration; HER2 – human epidermal growth factor receptor 2; MEK – mitogen-activated protein kinase; MET – mesenchymal-epithelial-transition; NSCLC – non-small cell lung cancer; od – once daily; PKIs – protein kinase inhibitors; RET – rearranged during transfection; NI – not important; ROS1 – proto-oncogene 1; TRK – tropomyosin receptor kinase

dosage using TDM have been demonstrated and its guideline has also been published (Clarke et al., 2021).

Therefore, the aim of this review is to summarize an overview of the current knowledge and evidence of the possibilities to tailor the dosage of selected PKIs using TDM, including the necessary pharmacokinetic parameters for personalized pharmacotherapy of patients with NSCLC.

Literature search

PubMed searches were performed using Boolean logic operations till January 2023. Search terms “pharmacokinetics”, “therapeutic drug monitoring”, “TDM”, “individualized dosing”, “exposure-response” and “exposure response” were combined with the name of the individual PKI registered by the European Medicines Agency (EMA) and US Food and Drug Administration (FDA) in NSCLC treatment to identify relevant references. Results were limited to studies in adult humans and English full-text articles published until January 2023. A total of 864 reports were identified from the initial literature search, out of which 15 relevant publications were found.

In addition, the references listed in the relevant articles were also examined and registration information from the EMA and FDA was reviewed.

Pharmacokinetics of currently approved PKIs in NSCLC

List of EMA- and FDA-approved small protein kinase inhibitors in NSCLC therapy with its basic characteristic is summarized in Table 1. Compared to traditional intravenously applied cytotoxic drugs, PKIs are administered orally on daily basis, particularly once a day, enabling outpatient treatment. An overview of pharmacokinetic (PK) properties of the selected PKIs is shown in Table 2.

Oral bioavailability ranges from 34% for larotrectinib up to 95% for dabrafenib. Some PKIs such as afatinib, dabrafenib, trametinib and erlotinib are recommended to be taken in the fasting state. The reason is that a high fat meal reduces C_{max} and AUC (area under concentration-time curve) and *vice versa* for erlotinib (approximately twofold higher exposure in fed condition) (Ling et al., 2008).

Most PKIs reach the maximum plasma concentration relatively fast (1–4 h), tepotinib is the only exception (8 h). The drugs are extensively distributed into tissues and are highly protein bound to alpha-1-acid glycoprotein and albumin resulting in a large volume of distribution and a long half-life.

Most of them undergo extensive metabolism, mainly via CYP3A4 with secondary contribution of other CYP enzymes. The exception is afatinib, which metabolism is negligible. The first mentioned PKIs are substrate of cytochrome P450 enzymes, the drug-drug interaction potential is considered high. Their exposure may be affected by concomitant use of other drugs that act on the same metabolic ways. Additionally, some of these drugs undergo auto-inhibition or auto-induction that make their metabolism at steady-state less predictable. Finally, cigarette smoking

has been known to induce CYP1A enzyme, thus significantly decreasing of erlotinib concentration, which is particularly important in the population of lung cancer patients (Petit-Jean et al., 2015).

All mentioned PKIs are predominantly excreted in the feces, with only a minor fraction being eliminated with the urine. These drugs are excreted as metabolites, except afatinib. Relatively large fraction of the dose of alectinib, ceritinib, crizotinib, pralsetinib and tepotinib may be excreted as parent compound.

Therapeutic drug monitoring of PKIs

Variability observed in clinical response between individuals ranges between 24–84% (Groenland et al., 2019). A broad range of factors, such as genetic heterogeneity of drug targets, pharmacogenetic background of the patient, patient's adherence to treatment, food intake, drug formulation, concomitant medication, and others, influence the absorption, distribution, metabolism, and excretion of drugs (Groenland et al., 2019; Janssen et al., 2020). Dose individualization through measurement of drug concentrations might reduce the interpatient variability in exposure and thereby favourably influence treatment outcome (de Wit et al., 2015).

In addition to individualized dosing, TDM can be used to diagnose unexpected toxicities or lack of therapeutic response, to detect and monitor drug interactions, to guide underdosing during dosage reduction or withdrawal of therapy, as well as to control adherence treatment (Kang and Lee, 2009). There are several general criteria for drugs to be suitable for TDM: availability of validated sensitive bioanalytical method, unpredictable and wide inter-individual pharmacokinetic variability in systemic exposure (which affects efficacy and tolerability), narrow therapeutic index, long-term therapy and correlation between plasma drug concentrations and clinical effects (Lankheet et al., 2014; Yu et al., 2014).

Proven relationship between exposure and response is fundamental for attempting to conduct TDM with added value (de Wit et al., 2015). Associations between drug concentration and therapeutic response have been summarized in several recent reviews (Verheijen et al., 2017; Janssen et al., 2020; Fahmy et al., 2021; Mueller-Schoell et al., 2021). Unfortunately, most PKIs don't have well defined thresholds for efficacy and toxicity, yet. In the absence of evidence-based TDM targets, Verheijen et al. (2017) suggest using the average population exposure of the approved effective dose, because the TDM targets of PKIs on average correspond to about 80% of the observed mean or median trough concentration (C_{min}). Proposed pharmacokinetic targets of PKIs are presented in Table 3.

To personalize PKIs dosing through TDM, the measurement of steady-state trough or just before the next dose concentration is often used in clinical practice (Verheijen et al., 2017). Trough levels are more practical than area under the plasma concentration-time curve due to daily dose and long half-life of PKIs and are less to be influenced by absorption and distribution problems (Kang and Lee, 2009). Ideally,

Table 2 – Summary of steady-state pharmacokinetics of PKIs after multiple daily oral doses in cancer patients

PKIs	Absorption			AUC (ng×h/ml)	Distribution	
	C _{max} (ng/ml)	T _{max} (h)	F (%)		Vd/F (l)	PPB (%)
Afatinib	38	3	92; ↓ with meal	631	2,870	95.0
Alectinib	676	4	37 ↑ with meal	5,400	4,016	99.0
Brigatinib	552 (90 mg) 1,452 (180 mg)	2	ND	8,165 (90 mg) 20,276 (180 mg)	153 (180 mg)	66.0
Capmatinib	4,780	1–2	70	20,200	164	96.0
Ceritinib	674 (750 mg)	4–6 ^a	ND ↑ with meal	14,000 (750 mg)	4,230 ^a (750 mg)	97.0
Crizotinib	327	4	43	3,084	1,177 ^b (50 mg)	91.0
Dabrafenib	1,478	2	95 ↓ with meal	4,341	70.3	99.7
Dacomitinib	108	6	80	2,342	1,889 ^b (20 mg)	98.0
Entrectinib	3,130 (nM)	4–6 ^a	>50	48,000 (nM×h)	551 (M5-81)	99.0
Erlotinib	1,995	4	59 ↑ with meal	41,300	232	95.0
Gefitinib	104.5 ^c	3–7	59	2,631 ^c	1,400	91.0
Larotrectinib	788	1	34	4,351	374 ^a	70.0
Lorlatinib	577	2	81	5,650	390 ^a	66.0
Mobocertinib	70.4	4	37	862 ^{ac}	3,510	99.0
Osimertinib	501 nmol/l	6	ND	11,258 nmol/l	986	99.0
Pralsetinib	2,830	2–4	ND	43,900	268	97.0
Selpercatinib	2,980 (180 mg)	2	73	51,600 (180 mg)	323 ^a	97.0
Tepotinib	1,291	8	72 ↑ with meal	27,438	34.6 ^b	98.0
Trametinib	22.2	1.5	72; ↓ with meal	370	214	97.4

PKIs are listed alphabetically. ^asingle dose administration; ^bsingle intravenous dose; ^chealthy volunteers
AUC – area under concentration-time curve; CL/F – apparent clearance; C_{max} – maximum concentration; F – oral bioavailability;
ND – not determined; OHD – hydroxy-dabrafenib; PKIs – protein kinase inhibitors; PPB – plasma protein binding;
T_{max} – time to reach C_{max}; T_{1/2} – half-life; UD – unchanged drug; Vd/F – apparent volume of distribution

Metabolism Enzymes (main metabolite)	T _{1/2} (h)	CL/F (l/h)	Excretion		References
			Feces (%)	Urine (%)	
negligible	36.3	64.2	85% UD	4% UD	Afatinib; Wind et al. (2017)
CYP3A4 (M4)	32	502	98 (84% UD 9% as M4)	<1	Alectinib; Hirota et al. (2019)
<i>in vitro</i> CYP2C8; CYP3A4	25	12.7 (180 mg)	65 (41% UD)	25 (86% UD)	Brigatinib; Hirota et al. (2019)
CYP3A4	6.54	19.8	78 (42% UD)	22	Capmatinib
<i>in vitro</i> CYP3A	41 ^a (750 mg)	33 (750 mg)	92 (68% UD)	1.3	Ceritinib; Hirota et al. (2019)
<i>in vitro</i> CYP3A	42 ^a	81	63 (53% UD)	22 (<2% UD)	Crizotinib; Hirota et al. (2019)
CYP2C8; CYP3A4 (OHD)	8	34.4	71	23	Dabrafenib
CYP2D6	70.3	26.9	78.8 (20% UD)	3.2 (<1% UD)	Dacomitinib
CYP3A4 (M5)	20 (M5-40)	19.6 (M5-52.4)	83 (22% as M5)	3	Entrectinib
CYP3A4/5 (OSI-420); CYP1A2	36.2	4.47	90 (1% UD)	9 (0.3% UD)	Erlotinib
CYP3A4; CYP2D6 (M523595)	41 ^b	30	80.8 (4% UD)	3.6 (0.5% UD)	Gefitinib
CYP3A4	2.9 ^a	98 ^a	58 (5% UD)	39 (20% UD)	Larotrectinib
CYP3A4; UGT1A4	23.6 ^a	17.7	41 (9% UD)	48 (<1% UD)	Lorlatinib
CYP3A (AP32960)	17.6	108	76 (6% UD)	3.57 (1.3% UD)	Mobocertinib; Zhang et al. (2021)
<i>in vitro</i> CYP3A4/5	48	14.2	67.8 (1.2% UD)	14.2 (0.8% UD)	Osimertinib; Brown et al. (2017)
<i>in vitro</i> CYP3A4; CYP2D6; CYP2A1	22.2	9.1	73 (66% UD)	6 (4.8% UD)	Pralsetinib (2020, 2021)
CYP3A4	37 ^{ac}	6	69 (14% UD)	24 (12% UD)	Selpercatinib
<i>in vitro</i> CYP3A4; CYP2C8	32	20.4	85 (50% UD)	15 (50% UD)	Tepotinib
non-CYP450	93.6–115.2	5.4	80	<0.1 UD	Trametinib

Table 3 – Summary of proposed pharmacokinetic targets of PKIs defined as trough plasma concentration

PKIs	Proposed target (ng/ml)	Mean/median exposure (ng/ml)	Exposure-response relationship	Associated parameter(s)	References
Afatinib	NA	$C_{\min,ss} \geq 14.4$	no		Verheijen et al. (2017), Wind et al. (2017)
Alectinib	≥ 435	$C_{\min,ss} = 517$	yes	PFS	Groenland et al. (2021)
Brigatinib	NA	$C_{\min,ss} = 226$ (90 mg) 520 (180 mg)	yes	PFS, OS	Brigatinib; Mueller-Schoell et al. (2021)
Capmatinib	NA	$C_{\min,ss} = 562.42$	not yet characterized		Capmatinib
Ceritinib	NA	$C_{\min,ss} = 871$ (750 mg)	inconclusive	ORR	Ceritinib; Verheijen et al. (2017)
Crizotinib	≥ 235	$C_{\min,ss} = 244$	yes	PFS	Groenland et al. (2021)
Dabrafenib	NA	$C_{\min,ss} = 46.6$	no		Dabrafenib; Ouellet et al. (2014)
Dacomitinib	NA	$C_{\min,ss} = 73.1$	inconclusive	PFS, tumour shrinkage	Dacomitinib
Entrectinib	NA	NA	no		Entrectinib
Erlotinib	> 500	$C_{\min,ss} = 1,011$	no		Hidalgo et al. (2001), Lankheet et al. (2014), Kenmotsu et al. (2022)

samples should be taken at steady-state, which is after 5 half-lives, e.g. 8 days for erlotinib.

Currently, validated analytical method combining liquid chromatography with tandem mass spectrometry is applied to facilitate therapeutic monitoring of the PKIs in routine practice (Zhou et al., 2021).

Afatinib

The relationship between plasma drug exposure and response for afatinib is sparse. No correlation between trough concentration and efficacy was found (Afatinib). Nevertheless, daily doses under 20 mg affected treatment effectiveness in terms of a significantly shorter progression free survival (PFS) (Lim et al., 2018). In contrast, the relationship between afatinib trough plasma concentrations and the occurrence of the adverse events were reported. The severity of diarrhea and rash positively

PKIs	Proposed target (ng/ml)	Mean/median exposure (ng/ml)	Exposure-response relationship	Associated parameter(s)	References
Gefitinib	≥ 200	$C_{\min,ss} = 266$	yes	OS	Zhao et al. (2011), Fahmy et al. (2021), Mueller-Schoell et al. (2021)
Larotrectinib	NA	$C_{\min,ss} = 33$	no		Larotrectinib
Lorlatinib	NA	$C_{\min,ss} = 114.97$	no		Chen et al. (2021)
Mobocertinib	NA		no		Gupta et al. (2022)
Osimertinib	NA	$C_{\min,ss} = 166$	no		Brown et al. (2017), Mueller-Schoell et al. (2021)
Pralsetinib	NA	$C_{\min,ss} = 1,150$	no		Pralsetinib (2020)
Selpercatinib	NA		not yet characterized		Selpercatinib
Tepotinib	NA		not yet characterized		Xiong et al. (2022)
Trametinib	≥ 10.6	$C_{\min} = 12.1$	yes	PFS	Trametinib; Ouellet et al. (2016)

PKIs are listed alphabetically; NA – not available; ORR – objective response rate; OS – overall survival; PFS – progression free survival; PKIs – protein kinase inhibitors

correlated with higher exposure of afatinib (Wind et al., 2017). Due to undefined TDM target, Verheijen et al. (2017) proposed to use a steady-state C_{\min} 14.4–27.4 ng/ml of the standard dose of afatinib 40 mg.

Alectinib

The previously proposed C_{\min} threshold of 435 ng/ml for alectinib was proven to prolong PFS in observational study with NSCLC patients (Groenland et al., 2021). The authors of the study state that TDM of alectinib should be part of the clinical routine (Groenland et al., 2021).

Brigatinib

Threshold for brigatinib has not been established yet. Exposure-response analyses showed positive trends in association between exposure to brigatinib represented mean of trough concentrations at steady-state and PFS and overall survival (OS) (Brigatinib).

Capmatinib

The exposure-response relationship was inconclusive due to small number of patients (Capmatinib).

Ceritinib

The results of exposure-response analyses for efficacy did not show a clear relationship between systemic exposure and objective response rate (ORR) or PFS in ALK-positive NSCLC patients. Only a trend towards higher ORR with higher C_{\min} was reported (Ceritinib; Verheijen et al., 2017). No threshold for ceritinib has been proposed so far. Meanwhile, ceritinib C_{\min} could be interpreted in reference to the mean C_{\min} of 871 ng/ml at dosage 750 mg od as target for TDM (Ceritinib; Verheijen et al., 2017).

Crizotinib

Significant exposure-therapeutic efficacy correlations have been described for crizotinib before. In an observational study in ALK-positive NSCLC patients, exposure-response (E-R) analyses were performed using a previously proposed C_{\min} threshold of ≥ 235 ng/ml for crizotinib (Groenland et al., 2021). In this study, the ≥ 235 ng/ml threshold was associated with longer PFS. As well as for alectinib, the authors of the study state that TDM of crizotinib should be part of the clinical routine (Groenland et al., 2021).

Dabrafenib

No consistent data for dabrafenib exposure-response relationship exist thus far. Recent study could not prove significant correlation between dabrafenib (measured as only parent drug) exposure and response (Raynal et al., 2022) in patients treated for metastatic melanoma. Verheijen et al. (2017) in the review suggested to target C_{\min} 99.6 ng/ml for guided dosing, which was based on the median sum of parent dabrafenib and its active hydroxyl metabolite in melanoma patients.

Dacomitinib

Only limited exposure-response data exists for dacomitinib in patients with locally advanced/metastatic NSCLC with EGFR-activating mutations. Drug exposure suggested slightly positive relationship E-R for PFS and statistically significant for tumour shrinkage (Dacomitinib).

Entrectinib

No apparent relationship between entrectinib parent (or M5 metabolite) steady-state exposure and efficacy was observed in E-R analyses in 76 patients with NTRK- (neurotrophic tyrosine receptor kinase), ROS1- (proto-oncogene 1), or ALK-positive, locally advanced or metastatic tumours. Results of the analyses suggested that doses higher than 600 mg are unlikely to produce greater efficacy (Mercier et al., 2022).

Erlotinib

Steady-state concentration ranged from 580 to 1,820 ng/ml in standard dosing regimen at 150 mg per day (Hidalgo et al., 2001). At this dosage in phase I study,

the values of the minimum concentration at steady-state exceeded 500 ng/ml in the majority of patients (Hidalgo et al., 2001). In preclinical studies, plasma concentration of 500 ng/ml showed EGFR inhibition associated with an antiproliferative activity (Hidalgo et al., 2001). This value was reported as a target threshold for erlotinib in several reviews (Yu et al., 2014; Verheijen et al., 2017; Mueller-Schoell et al., 2021) despite of lacking the relationship between efficacy and exposure of total and unbound erlotinib in patients with EGFR-mutated NSCLC (Kenmotsu et al., 2022).

Gefitinib

In study with NSCLC patients, overall survival was linked to gefitinib trough concentration. Patients with $C_{\min} \geq 200$ ng/ml had significantly higher overall survival (14.6 months compared to 4.7 months) (Zhao et al., 2011). Yet, a later retrospective analysis in NSCLC patients disputed it (Xin et al., 2015). The PFS for the group patients with lower trough concentration < 200 ng/ml were not inferior to patients with higher ($C_{\min} \geq 200$ ng/ml) trough concentration (Xin et al., 2015). For now, a threshold C_{\min} of ≥ 200 ng/ml for TDM gefitinib is reported in the most recent reviews (Fahmy et al., 2021; Mueller-Schoell et al., 2021).

Larotrectinib

Larotrectinib exposure did not have a statistically significant effect on the probability of a response (Larotrectinib).

Lorlatinib

The E-R analysis for efficacy was not statistically significant for either efficacy end points (ORR, intracranial ORR) in patients with NSCLC (Chen et al., 2021).

Mobocertinib

In the exposure-efficacy analyses, systemic exposure based on the molar sum of exposures to mobocertinib and its active metabolites was not a statistically significant predictor of clinical response (ORR) (Gupta et al., 2022).

Osimertinib

No evidence of relationship between osimertinib exposure (AUC_{ss}) and efficacy was observed at the dose range (20–240 mg) studied in patients with NSCLC (Brown et al., 2017). Interestingly, in recent study, increased osimertinib plasma exposure was associated with higher risk of death (shorter PFS and OS in unselected NSCLC patients) (Rodier et al., 2022). In the absence of an exposure-response target, the geometric mean C_{\min} of 166 ng/ml at approved dose of 80 mg od (once daily) could be used as a reference to guide TDM (Verheijen et al., 2017; Mueller-Schoell et al., 2021).

Pralsetinib

Results from registration-enabling study in patients with NSCLC revealed no relevant or consistent relationships between increasing pralsetinib exposure and efficacy or safety endpoints. However, pralsetinib mean C_{trough} of 1,150 ng/ml with the 400 mg od dose was associated with rapid declines in brain lesion size and prevention from developing new central nervous system metastases during the study. This value was close to the predicted brain IC₉₀ of pralsetinib for rearranged during transfection (RET) inhibition in humans (1,514 ng/ml) (Pralsetinib, 2020).

Selperetinib

The exposure-response relationship is largely unknown (Selpercatinib).

Tepotinib

The relationships between exposure and response for tepotinib is inconclusive because of the limited data. No clear association of tepotinib exposure (AUC) with efficacy and safety was observed in study by Xiong and his colleagues (2022).

Trametinib

Population pharmacokinetic analysis demonstrated association between clinical efficacy and trametinib trough concentrations (Ouellet et al., 2016). Patients with observed C_{min} above the median 10.6 ng/ml in phase II had longer PFS than those below median. This was not confirmed in phase III, where median was higher (13.6 ng/ml) (Ouellet et al., 2016). On the other hand, trametinib C_{min} threshold of 10.6 ng/ml is consistent with its preclinical target concentration of 10.4 ng/ml that inhibits the MEK (mitogen-activated protein kinase) pathway (Ouellet et al., 2016). Noted in study by Ouellet et al. (2016), exposure-response relationship was evaluated only for trametinib alone, not for combination therapy with dabrafenib. However, recent study did not confirm the above-mentioned positive relationship when combined with dabrafenib (Goldwirt et al., 2021).

Discussion and Conclusion

Current fixed dosing strategy is associated with decreased efficacy or on the other hand causing unnecessary toxicities (Lankheet et al., 2014; Groenland et al., 2019). There is growing evidence for potential benefits of dosing adjustment based on pharmacokinetic targets in treatment not only of lung cancer with most PKIs. The consensus guideline for TDM of imatinib has been already developed (Clarke et al., 2021). Positive examples of treatment optimization and individualization of PKIs from practice in patients with lung cancer are emerging (Catalán-Latorre et al., 2021).

We have summarized the available evidence on average C_{min} and proposed targets of PKIs for treatment of patients with NSCLC. Unfortunately, for a considerable number of PKIs, statistically significant exposure-response correlations are still lacking. Likewise, most of pharmacokinetic targets have not been established, yet, or they are

waiting to be validated in prospective studies. Currently, for none of the discussed agents, TDM is performed as the standard of care.

Despite the mentioned unknowns, provided data could be beneficial in cases of suspected nonadherence to therapy, pharmacokinetic drug-drug interactions, or unexpected toxicity (Groenland et al., 2019). After selecting the most effective drug for a specific tumour type, dose individualization could further help in the personalized treatment of NSCLC patients.

References

- Afatinib (2012) *Food and Drug Administration. Center for Drug Evaluation and Research. Clinical Pharmacology and Biopharmaceutics Review(s)*. Available at: www.accessdata.fda.gov/drugsatfda_docs/nda/2013/201292Orig1s000ClinPharmR.pdf (Accessed 10 March 2023)
- Alectinib (2016) *Committee for Medicinal Products for Human Use. European Medicines Agency. Alecensa. European public assessment report*. Available at: www.ema.europa.eu/en/documents/assessment-report/alecensa-epar-public-assessment-report_en.pdf (Accessed 11 March 2023)
- Arora, A., Scholar, E. M. (2005) Role of tyrosine kinase inhibitors in cancer therapy. *J. Pharmacol. Exp. Ther.* **315**, 971–979.
- Brigatinib (2017) *Food and Drug Administration. Center for Drug Evaluation and Research. NDA Multidisciplinary Review and Evaluation NDA 208772 ALUNBRIG (brigatinib)*. Available at: www.accessdata.fda.gov/drugsatfda_docs/nda/2017/208772Orig1s000MultidisciplineR.pdf (Accessed 10 March 2023)
- Brown, K., Comisar, C., Witjes, H., Maringwa, J., de Greef, R., Vishwanathan, K., Cantarini, M., Cox, E. (2017) Population pharmacokinetics and exposure-response of osimertinib in patients with non-small cell lung cancer. *Br. J. Clin. Pharmacol.* **83**, 1216–1226.
- Capmatinib (2022) *Committee for Medicinal Products for Human Use. European Medicines Agency. Tabrecta. European public assessment report*. Available at: www.ema.europa.eu/en/documents/assessment-report/tabrecta-epar-public-assessment-report_en.pdf (Accessed 11 March 2023)
- Catalán-Latorre, A., Sureda, M., Brugarolas-Masllorens, A., Escudero-Ortiz, V. (2021) Therapeutic drug monitoring of erlotinib in non-small cell lung carcinoma: A case study. *Ther. Drug Monit.* **43**, 447–450.
- Ceritinib (2014) *Food and Drug Administration. Center for Drug Evaluation and Research. Clinical Pharmacology and Biopharmaceutics Review(s)*. Available at: www.accessdata.fda.gov/drugsatfda_docs/nda/2014/205755Orig1s000ClinPharmR.pdf (Accessed 11 March 2023)
- Chen, J., Ruiz-García, A., James, L. P., Peltz, G., Thurm, H., Clancy, J., Hibma, J. (2021) Lorlatinib exposure-response analyses for safety and efficacy in a phase I/II trial to support benefit-risk assessment in non-small cell lung cancer. *Clin. Pharmacol. Ther.* **110**, 1273–1281.
- Clarke, W. A., Chatelut, E., Fotoohi, A. K., Larson, R. A., Martin, J. H., Mathijssen, R. H. J., Salamone, S. J. (2021) Therapeutic drug monitoring in oncology: International Association of Therapeutic Drug Monitoring and Clinical Toxicology consensus guidelines for imatinib therapy. *Eur. J. Cancer* **157**, 428–440.
- Cohen, P., Cross, D., Jänne, P. A. (2021) Kinase drug discovery 20 years after imatinib: Progress and future directions. *Nat. Rev. Drug Discov.* **20**, 551–569.
- Crizotinib (2011) *Food and Drug Administration. Center for Drug Evaluation and Research. Clinical Pharmacology and Biopharmaceutics Review(s)*. Available at: www.accessdata.fda.gov/drugsatfda_docs/nda/2011/202570Orig1s000ClinPharmR.pdf (Accessed 11 March 2023)
- Dabrafenib (2013) *Food and Drug Administration. Center for Drug Evaluation and Research. Clinical Pharmacology and Biopharmaceutics Review(s)*. Available at: www.accessdata.fda.gov/drugsatfda_docs/nda/2013/202806Orig1s000ClinPharmR.pdf (Accessed 11 March 2023)

- Dacomitinib (2018) *Food and Drug Administration. Center for Drug Evaluation and Research. NDA Multi-disciplinary Review and Evaluation NDA 212725 VIZIMPRO (dacomitinib)*. Available at: www.accessdata.fda.gov/drugsatfda_docs/nda/2018/211288Orig1s000MultidisciplineR.pdf (Accessed 11 March 2023)
- de Wit, D., Guchelaar, H. J., den Hartigh, J., Gelderblom, H., van Erp, N. P. (2015) Individualized dosing of tyrosine kinase inhibitors: Are we there yet? *Drug Discov. Today* **20**, 18–36.
- Entrectinib (2019) *Food and Drug Administration. Center for Drug Evaluation and Research. NDA Multi-disciplinary Review and Evaluation NDA 212725 ROZLYTEK (entrectinib)*. Available at: www.accessdata.fda.gov/drugsatfda_docs/nda/2019/212725Orig1s000,%20212726Orig1s000MultidisciplineR.pdf (Accessed 11 March 2023)
- Erlotinib (2021) *Product Monograph Tarceva (erlotinib)*. Available at: https://www.rocheCanada.com/PMs/Tarceva/Tarceva_PM_E.pdf (Accessed 11 March 2023)
- Fahmy, A., Hopkins, A. M., Sorich, M. J., Rowland, A. (2021) Evaluating the utility of therapeutic drug monitoring in the clinical use of small molecule kinase inhibitors: A review of the literature. *Expert Opin. Drug Metab. Toxicol.* **17**, 803–821.
- Gefitinib (2008) *Committee for Medicinal Products for Human Use. European Medicines Agency. Iressa. European public assessment report*. Available at: www.ema.europa.eu/en/documents/assessment-report/iressa-epar-public-assessment-report_en.pdf (Accessed 11 March 2023)
- Goldwirt, L., Louveau, B., Baroudjian, B., Allayous, C., Jouenne, F., Da Meda, L., Vu, L. T., Sauvageon, H., Herms, F., Delyon, J., Lebbé, C. Mourah, S. (2021) Dabrafenib and trametinib exposure-efficacy and tolerance in metastatic melanoma patients: A pharmacokinetic-pharmacodynamic real-life study. *Cancer Chemother. Pharmacol.* **88**, 427–437.
- Greer, J. A., Amoyal, N., Nisotel, L., Fishbein, J. N., MacDonald, J., Stagl, J., Lennes, I., Temel, J. S., Safren, S. A., Pirl, W. F. (2016) A systematic review of adherence to oral antineoplastic therapies. *Oncologist* **21**, 354–376.
- Groenland, S. L., Mathijssen, R. H. J., Beijnen, J. H., Huitema, A. D. R., Steeghs, N. (2019) Individualized dosing of oral targeted therapies in oncology is crucial in the era of precision medicine. *Eur. J. Clin. Pharmacol.* **75**, 1309–1318.
- Groenland, S. L., Geel, D. R., Janssen, J. M., de Vries, N., Rosing, H., Beijnen, J. H., Burgers, J. A., Smit, E. F., Huitema, A. D. R., Steeghs, N. (2021) Exposure-response analyses of anaplastic lymphoma kinase inhibitors crizotinib and alectinib in non-small cell lung cancer patients. *Clin. Pharmacol. Ther.* **109**, 394–402.
- Gupta, N., Largajolli, A., Witjes, H., Diderichsen, P. M., Zhang, S., Hanley, M. J., Lin, J., Mehta, M. (2022) Mobocertinib dose rationale in patients with metastatic NSCLC with EGFR exon 20 insertions: Exposure-response analyses of a pivotal phase I/II study. *Clin. Pharmacol. Ther.* **112**, 327–334.
- Hidalgo, M., Siu, L. L., Nemunaitis, J., Rizzo, J., Hammond, L. A., Takimoto, C., Eckhardt, S. G., Tolcher, A., Britten, C. D., Denis, L., Ferrante, K., Von Hoff, D. D., Silberman, S., Rowinsky, E. K. (2001) Phase I and pharmacologic study of OSI-774, an epidermal growth factor receptor tyrosine kinase inhibitor, in patients with advanced solid malignancies. *J. Clin. Oncol.* **19**, 3267–3279.
- Hirota, T., Muraki, S., Ieiri, I. (2019) Clinical pharmacokinetics of anaplastic lymphoma kinase inhibitors in non-small-cell lung cancer. *Clin. Pharmacokinet.* **58**, 403–420.
- Huang, L., Jiang, S., Shi, Y. (2020) Tyrosine kinase inhibitors for solid tumors in the past 20 years (2001–2020). *J. Hematol. Oncol.* **13**, 143.
- Janssen, J. M., Dorlo, T. P. C., Steeghs, N., Beijnen, J. H., Hanff, L. M., van Eijkelenburg, N. K. A., van der Lugt, J., Zwaan, C. M., Huitema, A. D. R. (2020) Pharmacokinetic targets for therapeutic drug monitoring of small molecule kinase inhibitors in pediatric oncology. *Clin. Pharmacol. Ther.* **108**, 494–505.
- Kang, J. S., Lee, M. H. (2009) Overview of therapeutic drug monitoring. *Korean J. Intern. Med.* **24**, 1–10.

- Kastelijin, E. A., de Langen, A. J., Peters, B. J. M. (2019) Treatment of oncogene-driven non-small cell lung cancer. *Curr. Opin. Pulm. Med.* **25**, 300–307.
- Kenmotsu, H., Imamura, C. K., Kawamura, T., Oyakawa, T., Omori, S., Nakashima, K., Wakuda, K., Ono, A., Taira, T., Naito, T., Murakami, H., Yamamoto, N., Takahashi, T., Tanigawara, Y. (2022) Prospective evaluation of the relationship between response and exposure of total and unbound erlotinib in non-small cell lung cancer patients. *Cancer Chemother. Pharmacol.* **90**, 115–123.
- Lankheet, N. A., Knapen, L. M., Schellens, J. H., Beijnen, J. H., Steeghs, N., Huitema, A. D. (2014) Plasma concentrations of tyrosine kinase inhibitors imatinib, erlotinib, and sunitinib in routine clinical outpatient cancer care. *Ther. Drug Monit.* **36**, 326–334.
- Larotrectinib (2018) *Food and Drug Administration. Center for Drug Evaluation and Research. NDA Multidisciplinary Review and Evaluation NDA 210861 and NDA 211710 VITRAKVI (larotrectinib)*. Available at: www.accessdata.fda.gov/drugsatfda_docs/nda/2018/210861Orig1s000_211710Orig1s000MultidisciplineR.pdf (Accessed 11 March 2023)
- Larotrectinib (2019) *Committee for Medicinal Products for Human Use. European Medicines Agency. Vitrakvi. European public assessment report*. Available at: www.ema.europa.eu/en/documents/assessment-report/vitrakvi-epar-public-assessment-report_en.pdf (Accessed 11 March 2023)
- Lim, C. K., Wei, Y. F., Tsai, M. S., Chen, K. Y., Shih, J. Y., Yu, C. J. (2018) Treatment effectiveness and tolerability of afatinib at different doses in patients with EGFR-mutated lung adenocarcinoma: How low can we go? *Eur. J. Cancer* **103**, 32–40.
- Ling, J., Fettner, S., Lum, B. L., Riek, M., Rakhit, A. (2008) Effect of food on the pharmacokinetics of erlotinib, an orally active epidermal growth factor receptor tyrosine-kinase inhibitor, in healthy individuals. *Anticancer Drugs* **19**, 209–216.
- Lorlatinib (2019) *Committee for Medicinal Products for Human Use. European Medicines Agency. Lorviqua. European public assessment report*. Available at: www.ema.europa.eu/en/documents/assessment-report/lorviqua-epar-public-assessment-report_en.pdf (Accessed 13 March 2023)
- Menz, B. D., Stocker, S. L., Verougstraete, N., Kocic, D., Galettis, P., Stove, C. P., Reuter, S. E. (2021) Barriers and opportunities for the clinical implementation of therapeutic drug monitoring in oncology. *Br. J. Clin. Pharmacol.* **87**, 227–236.
- Mercier, F., Djebli, N., González-Sales, M., Jaminion, F., Meneses-Lorente, G. (2022) Efficacy and safety exposure-response analyses of entrectinib in patients with advanced or metastatic solid tumors. *Cancer Chemother. Pharmacol.* **89**, 363–372.
- Mobocertinib (2021) *Food and Drug Administration. Center for Drug Evaluation and Research. NDA Multidisciplinary Review and Evaluation NDA 215310 EXKIVITY (mobocertinib)*. Available at: www.accessdata.fda.gov/drugsatfda_docs/nda/2021/215310Orig1s000MultidisciplineR.pdf (Accessed 13 March 2023)
- Mueller-Schoell, A., Groenland, S. L., Scherf-Clavel, O., van Dyk, M., Huisinga, W., Michelet, R., Jaehde, U., Steeghs, N., Huitema, A. D. R., Kloft, C. (2021) Therapeutic drug monitoring of oral targeted antineoplastic drugs. *Eur. J. Clin. Pharmacol.* **77**, 441–464.
- Osimertinib (2015) *Food and Drug Administration. Center for Drug Evaluation and Research. Clinical Pharmacology and Biopharmaceutics Review(s)*. Available at: www.accessdata.fda.gov/drugsatfda_docs/nda/2015/208065orig1s000clinpharmr.pdf (Accessed 13 March 2023)
- Ouellet, D., Gibiansky, E., Leonowens, C., O'Hagan, A., Haney, P., Switzky, J., Goodman, V. L. (2014) Population pharmacokinetics of dabrafenib, a BRAF inhibitor: Effect of dose, time, covariates, and relationship with its metabolites. *J. Clin. Pharmacol.* **54**, 696–706.
- Ouellet, D., Kassir, N., Chiu, J., Mouksassi, M. S., Leonowens, C., Cox, D., DeMarini, D. J., Gardner, O., Crist, W., Patel, K. (2016) Population pharmacokinetics and exposure-response of trametinib, a MEK inhibitor, in patients with BRAF V600 mutation-positive melanoma. *Cancer Chemother. Pharmacol.* **77**, 807–817.

- Petit-Jean, E., Buclin, T., Guidi, M., Quoix, E., Gourieux, B., Decosterd, L. A., Gairard-Dory, A. C., Ubeaud-Séquier, G., Widmer, N. (2015) Erlotinib: Another candidate for the therapeutic drug monitoring of targeted therapy of cancer? A pharmacokinetic and pharmacodynamic systematic review of literature. *Ther. Drug Monit.* **37**, 2–21.
- Pralsetinib (2020) *Food and Drug Administration. Center for Drug Evaluation and Research. NDA Multi-disciplinary Review and Evaluation NDA 213721 GAVRETO (pralsetinib)*. Available at: www.accessdata.fda.gov/drugsatfda_docs/nda/2020/213721Orig1s000MultidisciplineR.pdf (Accessed 13 March 2023)
- Pralsetinib (2021) *Committee for Medicinal Products for Human Use. European Medicines Agency. Gavreto. European public assessment report*. Available at: www.ema.europa.eu/en/documents/assessment-report/gavreto-epar-public-assessment-report_en.pdf (Accessed 13 March 2023)
- Raynal, M., Alvarez, J. C., Saiag, P., Beauchet, A., Funck-Brentano, C., Funck-Brentano, E. (2022) Monitoring of plasma concentrations of dabrafenib and trametinib in advanced BRAFV600^{mut} melanoma patients. *Ann. Dermatol. Venereol.* **149**, 32–38.
- Rodier, T., Puszkiel, A., Cardoso, E., Balakirouchenane, D., Narjoz, C., Arrondeau, J., Fallet, V., Khoudour, N., Guidi, M., Vidal, M., Declèves, X., Csajka, C., Alexandre, J., Cadranel, J., Fabre, E., Wislez, M., Goldwasser, F., Blanchet, B. (2022) Exposure-response analysis of osimertinib in patients with advanced non-small-cell lung cancer. *Pharmaceutics* **14**, 1844.
- Selpercatinib (2020) *Food and Drug Administration. Center for Drug Evaluation and Research. NDA Multi-disciplinary Review and Evaluation NDA 213246 RETEVMO (selpercatinib)*. Available at: www.accessdata.fda.gov/drugsatfda_docs/nda/2020/213246Orig1s000MultidisciplineR.pdf (Accessed 11 March 2023)
- Siegel, R. L., Miller, K. D., Fuchs, H. E., Jemal, A. (2022) Cancer statistics, 2022. *CA Cancer J. Clin.* **72**, 7–33.
- Tepotinib (2021) *Committee for Medicinal Products for Human Use. European Medicines Agency. Tepmetko. European public assessment report*. Available at: www.ema.europa.eu/en/documents/assessment-report/tepmetko-epar-public-assessment-report_en.pdf (Accessed 11 March 2023)
- Trametinib (2013) *Food and Drug Administration. Center for Drug Evaluation and Research. Clinical Pharmacology and Biopharmaceutics Review(s)*. Available at: www.accessdata.fda.gov/drugsatfda_docs/nda/2013/204114orig1s000clinpharmr.pdf (Accessed 11 March 2023)
- Verheijen, R. B., Yu, H., Schellens, J. H. M., Beijnen, J. H., Steeghs, N., Huitema, A. D. R. (2017) Practical recommendations for therapeutic drug monitoring of kinase inhibitors in oncology. *Clin. Pharmacol. Ther.* **102**, 765–776.
- Wind, S., Schnell, D., Ebner, T., Freiwald, M., Stopfer, P. (2017) Clinical pharmacokinetics and pharmacodynamics of afatinib. *Clin. Pharmacokinet.* **56**, 235–250.
- Xin, S., Zhao, Y., Wang, X., Huang, Y., Zhang, J., Guo, Y., Li, J., Li, H., Ma, Y., Chen, L., Hu, Z., Huang, M., Zhang, L. (2015) The dissociation of gefitinib trough concentration and clinical outcome in NSCLC patients with EGFR sensitive mutations. *Sci. Rep.* **5**, 12675.
- Xiong, W., Papasouliotis, O., Jonsson, E. N., Strotmann, R., Girard, P. (2022) Population pharmacokinetic analysis of tepotinib, an oral MET kinase inhibitor, including data from the VISION study. *Cancer Chemother. Pharmacol.* **89**, 655–669.
- Yu, H., Steeghs, N., Nijenhuis, C. M., Schellens, J. H., Beijnen, J. H., Huitema, A. D. (2014) Practical guidelines for therapeutic drug monitoring of anticancer tyrosine kinase inhibitors: Focus on the pharmacokinetic targets. *Clin. Pharmacokinet.* **53**, 305–325.
- Zhang, S., Jin, S., Griffin, C., Feng, Z., Lin, J., Baratta, M., Brake, R., Venkatakrishnan, K., Gupta, N. (2021) Single-dose pharmacokinetics and tolerability of the oral epidermal growth factor receptor inhibitor mobocertinib (TAK-788) in healthy volunteers: Low-fat meal effect and relative bioavailability of 2 capsule products. *Clin. Pharmacol. Drug Dev.* **10**, 1028–1043.

- Zhao, Y. Y., Li, S., Zhang, Y., Zhao, H. Y., Liao, H., Guo, Y., Shi, Y. X., Jiang, W., Xue, C., Zhang, L. (2011) The relationship between drug exposure and clinical outcomes of non-small cell lung cancer patients treated with gefitinib. *Med. Oncol.* **28**, 697–702.
- Zhou, L., Wang, S., Chen, M., Huang, S., Zhang, M., Bao, W., Bao, A., Zhang, P., Guo, H., Liu, Z., Xie, G., Gao, J., Wu, Z., Lou, Y., Fan, G. (2021) Simultaneous and rapid determination of 12 tyrosine kinase inhibitors by LC-MS/MS in human plasma: Application to therapeutic drug monitoring in patients with non-small cell lung cancer. *J. Chromatogr. B Analyt. Technol. Biomed. Life Sci.* **1175**, 122752.

Effects of Cannabidiol in Inflammation: A Review of Pre-clinical and Clinical Findings

Michaela Sklenárová, Martin Šíma, Ondřej Slanař

Institute of Pharmacology, First Faculty of Medicine, Charles University and General University Hospital in Prague, Prague, Czech Republic

Received April 12, 2023; Accepted August 17, 2023.

Key words: CBD – Cannabidiol – Arthritis – Inflammation – Pain

Abstract: Cannabidiol (CBD) is the second most abundant component of the plant *Cannabis sativa*. Currently, CBD is approved for Lennox-Gastaut and Dravet syndrome and newly for tuberous sclerosis complex. However, based on the available data, CBD might have a broad spectrum of potential therapeutic uses. Therefore, the aim of this review was to summarize the evidence on the effects of CBD on pain and inflammation of various causes. PubMed and Web of Science databases were searched until January 2023. The medical keyword term “cannabidiol” was combined with “pain”, “arthritis”, and “inflammation”. Based on the initial search for these terms, 9, 5, and 5 relevant publications have been selected. Based on the available data, it is not possible to draw a clear conclusion about the effect of CBD to relieve pain, because each study used a different route of administration or treatment regimen. The studies also differed in etiopathogenesis of pain (chronic, neuropathic, and possibly inflammatory pain), and in general included only small number of subjects. In case of anti-inflammatory qualities of CBD, its effect on the intestinal system is negligible. On the other hand, positive treatment results were observed in all publications dealing with the effect of CBD on arthritis.

This study was supported by the Charles University Cooperatio Program (research area PHAR) and grant No. SVV 260 638.

Mailing Address: Mgr. Michaela Sklenárová, Institute of Pharmacology, First Faculty of Medicine, Charles University and General University Hospital in Prague, Albertov 4, 128 00 Prague 2, Czech Republic; Phone: +420 224 968 163; e-mail: michaela.sklenarova@lf1.cuni.cz

Introduction

Cannabidiol (CBD) is the second most abundant component of the plant *Cannabis sativa* (Nahler et al., 2017). Nowadays, CBD substance is approved by regulatory authorities only for a few types of resistant epilepsies (Lennox-Gastaut and Dravet syndrome) and newly for tuberous sclerosis complex but is freely available in the form of food supplements. Typical oral forms (i.e., capsules) and parenteral forms can be encountered, but oral sublingual drops, sprays, or inhalation by aerosol, nebulizer, vapor, or cigarettes are also fairly common. The poor solubility of the compound in combination with significant first-pass effect cause low rate of gastrointestinal absorption (European Medicines Agency, 2023). On the other hand, CBD transport via the lymphatic system contributes significantly to the total drug exposure after peroral administration (Jelinek et al., 2022). Oral bioavailability has been described in range of 13–19% and can be notably increased by high-fat meal (Mechoulam et al., 2002; Lucas et al., 2018). The average bioavailability was 31% in 5 male participants after smoking (Ohlsson et al., 1986). CBD can be cumulated in adipose tissues. The metabolic pathways are mainly CYP2C19, CYP3A and uridine 5-diphosphate glucuronosyltransferase. The primary metabolite is the 7-OH-CBD metabolite, which is converted into 7-COOH-CBD metabolite (Lucas et al., 2018). It is not clear if CBD can convert to tetrahydrocannabinol (THC) in an acidic environment after dosing. There exists some evidence that acidic environments can support this transformation, but to date no *in vivo* experiments have confirmed this hypothesis (Wray et al., 2017). The elimination half-life ($t_{1/2}$) was 56 h (European Medicines Agency, 2023). Intravenous administration, smoking or chronic oral administration results in a longer $t_{1/2}$ of 24 hours, 31 hours, and 2–5 days, respectively (Ohlsson et al., 1986; Consroe et al., 1991). Major portion of CBD is excreted unchanged in the feces, while oxidized and glucuronidated metabolites are excreted via kidneys (Huestis, 2007; Ujvary and Hanus, 2016).

CBD influences a number of receptors. It is exogenous ligand that interact primarily with the endocannabinoid system, but the signaling is not completely understood (Pacher et al., 2020). CBD is negative allosteric modulator of cannabinoid receptors such as CB1 and CB2 (Laprairie et al., 2015; Cherkasova et al., 2022). CB1 receptors are primarily located in central nervous system compared to CB2 receptors (Ramirez et al., 2012). Some of the other most frequent targets of CBD include ligand-gated ion channels (NaV, GABAA), TRP channels (TRPV1, TRPV2, TRPA1, TRPM8), GPCRs (5-HT1A, α 1A, CB1, CB2, GPR18, GPR55), CYP450 enzymes, and nuclear receptors (PPAR γ) (Pertwee, 2005; Morales et al., 2017; Morales and Reggio, 2019). The complexity of CBD's interactions with its molecular targets suggests a very wide range of potential effects. Many of these have already been tested in various *in vitro/in vivo* and preclinical/clinical studies.

Because of that, this review aims to summarise the available evidence on the potential use of CBD in the treatment of inflammation and its symptoms.

Literature search

PubMed and Web of Science databases have been searched until January 2023. The medical subject headings term “cannabidiol” was combined with “pain”, “arthritis” and “inflammation” using Boolean operators in order to identify relevant references. Searches were limited only to original articles written in English. The search results for the term “pain” were limited only to articles dealing with inflammation-related pain. Finally, there were excluded studies testing the effects of CBD with combination with other medicine or using polycomponent mixtures of cannabinoids, except for mixtures in which the presence of substances with a majority of CBD was clearly declared.

There were 64, 68, and 481 results filtered based on the initial search for “pain”, “arthritis” and “inflammation” terms, respectively. Out of which 9, 5, and 5 relevant publications have been subsequently selected.

Effects of cannabidiol

Although THC has a similar molecular structure and sufficient affinity for both cannabinoid receptors (CB1 and CB2), CBD has only limited affinity (Pacher et al., 2020). Some studies in animal and human subjects have shown that the CB2 expression is the primary receptor that regulates the immunosuppressive effect release of pro-inflammatory cytokines including TNF α and Th1 helper response (Malfait et al., 2000; James, 2020). Several publications have demonstrated the potential anti-inflammatory effect of cannabinoids (Nagarkatti et al., 2009). Their mechanisms of action include activating receptors, inhibiting cytokines and cell proliferation, inducing apoptosis, etc. (Zurier and Burstein, 2016; Nichols and Kaplan, 2020). Human B cells, NK cells, neutrophils, CD8+ T cells, monocytes, and CD4+ T cells are expressed by CB1 and CB2. CB2 expressed changes correlated with inflammation. Arachidonic acid derivatives (2-arachidonylglycerol and anandamide) play the immunomodulatory role of CB2. Typically, CB2 stimulation decreases immune cell functions via intracellular signaling mechanisms, such as activation of mitogen-activated protein kinases and inhibition of adenylate cyclase activity by Gi/o proteins. In fact, CB2 can suppress the release of TNF-, IL-2, and IFN- from activated human peripheral lymphocytes and the synthesis of proinflammatory cytokines including TNF-, IL-6, and IL-8 in human macrophages and monocytes. Also, endocannabinoid synthesis is increased by toll-like receptor (TLR) activation, and cannabinoids decrease the TLR-induced inflammatory response (Pellati et al., 2018). Recent preclinical evidence suggests that CBD has anti-inflammatory, analgesic and antioxidant effects (Soliman et al., 2021). The anti-inflammatory effects of cannabinoids have been demonstrated in animal models of arthritis (Selvi et al., 2008). In animal models of arthritis, CBD provided pain relief and reduced inflammatory cell infiltration into the joint (Hammell et al., 2016). The reduction of neuropathic and cancer pain is known indications for the use of cannabinoids, and three cannabis-based drugs (Nabilone, Sativex

and Marinol) are used clinically for this purpose (Russo et al., 2007; Mucke et al., 2018).

Effects of cannabidiol in inflammation

As the publications to date on the effect of CBD on inflammation are very promising, several research groups are conducting further studies to demonstrate its effect in different tissues. Couch et al. (2017) used Caco-2 cultures and colonic samples from patients (bowel cancer [n=13], inflammatory bowel disease [n=6] or emergency appendectomies [n=6]). They observed that CBD prevented increase of cytokines in colonic samples and this effect were diminished by CB2 and TRPV1 anatagonists (Couch et al., 2017).

The anti-inflammatory effect of CBD and dexamethasone was also compared in another *in vitro* study. Inflammation was induced by lipopolysaccharide. Upon administering both substances, a similar effect was observed. However, the patterns of action differed substantially. CBD attenuated c-Jun N-terminal kinases phosphorylation levels, whereas dexamethazone attenuated only IκB kinase phosphorylation levels (Wang et al., 2022). According to a different, CBD has anti-arthritis activity and may help with joint inflammation particularly by reaching synovial fibroblasts in inflammatory disorders (Lowin et al., 2020). A low dose of CBD impacts the activity of G-proteins, which act as molecular switches transmitting signals from other stimuli to cells (De Petrocellis et al., 2011).

Two research groups tried to describe anti-inflammatory properties of CBD *in vivo* – in Institute of Cancer Research male mice and in rats (Borrelli et al., 2009; Jamontt et al., 2010). In the first study, the experimental colitis was induced in mice by dinitrobenzenesulfonic acid (DNBS) (intracolonic administration). In the second study, acute colitis in rats was induced by 2,4,6-trinitrobenzenesulfonic acid (TNBS). Both of studies observed reduction of proinflammatory interleukins. In rats, CBD not only reduced inflammation, but also reduced the incidence of functional disruptions.

The reduction of immune cell activation with CBD in the pancreatic microcirculation as well as lowering the risk of developing type 1 diabetes (T1D) was also demonstrated. These experiments show that untreated non-obese diabetic (NOD) mice developed T1D earlier (19.5 weeks) whereas CBD treated mice (24 weeks) (Lehmann et al., 2016). However, it should be remembered that T1D is a very specific type of inflammation.

In a clinical study, CBD was examined as an adjuvant to ongoing treatment for inflammatory bowel diseases. During the experiment, the disease activity was monitored as well as laboratory parameters during 8 weeks of treatment and 2 weeks after. Standard therapy was not changed. Totally, 19 of 20 patients completed the study. The effects of CBD were insignificant for Crohn's disease, but that could be caused by a small dosage of CBD, limited number of patients, or the lack of the necessary synergism with other cannabinoids (Naftali et al., 2017).

Table 1 – A summary of studies investigate effects of CBD on intestinal inflammation

References	Study sample (patient population, sample size, gender and age)	Treatment schedule	Study design	Conclusion
Borrelli et al. (2009)	male ICR mice (35–40 g), colitis was induced by the intracolonic administration of DNBS	CBD (1–10 mg/kg and 5 mg/kg) was injected once a day for 6 consecutive days starting 3 days before induction	disease-induced animal model	CBD reduced proinflammatory interleukins and the wet weight/colon length ratio of the inflamed tissue.
Jamontt et al. (2010)	wistar rats male induced acute colitis by TNBS	CBD were i.p. applied: 5, 10, 15 and 20 mg/kg (n=4, 6, 5 and 5, respectively) for vehicle group (n=11) sulphasalazine (n=7) was administered at 300 mg/kg p.o. One dose was given every 24 h during 3 days	disease-induced animal model	CBD not only reduced inflammation, but it also reduced the incidence of functional disruptions.
Naftali et al. (2017)	19 patients (11 men) (average 39 ± 15 years) with a Crohn's disease	per oral (10 mg) CBD/placebo twice a day. Test – 8 weeks of treatment and 2 weeks thereafter	randomized controlled	After 8 weeks of treatment, the index was very similar in the CBD and placebo groups CBD had no beneficial effects.
Lehmann et al. (2016)	19 seven-week-old female NOD mice	administered daily 5 mg/kg CBD/placebo i.p. 5 times a week for 10 weeks	disease-induced animal model	CBD-treated NOD mice exhibited substantially decreased leukocyte activation, and they also developed T1D later.
van Orten-Luiten et al. (2022)	32 female irritable bowel syndrome patients were randomized	chewing gum contain 50 mg CBD (max. 6 gums per day)	randomized, double-blinded, placebo-controlled cross-over	There were no group differences in pain scores or the number of gums used between CBD and placebo gum.

CBD – cannabidiol; ICR – Institute of Cancer Research; DNBS – dinitrobenzenesulfonic acid;

TNBS – trinitrobenzenesulfonic acid; NOD – non-obese diabetic

Also, we found publication where they focused on changing in glycemic and lipids metabolism after dosing CBD and others cannabinoids compare to placebo (Jadoon et al., 2016). The details about available studies are summarized in Table 1.

Effects of cannabidiol in arthritis

We evaluated 5 studies which met criteria for inclusion (Table 2). Two of these studies used a CBD extract, which included traceable amount of other substances. The study by Gamble et al. (2018) used extract contains low percentage of CBG, THC and other cannabinoids. The second research group – Heineman et al. (2022) – declared 99.07% pure isolate of CBD. Both these studies showed significant improvement in arthritis-related pain.

Similarly, to the previously mentioned studies, these groups administered CBD intraperitoneally and orally respectively. Based on Malfait's histological findings, we can confirm that optimal therapeutic effect has CBD at an i.p. dose of 5 mg/kg or an oral dose of 25 mg/kg. The therapeutic level of CBD is dose-dependent. According to their data, schematic administration can avoid the relapse of arthritis. Additionally, they examined the synovial cells, specifically before and after the administration of CBD. Synovial cell treated by CBD released significantly less TNF when cultivated *in vitro* (Malfait et al., 2000).

Effects of cannabidiol in inflammation-related pain

Pain management is a topic, where it is crucial to focus not only on the pain itself, but its origin. From the 64 found articles, we excluded cancer pain, palliative care, and pain caused by trauma. Due to these limitations, we were left with 9 publications, which we discuss below (Table 3).

In *in vitro* (human cells) and *in vivo* (mouse) models, CBD attenuated the production of proinflammatory cytokines IL-6 and TNF- α . These experiments were followed up by randomized, placebo-controlled veterinary study, when CBD significantly reduced pain and increased mobility in a dose-dependent manner in osteoarthritic dogs (Verrico et al., 2020).

Monosodium iodoacetate-induced osteoarthritis model in rats was used to assess the efficacy of CBD after intra-articular administration. CBD/placebo was administered in addition to using the CB1 receptor antagonist, the CB2 or the TRPV1 receptor antagonist. These three receptors are responsible for the anti-inflammatory and analgesic effects of CBD. The anti-inflammation effect of CBD arises from influencing only the CB2 and the TRPV1 receptor antagonist. Also, the binding of CBD to the TRPV1 receptor is responsible for the analgesic effect. Higher doses of CBD have only a local impact on secondary allodynia. Furthermore, in the acute phase of inflammation after CBD administration, a slowing of nerve demyelination versus placebo was observed on the 14th day after induction with monosodium iodoacetate (Philpott et al., 2017).

Table 2 – A summary of studies investigate effects of CBD on arthritis

References	Study sample (patient population, sample size, gender and age)	Treatment schedule	Study design	Conclusion
Malfait et al. (2000)	mices induced by model of murine CIA	p.o. applied – CBD doses were 10 mg/kg, 25 mg/kg, and 50 mg/kg (n=6 per group). Control group dose olive oil (n=6). Intraperitoneal administration – CBD – 20 mg/kg (n=12), 10 mg/kg (n=17), 5 mg/kg (n=15), and 2.5 mg/kg (n=9) and placebo (n=23)	disease-induced animal model	CBD was equally effective when administered i.p. or orally. The dose with an optimal effect at 5 mg/kg per day i.p. or 25 mg/kg per day orally. Clinical improvement was associated with the protection of the joints against severe damage.
Hammell et al. (2016)	54 rats were used in the experiments described here of which 21 were used as controls and 23 were subjected to adjuvant-induced arthritis	CBD gels (0.6, 3.1, 6.2 or 62.3 mg/day) were applied for 4 consecutive days after arthritis induction	parallel (control vs. disease-induced animal model)	Transdermal CBD gel with this dose significantly reduced joint swelling, limb posture scores as a rating of spontaneous pain, immune cell infiltration and thickening of the synovial membrane.
Jelinek et al. (2022)	14 rats with RA (induced by CIA)	7.5 mg of CBD per oral for 24 days	randomized, single-dose, laboratory-blinded	They observed the improvement of clinical parameters of RA after administration of CBD.
Gamble et al. (2018)	16 dogs diagnosed with osteoarthritis	CBD/placebo, 2 mg/kg every 12 h for 4 weeks. After 2-weeks of washouts period cross-over	randomized, placebo-controlled, owner and veterinarian double-blind, cross-over	Dogs were more comfortable and active when were treated by CBD.
Heineman et al. (2022)	18 participants with joint arthritis	treat by CBD twice a day 2 weeks (6.2 mg/ml CBD with shea butter) or placebo, followed by a 1-week washout period and then crossover	phase 2, double-blinded, randomized controlled	Topical CBD treatment showed a substantial reduction in associated disability and pain with specific joint arthritis.

CBD – cannabidiol; RA – rheumatoid arthritis; CIA – collagen-induced arthritis

CBD caused no clinical or statistically significant reduction of pain intensity in randomized, placebo-controlled study in 129 patients with osteoarthritis or psoriatic arthritis. For effect evaluation, primarily intensity of the pain (0–100 mm), but additionally Pittsburgh Sleep Quality Index, Hospital Anxiety and Depression Scale, Pain Catastrophizing Scale (PCS), and Health Assessment Questionnaire Disability Index were used. However, there are some notable limitations of this study. The patients absolved only 3 sessions with the doctors – first session where they were randomized, the second was made after 4 weeks via a phone call, and the last was made at the end of the study (after 12 weeks), and the dosage of CBD was 20–30 mg/day (Vela et al., 2022).

In contrast, Xu et al. (2020) reported that transdermal application of CBD can cause significant reduction in intense pain, sharp pain, and cold and itchy sensations in comparison with placebo. On the other hand, this study also has some limitations. The group of subjects is relatively small (n=29), and the pathology of examined diseases is heterogenous, which may affect the results. The final evaluation was done using a questionnaire and using the international scale for neuropatic pain (NPS) (Xu et al., 2020).

A balanced placebo design trial in healthy adults suggest that CBD and/or expectations for obtaining CBD can have a distinct effect on different pain outcomes. The notable limitations of this study are the fact that only a single dose of 50 mg CBD was used, and only a small group of young subjects were part of the trials (range 18–27 years) (De Vita et al., 2022).

Schneider et al. (2022) observed no significant effect of CBD on acute pain, hyperalgesia, and allodynia in comparison with placebo group. Similarly, to the previous study, the limitations include a single dose (although high), and relatively small sample of patients (Schneider et al., 2022).

Finally, CBD has not been shown to be superior to placebo as an adjunct medication for relief of acute non-traumatic back pain. Limitations of this study include application of only single dose of CBD, possible influence of analgesic medication used by patients before arrival, and also the verbal numerical pain scale may be biased by subjective evaluation (Bebbee et al., 2021).

Limitation of Wades study is variable range of CBDs dose (2.5–120 mg/24 hours). They also applied CBD extract which is not detailly described (Wade et al., 2003).

Conclusion

This review provides a structured summarization of available and published evidence on the effects of CBD in a range of examined diseases. Each research group used different formulations, routes of administration, treatment regimens, as well as different groups of subjects. These inconsistencies make it difficult to draw objective conclusions. Finally, we would also like to note that our review focused on studies examining CBD's effect on pain, which also used different etiopathogenesis of pain (e.g., chronic, neuropathic, or inflammatory pain).

Table 3 – A summary of studies investigate effects of CBD on pain

References	Study sample (patient population, sample size, gender and age)	Treatment schedule	Study design	Conclusion
Verrico et al. (2020)	spontaneous canine model of OA on mice	4-week liposomal CBD (20 mg/day) and nonliposomal CBD (50 mg/day)	randomized, double-blind, placebo-controlled study	CBD significantly decreased pain and increased mobility in a dose-dependent among animals. Liposomal CBD (20 mg/day) was as effective as the highest dose of nonliposomal CBD (50 mg/day) in clinical outcomes.
Philpott et al. (2017)	17 rats induced osteoarthritis by monosodium iodoacetate	administered i.artic.vehicle (50 ml) / CBD (100–300 mg/50 ml). In groups administered (s.c.) around joint the CB1 receptor antagonist (75 mg/50 ml) / the CB2 receptor antagonist (75 mg/50 ml) / the TRPV1 receptor antagonist (30 mg/50 ml)	disease-induced animal model	Local CBD therapy decreased acute, temporary joint inflammation. The early onset of pain and nerve damage in these OA joints was stopped by prophylactic CBD therapy. These results imply that CBD may be a secure and beneficial treatment for managing OA joint neuropathic pain.
Wade et al. (2003)	20 patient – 14 diagnoses of multiple sclerosis, 4 spinal cord injuries, 1 brachial plexus lesion with associated neuropathy, and 1 phantom limb pain following an amputation	2-week treatment periods range of 2.5–120 mg/24 hours	double-blinded, randomized placebo-controlled crossover study	Muscle spasms, spasticity, and bladder control did not improve statistically using CBD compared to placebo.
Vela et al. (2022)	129 patients randomized to CBD/placebo group	synthetic CBD 20 to 30 mg or placebo daily for 12 weeks	randomized, double-blind, placebo-controlled design	When compared to placebo, they found no clinically or statistically effects of CBD on pain intensity in individuals with hand osteoarthritis and psoriatic arthritis.
Xu et al. (2020)	29 patients (range 35–79 years, 37.9% females) with symptomatic peripheral neuropathy with different origin	250 mg of CBD per 3 fl. oz container, topical application 4 times a day during 4 weeks	double-blind, randomized placebo-controlled crossover	When compared to the placebo group, the CBD group saw a notable reduction in pain, cold, and itching feelings.

Haffar et al. (2022)	80 patients undergoing primary unilateral total knee arthroplasty applied topical CBD (CBD; n=19), essential oil (EO; n=21), CBD and essential oil (CBD + EO; n=21), or placebo (PLA; n=19) three times a day around the knee for two weeks postoperatively	CBD alone (group CBD), essential oils (group EO), CBD and essential oils (group CBD-EO), and placebo with no CBD or EO (group PLA)	randomized double-blinded placebo-controlled	No statistically significant differences existed for Visual Analogue Scale scores at other times.
De Vita et al. (2022)	15 healthy adults (between 18 and 27 years) each completed 4 separate experimental sessions	4 groups – control (told inactive-given inactive); expectancy (told active CBD-given inactive); drug (told inactive-given active CBD); and expectancy + drug (told active CBD-given active CBD). 50 mg of hemp-derived CBD isolate in a 0.3 ml oil solution administered sublingually via dropper	crossover, 2x2 factorial balanced placebo design	These results suggest that CBD and/or expectations for obtaining CBD can have a distinct effect on different pain outcomes.
Schneider et al. (2022)	20 healthy volunteers with acute pain model with intradermal electrical stimulation	single 800-mg orally administered CBD compared with placebo	randomized, placebo-controlled, double-blinded, crossover	When compared to a placebo, there was no significant difference in pain scores after CBD application. Also hyperalgesia and allodynia were not significantly different after CBD administration versus placebo.
Beebe et al. (2021)	100 patients with acute, non-traumatic low back pain (34–60 years), 56 men	400 mg of synthetic CBD or placebo	randomised, double blinded, placebo-controlled	The two-hour mean pain scores for both the CBD and placebo groups were comparable. The two groups reported adverse reactions and oxycodone use in the four hours before and after the four hours of administering CBD or a placebo were comparable.

CBD – cannabidiol; OA – osteoarthritis; EO – essential oil; PLA – placebo; s.c. – subcutaneously

After evaluating the effects of CBD on intestinal inflammation, it can be concluded that the positive effect is not proven beyond doubt. On the other hand, all available data suggest that CBD has a positive effect on joint inflammation (arthritis) and exhibits a reduction of pro-inflammatory markers.

Acknowledgements: Michaela Sklenárová wishes to acknowledge the support provided by Pharmaceutical Applied Research Centre (The PARC) for her scientific work.

References

- Bebee, B., Taylor, D. M., Bourke, E., Pollack, K., Foster, L., Ching, M., Wong, A. (2021) The CANBACK trial: A randomised, controlled clinical trial of oral cannabidiol for people presenting to the emergency department with acute low back pain. *Med. J. Aust.* **214**, 370–375.
- Borrelli, F., Aviello, G., Romano, B., Orlando, P., Capasso, R., Maiello, F., Guadagno, F., Petrosino, S., Capasso, F., Di Marzo, V., Izzo, A. A. (2009) Cannabidiol, a safe and non-psychotropic ingredient of the marijuana plant *Cannabis sativa*, is protective in a murine model of colitis. *J. Mol. Med. (Berl.)* **87**, 1111–1121.
- Cherkasova, V., Wang, B., Gerasymchuk, M., Fiselier, A., Kovalchuk, O., Kovalchuk, I. (2022) Use of cannabis and cannabinoids for treatment of cancer. *Cancers* **14**, 5142.
- Consroe, P., Laguna, J., Allender, J., Snider, S., Stern, L., Sandyk, R., Kennedy, K., Schram, K. (1991) Controlled clinical trial of cannabidiol in Huntington's disease. *Pharmacol. Biochem. Behav.* **40**, 701–708.
- Couch, D. G., Tasker, C., Theophilidou, E., Lund, J. N., O'Sullivan, S. E. (2017) Cannabidiol and palmitoylethanolamide are anti-inflammatory in the acutely inflamed human colon. *Clin. Sci. (Lond.)* **131**, 2611–2626.
- De Petrocellis, L., Ligresti, A., Moriello, A. S., Allara, M., Bisogno, T., Petrosino, S., Stott, C. G., Di Marzo, V. (2011) Effects of cannabinoids and cannabinoid-enriched Cannabis extracts on TRP channels and endocannabinoid metabolic enzymes. *Br. J. Pharmacol.* **163**, 1479–1494.
- De Vita, M. J., Maisto, S. A., Gilmour, C. E., McGuire, L., Tarvin, E., Moskal, D. (2022) The effects of cannabidiol and analgesic expectancies on experimental pain reactivity in healthy adults: A balanced placebo design trial. *Exp. Clin. Psychopharmacol.* **30**, 536–546.
- European Medicines Agency (2023) Epidyolex. Accessed March 27, 2023. Available at: https://www.ema.europa.eu/en/documents/product-information/epidyolex-epar-product-information_en.pdf
- Gamble, L. J., Boesch, J. M., Frye, C. W., Schwark, W. S., Mann, S., Wolfe, L., Brown, H., Berthelsen, E. S., Wakshlag, J. J. (2018) Pharmacokinetics, safety, and clinical efficacy of cannabidiol treatment in osteoarthritic dogs. *Front. Vet. Sci.* **5**, 165.
- Haffar, A., Khan, I. A., Abdelaal, M. S., Banerjee, S., Sharkey, P. F., Lonner, J. H. (2022) Topical cannabidiol (CBD) after total knee arthroplasty does not decrease pain or opioid use: A prospective randomized double-blinded placebo-controlled trial. *J. Arthroplasty* **37**, 1763–1770.
- Hammell, D. C., Zhang, L. P., Ma, F., Abshire, S. M., McIlwrath, S. L., Stinchcomb, A. L., Westlund, K. N. (2016) Transdermal cannabidiol reduces inflammation and pain-related behaviours in a rat model of arthritis. *Eur. J. Pain* **20**, 936–948.
- Heineman, J. T., Forster, G. L., Stephens, K. L., Cottler, P. S., Timko, M. P., DeGeorge, B. R. Jr. (2022) A randomized controlled trial of topical cannabidiol for the treatment of thumb basal joint arthritis. *J. Hand Surg. Am.* **47**, 611–620.
- Huestis, M. A. (2007) Human cannabinoid pharmacokinetics. *Chem. Biodivers.* **4**, 1770–1804.
- Jadoon, K. A., Ratcliffe, S. H., Barrett, D. A., Thomas, E. L., Stott, C., Bell, J. D., O'Sullivan, S. E., Tan, G. D. (2016) Efficacy and safety of cannabidiol and tetrahydrocannabinol on glycemic and lipid parameters in

- patients with type 2 diabetes: A randomized, double-blind, placebo-controlled, parallel group pilot study. *Diabetes Care* **39**, 1777–1786.
- James, S. (2020) *A Clinician's Guide to Cannabinoid Science, Chapter 9: Cannabinoids and Inflammation and Autoimmune Disorders*. Cambridge University Press, Cambridge.
- Jamontt, J. M., Molleman, A., Pertwee, R. G., Parsons, M. E. (2010) The effects of delta-tetrahydrocannabinol and cannabidiol alone and in combination on damage, inflammation and *in vitro* motility disturbances in rat colitis. *Br. J. Pharmacol.* **160**, 712–723.
- Jelinek, P., Rousarova, J., Rysanek, P., Jezkova, M., Havlujova, T., Pozniak, J., Kozlik, P., Krizek, T., Kucera, T., Sima, M., Slanar, O., Soos, M. (2022) Application of oil-in-water cannabidiol emulsion for the treatment of rheumatoid arthritis. *Cannabis Cannabinoid Res.* (Epub ahead of print)
- Laprairie, R. B., Bagher, A. M., Kelly, M. E. M., Denovan-Wright, E. M. (2015) Cannabidiol is a negative allosteric modulator of the cannabinoid CB1 receptor. *Br. J. Pharmacol.* **172**, 4790–4805.
- Lehmann, C., Fisher, N. B., Tugwell, B., Szczesniak, A., Kelly, M., Zhou, J. (2016) Experimental cannabidiol treatment reduces early pancreatic inflammation in type 1 diabetes. *Clin. Hemorheol. Microcirc.* **64**, 655–662.
- Lowin, T., Tingting, R., Zurmahr, J., Classen, T., Schneider, M., Pongratz, G. (2020) Cannabidiol (CBD): A killer for inflammatory rheumatoid arthritis synovial fibroblasts. *Cell Death Dis.* **11**, 714.
- Lucas, C. J., Galettis, P., Schneider, J. (2018) The pharmacokinetics and the pharmacodynamics of cannabinoids. *Br. J. Clin. Pharmacol.* **84**, 2477–2482.
- Malfait, A. M., Gallily, R., Sumariwalla, P. F., Malik, A. S., Andreakos, E., Mechoulam, R., Feldmann, M. (2000) The nonpsychoactive cannabis constituent cannabidiol is an oral anti-arthritic therapeutic in murine collagen-induced arthritis. *Proc. Natl. Acad. Sci. U. S. A.* **97**, 9561–9566.
- Mechoulam, R., Parker, L. A., Gallily, R. (2002) Cannabidiol: An overview of some pharmacological aspects. *J. Clin. Pharmacol.* **42**, 11s–19s.
- Morales, P., Reggio, P. H. (2019) CBD: A new hope? *ACS Med. Chem. Lett.* **10**, 694–695.
- Morales, P., Hurst, D. P., Reggio, P. H. (2017) Molecular targets of the phytocannabinoids: A complex picture. *Prog. Chem. Org. Nat. Prod.* **103**, 103–131.
- Mucke, M., Phillips, T., Radbruch, L., Petzke, F., Hauser, W. (2018) Cannabis-based medicines for chronic neuropathic pain in adults. *Cochrane Database Syst. Rev.* **3**, CD012182.
- Naftali, T., Mechulam, R., Marii, A., Gabay, G., Stein, A., Bronshtain, M., Laish, I., Benjaminov, F., Konikoff, F. M. (2017) Low-dose cannabidiol is safe but not effective in the treatment for Crohn's disease, a randomized controlled trial. *Dig. Dis. Sci.* **62**, 1615–1620.
- Nagarkatti, P., Pandey, R., Rieder, S. A., Hegde, V. L., Nagarkatti, M. (2009) Cannabinoids as novel anti-inflammatory drugs. *Future Med. Chem.* **1**, 1333–1349.
- Nahler, G., Grotenhermen, F., Zuardi, A. W., Crippa, J. A. S. (2017) A conversion of oral cannabidiol to delta9-tetrahydrocannabinol seems not to occur in humans. *Cannabis Cannabinoid Res.* **2**, 81–86.
- Nichols, J. M., Kaplan, B. L. F. (2020) Immune responses regulated by cannabidiol. *Cannabis Cannabinoid Res.* **5**, 12–31.
- Ohlsson, A., Lindgren, J. E., Andersson, S., Agurell, S., Gillespie, H., Hollister, L. E. (1986) Single-dose kinetics of deuterium-labelled cannabidiol in man after smoking and intravenous administration. *Biomed. Environ. Mass Spectrom.* **13**, 77–83.
- Pacher, P., Kogan, N. M., Mechoulam, R. (2020) Beyond THC and endocannabinoids. *Annu. Rev. Pharmacol. Toxicol.* **60**, 637–659.
- Pellati, F., Borgonetti, V., Brighenti, V., Biagi, M., Benvenuti, S., Corsi, L. (2018) *Cannabis sativa* L. and nonpsychoactive cannabinoids: Their chemistry and role against oxidative stress, inflammation, and cancer. *Biomed Res. Int.* **2018**, 1691428.

- Pertwee, R. G. (2005) Inverse agonism and neutral antagonism at cannabinoid CB1 receptors. *Life Sci.* **76**, 1307–1324.
- Philpott, H. T., O'Brien, M., McDougall, J. J. (2017) Attenuation of early phase inflammation by cannabidiol prevents pain and nerve damage in rat osteoarthritis. *Pain* **158**, 2442–2451.
- Ramirez, S. H., Hasko, J., Skuba, A., Fan, S., Dykstra, H., McCormick, R., Reichenbach, N., Krizbai, I., Mahadevan, A., Zhang, M., Tuma, R., Son, Y. J., Persidsky, Y. (2012) Activation of cannabinoid receptor 2 attenuates leukocyte-endothelial cell interactions and blood-brain barrier dysfunction under inflammatory conditions. *J. Neurosci.* **32**, 4004–4016.
- Russo, E. B., Guy, G. W., Robson, P. J. (2007) Cannabis, pain, and sleep: Lessons from therapeutic clinical trials of Sativex, a cannabis-based medicine. *Chem. Biodivers.* **4**, 1729–1743.
- Schneider, T., Zurbriggen, L., Dieterle, M., Mauermann, E., Frei, P., Mercer-Chalmers-Bender, K., Ruppen, W. (2022) Pain response to cannabidiol in induced acute nociceptive pain, allodynia, and hyperalgesia by using a model mimicking acute pain in healthy adults in a randomized trial (CANAB I). *Pain* **163**, e62–e71.
- Selvi, E., Lorenzini, S., Garcia-Gonzalez, E., Maggio, R., Lazzarini, P. E., Capecchi, P. L., Balistreri, E., Spreafico, A., Niccolini, S., Pompella, G., Natale, M. R., Guideri, F., Laghi Pasini, F., Galeazzi, M., Marcolongo, R. (2008) Inhibitory effect of synthetic cannabinoids on cytokine production in rheumatoid fibroblast-like synoviocytes. *Clin. Exp. Rheumatol.* **26**, 574–581.
- Soliman, N., Haroutounian, S., Hohmann, A. G., Krane, E., Liao, J., Macleod, M., Segelcke, D., Sena, C., Thomas, J., Vollert, J., Wever, K., Alaverdyan, H., Barakat, A., Barthlow, T., Bozer, A. L. H., Davidson, A., Diaz-delCastillo, M., Dolgorukova, A., Ferdousi, M. I., Healy, C., Hong, S., Hopkins, M., James, A., Leake, H. B., Malewicz, N. M., Mansfield, M., Mardon, A. K., Mattimoe, D., McLoone, D. P., Noes-Holt, G., Pogatzki-Zahn, E. M., Power, E., Pradier, B., Romanos-Sirakis, E., Segelcke, A., Vinagre, R., Yanes, J. A., Zhang, J., Zhang, X. Y., Finn, D. P., Rice, A. S. C. (2021) Systematic review and meta-analysis of cannabinoids, cannabis-based medicines, and endocannabinoid system modulators tested for antinociceptive effects in animal models of injury-related or pathological persistent pain. *Pain* **162**, S26–S44.
- Ujvary, I., Hanus, L. (2016) Human metabolites of cannabidiol: A review on their formation, biological activity, and relevance in therapy. *Cannabis Cannabinoid Res.* **1**, 90–101.
- van Orten-Luiten, A. B., de Roos, N. M., Majait, S., Witteman, B. J. M., Witkamp, R. F. (2022) Effects of cannabidiol chewing gum on perceived pain and well-being of irritable bowel syndrome patients: A placebo-controlled crossover exploratory intervention study with symptom-driven dosing. *Cannabis Cannabinoid Res.* **7**, 436–444.
- Vela, J., Dreyer, L., Petersen, K. K., Arendt-Nielsen, L., Duch, K. S., Kristensen, S. (2022) Cannabidiol treatment in hand osteoarthritis and psoriatic arthritis: A randomized, double-blind, placebo-controlled trial. *Pain* **163**, 1206–1214.
- Verrico, C. D., Wesson, S., Konduri, V., Hofferek, C. J., Vazquez-Perez, J., Blair, E., Dunner, K. Jr., Salimpour, P., Decker, W. K., Halpert, M. M. (2020) A randomized, double-blind, placebo-controlled study of daily cannabidiol for the treatment of canine osteoarthritis pain. *Pain* **161**, 2191–2202.
- Wade, D. T., Robson, P., House, H., Makela, P., Aram, J. (2003) A preliminary controlled study to determine whether whole-plant cannabis extracts can improve intractable neurogenic symptoms. *Clin. Rehabil.* **17**, 21–29.
- Wang, Y., Wang, X., Yang, Y., Quan, Q., Huo, T., Yang, S., Ju, R., An, Q. (2022) Comparison of the *in vitro* anti-inflammatory effect of cannabidiol to dexamethasone. *Clin. Cosmet. Investig. Dermatol.* **15**, 1959–1967.
- Wray, L., Stott, C. G., Jones, N. A., Wright, S. (2017) Cannabidiol does not convert to Δ^9 -tetrahydrocannabinol in an *in vivo* animal model. *Cannabis Cannabinoid Res.* **2**, 282–287.

- Xu, D. H., Cullen, B. D., Tang, M., Fang, Y. (2020) The effectiveness of topical cannabidiol oil in symptomatic relief of peripheral neuropathy of the lower extremities. *Curr. Pharm. Biotechnol.* **21**, 390–402.
- Zurier, R. B., Burstein, S. H. (2016) Cannabinoids, inflammation, and fibrosis. *FASEB J.* **30**, 3682–3689.

Effect of Convalescent Plasma Therapy on Mortality and Viral Load in Severely Ill Patients with COVID-19

**Jan Moravec¹, Martin Müller¹, Petr Turek², Michal Moravec¹,
Tomáš Nejtek¹, Roman Zazula¹**

¹Department of Anesthesiology and Intensive Care, First Faculty of Medicine, Charles University and Thomayer University Hospital, Prague, Czech Republic;

²Department of Blood Transfusion, Thomayer University Hospital, Prague, Czech Republic

Received February 27, 2023; Accepted August 27, 2023.

Key words: Severe COVID-19 – Convalescent plasma – Viral load

Abstract: The use of convalescent plasma (CP) appeared to be a promising, easily available and safe way of treatment of severe COVID-19 at the onset of the pandemic in early 2020. Conducted in 2020 and 2021, our study of 52 severely to critically ill COVID-19 patients who received CP plasma as a treatment and of 97 controls found no difference in 30-day or 90-day mortality rates. A significant viral load drop in most patients (4.7 log₁₀ [p<0.001] copies/ml) was observed following CP administration. Retrospective analysis of selected inflammatory markers and immunoglobulins showed higher C-reactive protein levels among the study group, and their decrease on Day 7.

This study was supported by the Ministry of Health of the Czech Republic, grant no. NU22-A-123, and by MH CZ – DRO (Thomayer University Hospital – TUH, 00064190).

Mailing Address: Jan Moravec, MD., Department of Anesthesiology and Intensive Care, First Faculty of Medicine, Charles University and Thomayer University Hospital, Vídeňská 800, 140 59 Prague 4, Czech Republic; e-mail: jan.moravec@ftn.cz

Introduction

The history of convalescent plasma (CP)/serum therapy goes back to administration of horse serum for diphtheria in the 1890s (Behring, 1890; Bracha and Tan, 2011). The first widespread use of CP as a therapy came with the 1918 Spanish influenza pandemic caused by the A/H1N1 virus. A later meta-analysis found a lower mortality risk in patients infected with the Spanish influenza who later developed pneumonia and received CP treatment (Luke et al., 2006). Prior to introduction of antibiotics, convalescent serum obtained from immunized animals was widely used to battle serious bacterial infections. The antibiotic boom after the Second World War substantially reduced clinical use of CP therapy.

The novel COVID-19 disease brought CP into the spotlight of therapeutic options in the early pandemic. The use of plasma collected from recovered patients seemed to be a feasible, readily available and safe treatment.

Those who have recovered from COVID-19 produce and increase the levels of specific antibodies within three weeks following the onset of the first symptoms. Initially, IgM and IgA antibodies are created, followed by IgG antibodies about a week later. The IgM and IgA levels begin to fall after three weeks since the first symptoms occurred. The protective effect of IgG antibodies lasts longer: their levels decrease after about six months. Nevertheless, there is a high inter-individual variability in both the serum levels and production length for each antibody type (Mallano et al., 2022).

These antibodies can help neutralize the virus and modify the inflammatory response. Therefore, the use of COVID-19 convalescent plasma containing anti-SARS-CoV-2 antibodies was considered a suitable experimental therapy for this disease (Wang et al., 2020).

Material and Methods

Approved by the Ethical Committee of the Institute for Clinical and Experimental Medicine and the Thomayer University Hospital and conducted at the DAIC (Department of Anesthesiology and Intensive Care, First Faculty of Medicine, Charles University and Thomayer University Hospital), our study researched and evaluated experimental treatment of severely ill COVID-19 inpatients with CP collected from recovered donors. The patients received two transfusion units of CP (approx. 200–250 ml each) from different donors. The study protocol reflected the expert guidelines of CSARIM (Czech Society for Anesthesiology, Resuscitation and Intensive Medicine) (Balík et al., 2020). The patients signed a consent about the nature and the extent of proposed plasma therapy, laboratory parameters to be monitored and expected benefits and risks of the study. Where the informed consent could not be obtained from the patients, it was signed by a closed relative.

The anti-SARS-CoV-2 convalescent plasma was collected in three large hospitals, all of them located in the Czech capital of Prague (Thomayer University Hospital, Institute of Haematology and Blood Transfusion, and General University Hospital in

Prague). The plasma donation was mandated by complete recovery from laboratory-confirmed COVID-19, at least 14 days since recovery or end of isolation/quarantine, good general health, eligibility and standard requirements for blood donation (Turek, 2020).

Given the urgency of the situation, the presence of anti-SARS-CoV-2 antibodies in the CP was only confirmed by a rapid test (by Innovita) before its administration to the first 4 patients. The plaque reduction neutralization test (virus neutralisation test) and IgG/IgA ELISA test to determine the levels of antibodies were taken subsequently. The plaque reduction neutralization tests were performed at the Central Military Health Institute, Těchonín, Czech Republic.

Plaque reduction neutralization test: to determine antibody titer, the plasma sample is incubated in different diluted concentrations with a standard concentration of virus suspension, and subsequently added to the cell culture. The pathogens that have not been neutralized by the antibodies then infect the cells. The result is read under microscope as the cytopathic effect of the virus. A negative result means a lower antibody titer in the sample than the dilution.

Specific antibody levels: simultaneously with the plaque reduction neutralization test, the levels of IgG anti-SARS-CoV-2 antibodies were measured at the Thomayer University Hospital and the Institute of Haematology and Blood Transfusion using the ELISA test (by Euroimmun, Lübeck, Germany), which contains the recombinant S1 spike protein domain and intern calibrator allowing for a semi-quantitative reading. A later comparison showed a correlation between the neutralization test and the ELISA test results (Figure 1) (Turek et al., 2020). From November 2020, only CP with a COVID-IgG index value > 3.7 , and from January 2021, only CP with a COVID-IgG levels > 80 BAU (binding antibody units)/ml (equivalent to an index value of approx. 4.5) were administered to patients.

Viral load: a sample of nasopharyngeal swab or tracheal aspirate culture was taken before the first CP transfusion to establish the SARS-CoV-2 viral load using the real-

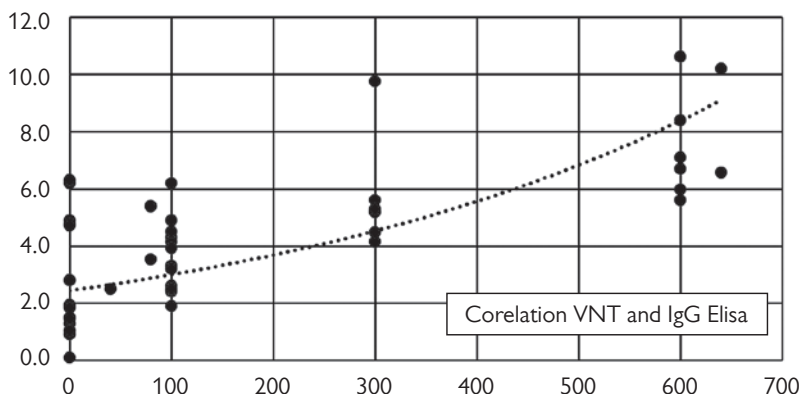


Figure 1 – ELISA virus neutralisation test.

Table 1 – COVID-19 severity by NIH

Severity	Definition by NIH
Asymptomatic or presymptomatic infection	PCR SARS-CoV-2 positivity without any symptoms.
Mild illness	Patients with mild illness may exhibit a variety of signs and symptoms (e.g., fever, cough, sore throat, malaise, headache, muscle pain, nausea, vomiting, diarrhea, loss of taste and smell). They do not have shortness of breath, dyspnea on exertion, or abnormal imaging.
Moderate illness	Moderate illness is defined as evidence of lower respiratory disease during clinical assessment or imaging, with SpO ₂ ≥ 94% on room air at sea level.
Severe illness	Patients with COVID-19 are considered to have severe illness if they have SpO ₂ < 94% on room air at sea level, PaO ₂ /FiO ₂ < 300 mm Hg, a respiratory rate > 30 breaths/min, or lung infiltrates > 50%.
Critical illness	Acute respiratory distress syndrome, virus-induced distributive (septic) shock, cardiac shock, an exaggerated inflammatory response, thrombotic disease, and exacerbation of underlying comorbidities caused by SARS-CoV-2 infection.

Coronavirus Disease 2019 (COVID-19) Treatment Guidelines
 NIH – National Institutes of Health

time PCR technique (RT-PCR). The second RT-PCR test was performed on Day 7 following the CP application. Viral load was not measured in the control group due to technical and logistic reasons.

Study population: the study group consisted of DAIC patients with severe or critical illness as defined by the National Institutes of Health (NIH) Guidelines (Table 1) (Coronavirus Disease 2019 [COVID-19] Treatment Guidelines). The control group comprised severely and critically ill patients who were admitted in our department in the same time period and received the same treatment as the study group except CP therapy.

The primary outcome of our study was 30-day and 90-day mortality rates in both groups. As the secondary outcome, we evaluated the non-specific immunoglobulin levels (IgA, IgM, IgG), inflammatory parameters (C-reactive protein – CRP, procalcitonin – PCT, and interleukin 6 – IL-6), leucocytes and their populations (neutrophils, lymphocytes and neutrophil-to-lymphocyte ratio – NLR). The blood samples were taken before CP administration and on Day 7. In the control group the tests were taken on the admission day, and on Day 7 intensive care unit (ICU) stay.

The statistic comparison of the discrete data was performed by Pearson's chi-squared test with Yates' correction for continuity. The effect of CP on the development of the individual parameters under observation was tested by a linear mixed effect model. R software, version 4.1.3 (Vienna, Austria), with the RStudio

interface was used for the statistical analysis. Statistically significant was considered $p < 0.05$.

Results

From April 2020 to March 2021, CP was administered to 52 patients hospitalised at DAIC with PCR confirmed COVID-19, bilateral viral pneumonia and respiratory failure requiring treatment with either high flow oxygen therapy, non-invasive ventilation or mechanical ventilation. One patient was treated solely with conventional oxygen therapy. 50 patients obtained 2 transfusion units of CP from different donors, with a minimum interval of 2 hours between each unit. 2 patients only received one transfusion unit (due to a transfusion-associated circulatory reaction in 1 patient, and a critical condition following cardiopulmonary resuscitation with a very poor prognosis in another patient). Along with CP, the patients were treated with low molecular weight heparin and systemic corticosteroids. Further medication, which reflected the current knowledge and drug availability at the time, is included in Table 2. The average age of patients treated with CP was 65.2 ± 13.3 years (average age \pm standard deviation). There were 37 men (71%) and 15 women (29%) in the study group.

Out of the 97 patients in the control group, 95 required either high flow oxygen therapy or non-invasive ventilation or mechanical ventilation, 2 patients received only conventional oxygen therapy. The average age of controls was 67.5 ± 10.7 years. There were 64 men (66%) and 33 women (34%) in the control group.

The data on 30-day and 90-day mortality rates were obtained from all patients both in the study and control group. 30-day mortality among CP-treated patients was 40.4%, and 48.5% in control group (Figure 2). 90-day mortality was 55.8% in the study group and 56.7% among controls (Figure 3). No statistically significant difference was found in both 30-day mortality ($p=0.44$) and 90-day mortality ($p=1$).

Table 2 – Overview of medication

Treatment	Number of patients receiving in study group	Number of patients receiving in control group
Low molecular weight heparin	52 (100%)	97 (100%)
Systemic corticotherapy	52 (100%)	94 (97%)
Remdesivir	29 (56%)	32 (33%)
Favipiravir	5 (10%)	19 (20%)
Hydroxychloroquine + isoprinosine	3 (6%)	0
Remdesivir + ivermectin	2 (4%)	2 (2%)
Favipiravir + ivermectin	2 (4%)	1 (1%)
Remdesivir + isoprinosine	1 (2%)	0
Ivermectin + isoprinosine	1 (2%)	0
Baricitinib	0	2 (2%)

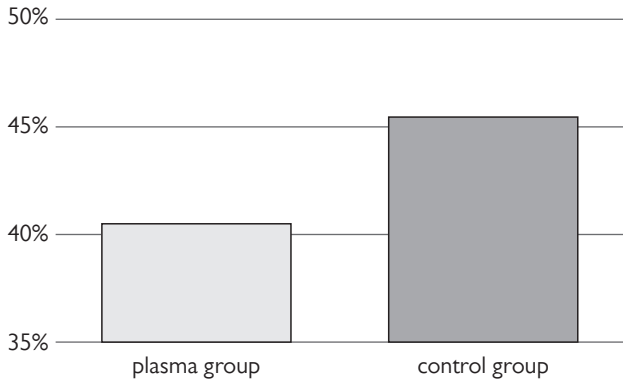


Figure 2 – 30-day mortality.

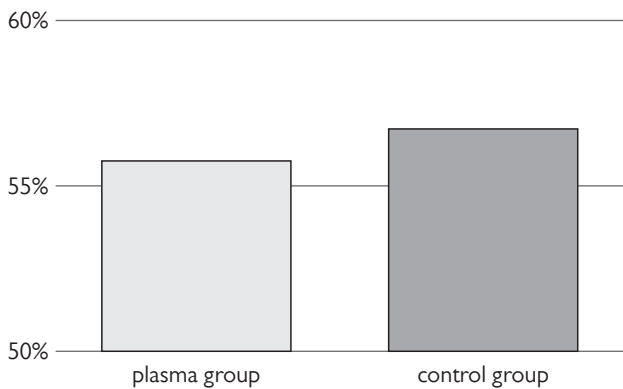


Figure 3 – 90-day mortality.

The median value (first quartile; third quartile) of length of hospital stay was 16.0 (10.8; 24.0) days in the study group. In the control group, the length of hospital stay was only 13.0 (8.0; 19.0) days. The difference in the length of hospital stay between the study and control groups is borderline statistically significant ($p=0.04$).

The median length of mechanical ventilation was 284 (155; 485) hours in the study group, and 262 (151; 347) hours in the control group. The difference in the length of mechanical ventilation was not statistically significant ($p=0.053$).

Complete data on viral load were obtained from 28 patients: their levels dropped in 23 patients, rose in 4 of them, and remained unchanged in 1 patient. 11 patients became PCR SARS-CoV-2 negative on Day 7. On average, the viral load decreased by 4.7 \log_{10} ($p<0.001$) copies/ml over the 7 days following CP administration (Figure 4).

A comparison was made between the levels of inflammatory markers measured in the study and control groups on T 0 (patient's admission to DAIC, that is, before CP administration), and on Day 7 (eighth day of ICU stay). The following data are presented as median values (first quartile; third quartile).

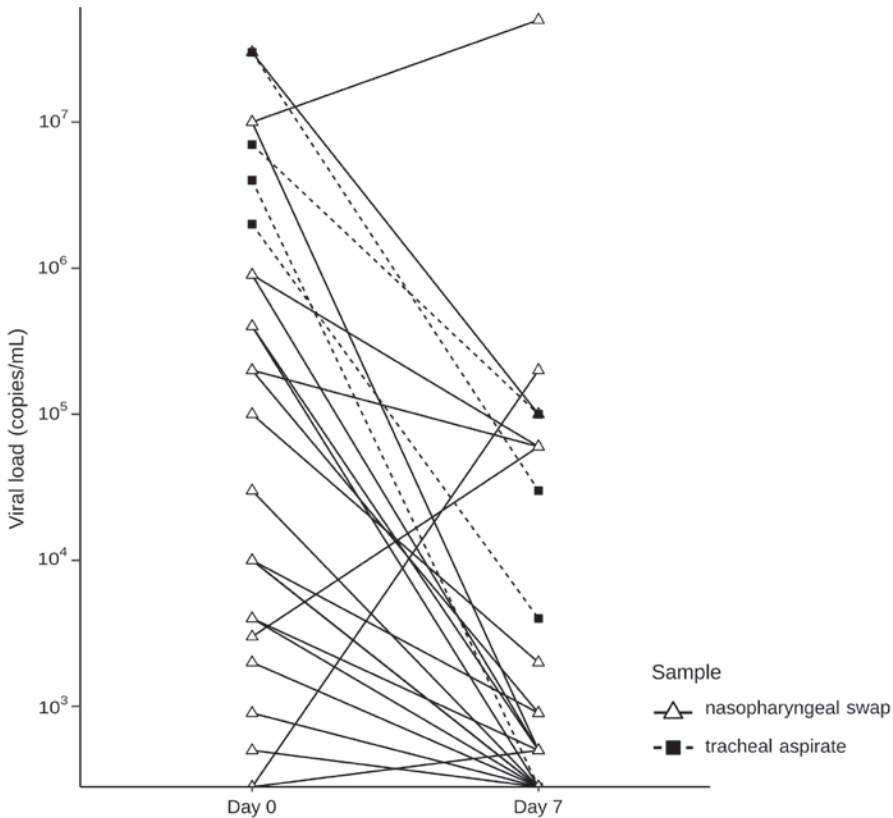


Figure 4 – Viral load over time.

Complete data on C-reactive protein values were obtained on T 0 from all patients, on Day 7 the data is missing from 11 patients in the study group and from 22 patients in the control group. On the admission day, the CRP levels were significantly higher in the study group – 171.9 (113.5; 234.9) mg/l, than in the control group – 113.2 (41.0; 157.0) mg/l, $p < 0.001$. On Day 7, the CRP levels were lower in the study group – 83.6 (21.4; 134.0) mg/l, compared to the control group – 98.1 (21.8; 134.4) mg/l, with an average decrease of 74.1 mg/l ($p < 0.001$) in the study group. Among the controls, the decrease in the CRP levels was insignificant ($p = 0.26$) (Figure 5).

We also compared the procalcitonin levels, which, however, did not show any significant difference between the groups on T 0, nor was there any significant change in PCT levels on Day 7.

A significantly lower level of leucocytes was found in the study group on T 0 ($p = 0.009$). On Day 7, however, the change in the leucocyte levels was insignificant both in the study and control group (Figure 6).

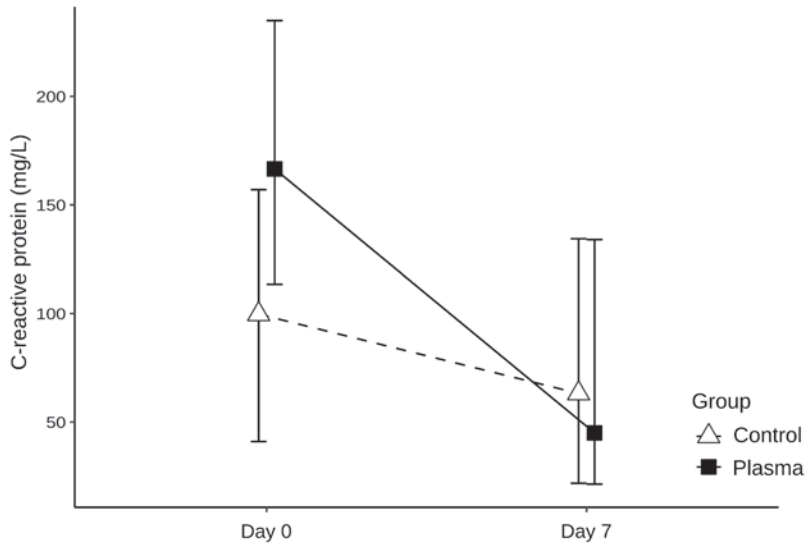


Figure 5 – C-reactive protein.

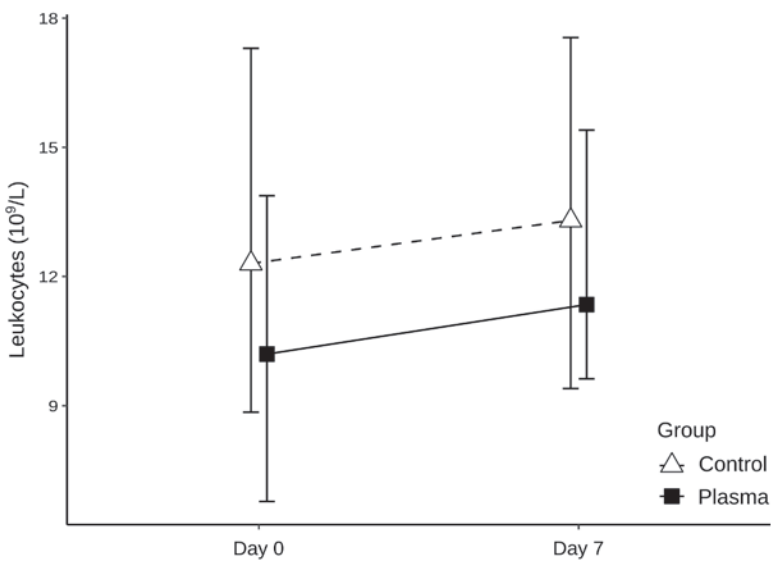


Figure 6 – Leukocytes.

A comparison was made of leucocyte populations, namely lymphocytes. No significant difference was found in the absolute number of lymphocytes between the groups, whether on T 0 or on Day 7.

Another potentially interesting inflammatory marker that we evaluated was neutrophil-to-lymphocyte ratio (NLR), the high levels of which are associated with

higher mortality (Vafadar Moradi et al., 2021). We did not find any statistically significant difference in the NLR levels between the study and control groups either on T 0 or on Day 7.

We also chose to examine the levels of individual immunoglobulins (IgA, IgM, and IgG) as potentially interesting markers of antibody immunity response. Despite a rise in the IgM levels among the controls on Day 7, we found no statistically significant difference between the groups ($p=0.07$). The IgA and IgG levels showed no significant difference between the groups both on Day 0 and Day 7.

Discussion

At the turn of spring 2020, the world, was hit by the COVID-19 pandemic. With the speed of the pandemic onset, it was necessary to prepare the inpatient wards for a surge of patients requiring an isolation regime, and also actively search the available resources for methods to treat the novel disease. Convalescent plasma appeared to be a relatively quickly available, proven and inexpensive option for treatment. Our hospital was among the first ones in the Czech Republic to use convalescent plasma as a treatment of COVID-19 patients. Before the first administration of CP, a study protocol was designed to allow for a retrospective analysis of the CP efficacy.

Despite the well-known complications of blood plasma transfusion as such, a serious adverse reaction (hypotension) only occurred in one out of 102 CP administrations. None of the patients developed a circulatory overload that would lead to heart failure, allergic or anaphylactic reaction, transfusion-related acute lung injury, haemolytic reaction or transfusion-related infection. Although our study did not prove the CP efficacy, it also did not prove to be harmful for the patients and increase morbidity and/or mortality.

Owing to the limited availability of CP and logistic obstacles of the plaque reduction test in the early pandemic, some patients received CP without establishing its titer value from neutralisation effect. Subsequent tests revealed a low antibody titer in several CP units that had been administered, which could have been the other potential confounding factor for non-superiority of CP over standard treatment (see Methods above).

The crucial limitation of our study is the absence of data on the dynamics of viral load in the control group. Its comparison with the data on the study group could have revealed the effect of CP on the clearance of the virus. On a sample of 231 patients, Fajnzylber et al. (2020) showed a viral load median value of 4.4 log₁₀ in sputum, and its decrease over time in most patients both in sputum and nasopharyngeal swab. However, a systematic review on viral load and disease severity by Dadras et al. (2022) found that even relationship between COVID-19 severity and viral load is inconclusive.

The other limitation of the study is the absence of randomisation. At the time of the study, the indication criteria for administration were based on the expert

guidelines of CSARIM, therefore only patients with a severe course were included in the study in accordance with the guidelines (Balík et al., 2020).

There are probably several reasons for the unsatisfactory outcome of CP treatment. One of them might be timing: CP was applied to patients who already required high flow oxygen therapy or ventilatory support and their illness has reached an advanced stage where the inflammation was difficult to control. Some studies describe the cytokine-storm rather than the direct cytopathogenic effect of SARS-CoV-2 to be the primary factor of the tissue damage and respiratory failure (Yang et al., 2021). According to some studies, application of a different immunomodulation treatment, namely IL-6 inhibitor (e.g., tocilizumab), leads to a better prognosis and shorter hospitalisation (RECOVERY Collaborative Group, 2021), while other studies have not proven its effect on mortality rate (Rosas et al., 2021).

Despite that the fact, that there is currently no evidence for benefit of CP therapy for COVID-19, which was also the conclusion of our study, there are still weak recommendation for use a CP (Coronavirus Disease 2019 [COVID-19] Treatment Guidelines) and some studies suggested a potential benefit for immunocompromised patients when administrated early (Writing Committee for the REMAP-CAP Investigators et al., 2021; Denkinger et al., 2023) and CP holds the potential to evolve in real-time with virus and retain activity against new variants unlike monoclonal antibodies.

Conclusion

Despite the statistically insignificant difference in 30-day mortality, the 90-day mortality rate was practically the same in both groups.

This finding corresponds with the outcomes of other large multicentric studies (Bégin et al., 2021; Writing Committee for the REMAP-CAP Investigators et al., 2021).

The viral load decrease following CP treatment was evident in most patients, but it could have been caused by many factors, and its evaluation would require comparison with the control group.

At the onset of the COVID-19 pandemic, convalescent plasma appeared to be a promising treatment with the unavailability of targeted therapy and rapid growth in the patients' numbers. Today, the therapeutic potential of convalescent plasma seems to be minimal. Currently, there is an array of accessible antiviral drugs, monoclonal antibodies and immunomodulatory agents. Although CP administration did not result in better clinical outcome, it was not harmful for the patients (did not increase mortality). According to the NIH, CP therapy is not recommended for immunocompetent patients anymore (Coronavirus Disease 2019 [COVID-19] Treatment Guidelines). According to the multidisciplinary expert position of CSARIM, CP therapy is not recommended for patients receiving any ventilation support or on high flow oxygen therapy (Bohoněk et al., 2021).

References

- Balík, M., Bohoněk, M., Černý, V., Holub, M., Kümpel, P., Plíšek, S., Roháčová, H. (2020) Doporučení postup pro použití rekonvalescentní plazmy v léčbě dospělých pacientů s COVID-19. *Česká Společnost Anesteziologie, Resuscitace a Intenzivní Medicíny ČLS JEP*. Available at: https://www.csarim.cz/getmedia/975c0db9-cc03-4b15-812a-377d41713e61/08_dp_covid_stl_csarim_sil_rekonvalesc_plazma_300420_2.pdf.aspx (Accessed 12. 12. 2022)
- Bégin, P., Callum, J., Jamula, E., Cook, R., Heddle, N. M., Timmouth, A., Zeller, M. P., Beaudoin-Bussièeres, G., Amorim, L., Bazin, R., Loftsgard, K. C., Carl, R., Chassé, M., Cushing, M. M., Daneman, N., Devine, D. V., Dumaresq, J., Fergusson, D. A., Gabe, C., Glesby, M. J., Li, N., Liu, Y., McGeer, A., Robitaille, N., Sachais, B. S., Scales, D. C., Schwartz, L., Shehata, N., Turgeon, A. F., Wood, H., Zarychanski, R., Finzi, A.; CONCOR-1 Study Group; Arnold, D. M. (2021) Convalescent plasma for hospitalized patients with COVID-19: An open-label, randomized controlled trial. *Nat. Med.* **27**, 2012–2024.
- Behring, E. A. (1890) Untersuchungen über das Zustandekommen der Diphtherie-Immunität bei Thieren. *Dtsch. Med. Wochenschr.* **1890**, 1145–1148.
- Bohoněk, M., Černý, V., Holub, M., Dlouhý, P., Vašáková, M. (2021) Mezioborové stanovisko (evidenční číslo ČSARIM: 18/2021) k podávání rekonvalescentní plazmy u pacientů s COVID-19. *Česká Společnost Anesteziologie, Resuscitace a Intenzivní Medicíny ČLS JEP*. Available at: https://www.csarim.cz/getmedia/0d4a80ec-41de-459b-aa2c-1f6a2f1042a5/2021_PP_18_CSARIM_STL_SIL_CPFS_Rekonv_plazma_final_020321.pdf
- Bracha, A., Tan, S. Y. (2011) Emil von Behring (1854–1917): Medicine's first Nobel laureate. *Singapore Med. J.* **52**, 1–2.
- Coronavirus Disease 2019 (COVID-19) Treatment Guidelines. *NIH COVID-19 Treatment Guidelines*. Available at: <https://files.covid19treatmentguidelines.nih.gov/guidelines/covid19treatmentguidelines.pdf>
- Dadras, O., Afsahi, A. M., Pashaei, Z., Mojdeganlou, H., Karimi, A., Habibi, P., Barzegary, A., Fakhfourli, A., Mirzapour, P., Janfaza, N., Dehghani, S., Afroughi, F., Dashti, M., Khodaei, S., Mehraeen, E., Voltarelli, F., Sabatier, J.-M., SeyedAlinaghi, S. (2022) The relationship between COVID-19 viral load and disease severity: A systematic review. *Immun. Inflamm. Dis.* **10**, e580.
- Denkinger, C. M., Janssen, M., Schäkel, U., Gall, J., Leo, A., Stelmach, P., Weber, S. F., Krisam, J., Baumann, L., Stermann, J., Merle, U., Weigand, M. A., Nussbag, C., Bullinger, L., Schrezenmeier, J.-F., Bornhäuser, M., Alakel, N., Witzke, O., Wolf, T., Vehreschild, M. J. G. T., Schmiedel, S., Addo, M. M., Herth, F., Kreuter, M., Tepas, P.-R., Hertenstein, B., Hänel, M., Morgner, A., Kiehl, M., Hopfer, O., Wattad, M.-A., Schimanski, C. C., Celik, C., Pohle, T., Ruhe, M., Kern, W. V., Schmitt, A., Lorenz, H.-M., Souto-Carneiro, M., Gaeddert, M., Halama, N., Meuer, S., Kräusslich, H.-G., Müller, B., Schnitzler, P., Parthé, S., Bartschlag, R., Gronkowski, M., Klemmer, J., Schmitt, M., Dreger, P., Kriegsmann, K., Schlenk, R. F., Müller-Tidow, C. (2023) Anti-SARS-CoV-2 antibody-containing plasma improves outcome in patients with hematologic or solid cancer and severe COVID-19: A randomized clinical trial. *Nat. Cancer* **4**, 96–107.
- Fajnzylber, J., Regan, J., Coxen, K., Corry, H., Wong, C., Rosenthal, A., Worrall, D., Giguel, F., Piechocka-Trocha, A., Atyeo, C., Fischinger, S., Chan, A., Flaherty, K. T., Hall, K., Dougan, M., Ryan, E. T., Gillespie, E., Chishty, R., Li, Y., Jilg, N., Hanidziar, D., Baron, R. M., Baden, L., Tsibris, A. M., Armstrong, K. A., Kuritzkes, D. R., Alter, G., Walker, B. D., Yu, X., Li, J. Z. (2020) SARS-CoV-2 viral load is associated with increased disease severity and mortality. *Nat. Commun.* **11**, 5493.
- Luke, T. C., Kilbane, E. M., Jackson, J. L., Hoffman, S. L. (2006) Meta-analysis: Convalescent blood products for Spanish influenza pneumonia: A future H5N1 treatment? *Ann. Intern. Med.* **145**, 599–609.
- Mallano, A., Ascione, A., Flego, M. (2022) Antibody response against SARS-CoV-2 infection: Implications for diagnosis, treatment and vaccine development. *Int. Rev. Immunol.* **41**, 393–413.

- RECOVERY Collaborative Group (2021) Tocilizumab in patients admitted to hospital with COVID-19 (RECOVERY): A randomised, controlled, open-label, platform trial. *Lancet* **397**, 1637–1645.
- Rosas, I. O., Bräu, N., Waters, M., Go, R. C., Hunter, B. D., Bhagani, S., Skiest, D., Aziz, M. S., Cooper, N., Douglas, I. S., Savic, S., Youngstein, T., Del Sorbo, L., Cubillo Gracian, A., De La Zerda, D. J., Ustianowski, A., Bao, M., Dimonaco, S., Graham, E., Matharu, B., Spotswood, H., Tsai, L., Malhotra, A. (2021) Tocilizumab in hospitalized patients with severe Covid-19 pneumonia. *N. Engl. J. Med.* **384**, 1503–1516.
- Turek, P. (2020) Darování plazmy po prodělané infekci koronavirem (COVID-19). *Transfuzní Oddělení, Fakultní Thomayerova nemocnice*. Available at: https://www.ftn.cz/upload/ftn/Kliniky/Transfuzni_odd/Dokumenty/TN_TRA_COVID-19_nabor.pdf
- Turek, P., Dresler, J., Hamšíková, E., Gašová, Z., Dušková, D., Ibrahimová, M., Kabičková, H., Kubičková, P. (2020) Vyšetření anti-SARS-CoV-2 virus-neutralizačním testem a IgG Elisa testem Euroimmun. *Transfuzní a Hematologie Dnes* **26**, 27.
- Vafadar Moradi, E., Teimouri, A., Rezaee, R., Morovatdar, N., Foroughian, M., Layegh, P., Rezvani Kakhki, B., Ahmadi Koupaei, S. R., Ghorani, V. (2021) Increased age, neutrophil-to-lymphocyte ratio (NLR) and white blood cells count are associated with higher COVID-19 mortality. *Am. J. Emerg. Med.* **40**, 11–14.
- Wang, X., Guo, X., Xin, Q., Pan, Y., Hu, Y., Li, J., Chu, Y., Feng, Y., Wang, Q. (2020) Neutralizing antibody responses to severe acute respiratory syndrome coronavirus 2 in coronavirus disease 2019 inpatients and convalescent patients. *Clin. Infect. Dis.* **71**, 2688–2694.
- Writing Committee for the REMAP-CAP Investigators; Estcourt, L. J., Turgeon, A. F., McQuilten, Z. K., McVerry, B. J., Al-Beidh, F., Annane, D., Arabi, Y. M., Arnold, D. M., Beane, A., Bégin, P., van Bentum-Puijk, W., Berry, L. R., Bhimani, Z., Birchall, J. E., Bonten, M. J. M., Bradbury, C. A., Brunkhorst, F. M., Buxton, M., Callum, J. L., Chassé, M., Cheng, A. C., Cove, M. E., Daly, J., Derde, L., Detry, M. A., De Jong, M., Evans, A., Fergusson, D. A., Fish, M., Fitzgerald, M., Foley, C., Goossens, H., Gordon, A. C., Gosbell, I. B., Green, C., Haniffa, R., Harvala, H., Higgins, A. M., Hills, T. E., Hoad, V. C., Horvat, C., Huang, D. T., Hudson, C. L., Ichihara, N., Laing, E., Lamikanra, A. A., Lamontagne, F., Lawler, P. R., Linstrum, K., Litton, E., Lorenzi, E., MacLennan, S., Marshall, J., McAuley, D. F., McDyer, J. F., McGlothlin, A., McGuinness, S., Mifflin, G., Montgomery, S., Mouncey, P. R., Murthy, S., Nichol, A., Parke, R., Parker, J. C., Priddee, N., Purcell, D. F. J., Reyes, L. F., Richardson, P., Robitaille, N., Rowan, K. M., Rynne, J., Saito, H., Santos, M., Saunders, C. T., Serpa Neto, A., Seymour, C. W., Silversides, J. A., Tinmouth, A. A., Triulzi, D. J., Turner, A. M., van de Veerdonk, F., Walsh, T. S., Wood, E. M., Berry, S., Lewis, R. J., Menon, D. K., McArthur, C., Zarychanski, R., Angus, D. C., Webb, S. A., Roberts, D. J., Shankar-Hari, M. (2021) Effect of convalescent plasma on organ support-free days in critically ill patients with COVID-19: A randomized clinical trial. *JAMA* **326**, 1690–1702.
- Yang, L., Xie, X., Tu, Z., Fu, J., Xu, D., Zhou, Y. (2021) The signal pathways and treatment of cytokine storm in COVID-19. *Signal Transduct. Target. Ther.* **6**, 1–20.

The Predictive Value of Serum Aldosterone Level for Coronary Artery Calcium Score in Patients with Chronic Kidney Disease: A Single-center Study

Viktor V. Semenov¹, Jizzo R. Bosdriesz², Olexandr Kuryata¹

¹Department of Internal Medicine 2 and Phthisiology, Dnipro State Medical University, Dnipro, Ukraine;

²ERA-EDTA Registry, Department of Medical Informatics, Amsterdam UMC, University of Amsterdam, Amsterdam Public Health Research Institute, Amsterdam, The Netherlands

Received September 21, 2022; Accepted August 27, 2023.

Key words: Aldosterone – Chronic kidney disease – Coronary artery calcium score – Prediction

Abstract: Patients with chronic kidney disease (CKD) have high cardiovascular risk (CVR), which is often underestimated by conventional tools. The coronary artery calcium score (CACS) significantly improves CVR stratification by conventional tools, but it is often not available in low-resources settings. Aldosterone may be a cheaper alternative to CACS for CVR assessment in CKD patients. The aim was to assess the ability of serum aldosterone level to predict CACS in patients with CKD in comparison to standard predictors. This single-center study included 57 patients aged 40 to 67 years with CKD (estimated glomerular filtration rate [eGFR] ≥ 45 ml/min) and arterial hypertension. Serum aldosterone, sex, age, body mass index, blood pressure, total cholesterol, eGFR, and proteinuria were used for prediction of CACS > 0 Agatston units (AU) and CACS > 100 AU. The area under the curve (AUC) with 95% confidence intervals (CI) and the mean Brier scores were examined for predictors of CACS. Aldosterone predicted a CACS > 100 AU

This study was supported from European Renal Association – European Dialysis and Transplantation Association during ERA-EDTA Registry Fellowship at the Department of Medical Informatics, Amsterdam UMC, University of Amsterdam. The reagent for measurement of serum aldosterone was purchased with the support from Dnipro State Medical University, Dnipro, Ukraine.

Mailing Address: Viktor V. Semenov, PhD., Dnipro State Medical University, Vernadskoho Street 9, Dnipro, 49000, Ukraine; Phone: +380 984 334 841; e-mail: semenoviktikt@gmail.com

(AUC = 0.72, 95% CI: 0.56–0.88), but not a CACS>0 AU. Age predicted a CACS>100 AU (AUC = 0.80, 95% CI: 0.67–0.93) and a CACS>0 AU (AUC = 0.75, 95% CI: 0.62–0.89). The addition of aldosterone to age for prediction of a CACS>100 AU improved the mean Brier score, compared to the model with age alone, from 0.16 to 0.14, but not the AUC (0.83, 95% CI: 0.70–0.95). Aldosterone was a significant predictor of a CACS>100 AU in patients with CKD, but aldosterone was not a better predictor than age alone.

Introduction

Patients with chronic kidney disease (CKD) are known to have increased overall and cardiovascular mortality (Matsushita et al., 2016), mostly due to a higher risk of atherosclerosis development (Valdivielso et al., 2019). Cardiovascular risk stratification is usually done with simple and reliable tools, such as the SCORE and Framingham risk chart (D'Agostino et al., 2008; Piepoli et al., 2016). These tools work well in the general population, but underestimate risk in individuals with CKD (Matsushita et al., 2016). Accounting for additional markers may improve the predictive ability of standard tools. The most powerful improvement of cardiovascular risk prediction made by standard tools was shown by coronary artery calcium score (CACS) (Osawa et al., 2016; De Lemos et al., 2017), which works well both for the general population and for patients with CKD (Chen et al., 2017). CACS is based on computed tomography scanning of the heart with the measurement of the calcium in the coronary arteries. It is a simple and reliable test for risk reassessment which does not require special preparation of the patient (Zhao et al., 2014). However, its implementation in low-income countries may be problematic. For instance, in Ukraine, the healthcare system provides approximately 25 \$ for the yearly follow-up of a middle-aged person in primary care (Orange Health Consultants, 2018), while the lowest estimated cost for the use of CACS is 85 \$ (Van Kempen et al., 2011). Feasibility is a crucial factor of tests for early diagnosis of cardiovascular disease. Moreover, in low- and middle-income regions (including Eastern Europe), only modest reductions in coronary artery disease related mortality have been observed in the last decades, which may be related to the lower investments in their healthcare systems (Moran et al., 2014).

For individuals with limited access to CACS, aldosterone may be a candidate biomarker for the identification of persons with poor cardiovascular prognosis. CKD itself predisposes to excessive production of aldosterone (Hayashi et al., 2018). In addition, up to 86% of patients with CKD have arterial hypertension (HTN) (Judd and Calhoun, 2015), for which the first-line drugs are angiotensin-converting enzyme inhibitors (ACEi) or angiotensin receptor blockers (ARB) (Whelton et al., 2018; Williams et al., 2018). Their usage may result in a higher production of aldosterone, which is also called aldosterone “breakthrough” (Schrier, 2010). Aldosterone is the main driver of the renin-angiotensin-aldosterone (RAAS) system,

which has pleiotropic effects on the cardiovascular system (rising of systemic blood pressure [BP], cardiac fibrosis, pro-inflammatory activity, vascular calcification) and kidneys (renal fibrosis, CKD progression) (Donderski et al., 2017). Measuring the aldosterone level is much simpler and more feasible than the investigation of coronary calcium, and therefore may be implemented in routine clinical practice in the settings of limited access to CACS measurement.

To date, no study assessed the potential prognostic value of aldosterone for cardiovascular events in patients with CKD. The ability of aldosterone to predict cardiovascular mortality or hospitalization was not yet assessed in patient with CKD, but in two previously performed prognostic studies in patients with heart failure it was assessed, with inconsistent results (Güder et al., 2007; Kobayashi et al., 2020). Therefore, the aim of this study was to assess the ability of serum aldosterone level to predict CACS in patients with CKD.

Methods

Study population

Patients for this study were enrolled from January 2018 till July 2019 at the Dnipropetrovsk Mechnikov Regional Hospital, Dnipro, Ukraine. Inclusion criteria were: age between 40 and 70 years, established diagnosis of CKD stages 1–3a (estimated glomerular filtration rate [eGFR] \geq 45 ml/min), grades I–II HTN (systolic BP $<$ 180 mm Hg, diastolic BP $<$ 110 mm Hg), and treatment with ACEi/ARB in combination with other first-line antihypertensive drug for at least 3 months prior to the enrolment to the study. None of the patients were treated with aldosterone receptor blockers at the moment of data collection. 33 of 57 patients (57.9%) were receiving treatment with statins at the moment of data collection. Exclusion criteria were: the presence of cardiovascular disease, nephrotic syndrome (urine protein loss $>$ 3.5 g/24 hours), severe deviations of serum potassium level ($<$ 3 or $>$ 6 mmol/l), type 1 diabetes mellitus (DM), type 2 DM requiring insulin therapy, arrhythmia that required pharmacological treatment, thyroid gland function abnormalities, and presence of malignancies or hereditary anomalies of the urinary tract.

Diagnosis of CKD was based on KDIGO Guidelines for Evaluation and Management of CKD (Eknoyan et al., 2013). Patients in the study who fulfilled the diagnosis of CKD had abnormalities of kidney function or structure for more than 3 months (eGFR $<$ 60 ml/min, or albuminuria $>$ 30 mg/24 hours, or urine sediment abnormalities, or structural kidney abnormalities detected by kidney ultrasound) (Eknoyan et al., 2013). Diagnosis of HTN was established according to ESC Guidelines for the Management of Arterial Hypertension (Mancia et al., 2013; Williams et al., 2018). Patients were recommended to restrict salt intake to less than 5 g per day for at least 3 months prior to the enrolment to the study (Eknoyan et al., 2013).

Compliance with ethical standards

All the patients gave their written informed consent to the collection and processing of the data. The study was approved by the Ethical Committee of Dnipropetrovsk Mechnikov Regional Hospital, Dnipro, Ukraine.

Measurements

CACS

CACS was obtained using computed tomography coronarography, and computed tomography scans were performed using Optima CT660 (GE Healthcare, Wisconsin, USA). CACS was reported in Agatston units (AU). The decision to classify CACS as negative (0 AU), moderate (1–100 AU) or high (>100 AU) was based on the 2019 ESC/EAS Guidelines for the management of dyslipidaemias (Mach et al., 2020) and on the study of Chen et al. (2017).

Aldosterone

Evaluation of the serum aldosterone level was performed using reagent Diagnostics Biochem Canada Aldosterone Elisa Kit, CAN-ALD-450. Blood for the analysis was taken after at least 8 hours of fasting and after the patient had been seated for 15 minutes. Blood samples were immediately centrifuged at room temperature at 2,000 rpm for 15 minutes. Serum was collected and stored at -20°C . Serum aldosterone level was reported in pg/ml.

Other variables

The following variables were investigated: sex, age, smoking status, body mass index (BMI), systolic BP (SBP), diastolic BP (DBP), total cholesterol (TC), eGFR and the presence of proteinuria.

Age was reported in years. BMI was calculated as weight (kg)/height (m)². BP evaluation was performed using the automated method and reported in mm Hg. Assessment of blood TC, creatinine and urine protein presence were performed using standard methods. eGFR was calculated using the CKD-EPI equation, which requires patients' sex, ethnicity, age and serum creatinine, and reported in ml/min (Eknoyan et al., 2013). Proteinuria was defined as the presence of protein or protein trace in morning void.

Missing data

There were missing data for TC (13 patients, 22.8%) and eGFR (2 patients, 3.5%). Missing continuous values were omitted from the calculations.

Statistical analysis

Statistical analyses were performed using LibreOffice and R, version 3.6.3 (Sing et al., 2005; Robin et al., 2011; López-Ratón et al., 2014; Lele et al., 2019; Firke, 2020; R Core Team, 2020). The type of data distribution was assessed using a Shapiro-

Wilk test. In case of normal distribution, continuous data were presented as mean (with standard deviation) and groups were compared using one-way analysis of variance. In the case of non-normal distribution, continuous data were presented as median (with 25th and 75th percentiles) and groups were compared using the Kruskal-Wallis test. Categorical data were presented as n (%), and groups were compared using chi-square test.

The ability of variables in the study to predict a CACS > 0 AU and CACS > 100 AU was assessed. First, all variables available in clinical practice that are potentially associated with coronary calcification (i.e., sex, age, smoking status, BMI, SBP, DBP, TC, and eGFR), and serum aldosterone were included in univariate logistic regression models. Next, only significant predictors were included to the multivariate logistic regression model with addition of serum aldosterone (per 10 pg/ml) to assess its ability to improve the prediction. The assumption of linearity of eGFR with log odds of the outcome was violated and therefore the natural logarithm of eGFR was included in the logistic regression model. The mean Brier score was used to estimate the accuracy of the models (scores could range from 0 [perfect accuracy] to 0.25 [of no value]). To determine how well the model distinguished between individuals with and without the outcome, a receiver operating characteristic (ROC) curve was built with estimation of the area under the curve (AUC). Comparison of two AUCs was performed with the method by DeLong et al. (1988). For statistically significant predictors, optimal cut-off points were determined (i.e., values of the predictors that classify the highest number of study participants correctly) with the highest Youden's index (the sum of specificity and sensitivity). Calibration of the model was assessed with the Hosmer-Lemeshow goodness-of-fit test. The threshold for confirming statistical hypotheses was set at <0.05.

Results

The study included 57 patients of Caucasian ethnicity aged 40 to 67 years (Table 1). Mean eGFR of the patients in the study was 77.2 ml/min, and ranged from 45.3 ml/min to 108.3 ml/min. CKD stage 1 was diagnosed in 11 patients (19.3%), CKD stage 2 was diagnosed in 41 patients (71.9%), and CKD stage 3a was diagnosed in 5 patients (8.8%). 42 (73.7%) of the patients were females. Age and serum aldosterone differed significantly between patients with a CACS of 0 AU, 1–100 AU and >100 AU. Median serum aldosterone was the highest in patients with CACS > 100 AU, but there was no linear relation between aldosterone and CACS category. The proportion of females, smoking status, patients with diabetes mellitus and patients with proteinuria as well as the mean BMI, SBP, TC, eGFR and median DBP were not different between patients with CACS of 0 AU, 1–100 AU and >100 AU.

Using univariate logistic regression, age was the only significant predictor of CACS > 0 AU, whereas both age and aldosterone were significant predictors of CACS > 100 AU (Table 2). In the multivariate logistic regression model, both age and aldosterone significantly predicted CACS > 100 AU (Table 2).

Table 1 – Demographic, clinical and laboratory characteristics of CKD patients with CACS of 0 AU, 1–100 AU and > 100 AU

Variable	Total (n=57)	CACS			p-value
		0 AU (n=20)	1–100 AU (n=22)	> 100 AU (n=15)	
Age, years	56 (53; 59)	53 (49; 55)	55 (53; 59)	60 (57; 63)	<0.01
Females, n (%)	42 (73.7)	16 (80.0)	15 (68.2)	11 (73.3)	0.69
Smoking, n (%)	6 (10.5)	2 (10.0)	3 (13.6)	1 (6.7)	0.79
DM, n (%)	11 (19.3)	2 (10.0)	5 (22.7)	4 (26.7)	0.48
BMI, kg/m ²	31.9 (7.5)	29.6 (6.9)	33.5 (7.0)	32.5 (8.5)	0.21
SBP, mm Hg	139 (17.5)	138.5 (15.4)	137.4 (19.2)	142.2 (18.3)	0.58
DBP, mm Hg	85 (80; 95)	90 (80; 91.2)	85 (80; 96.5)	85 (80; 90.5)	0.99
TC, mmol/l	5.4 (1.1)	5.6 (1.3)	5.5 (1.2)	5.2 (1.0)	0.38
eGFR, ml/min	77.2 (13.4)	81.7 (12.8)	74.1 (14.4)	75.8 (12.0)	0.18
Proteinuria, n (%)	33 (57.9)	13 (65.0)	11 (50.0)	9 (60.0)	0.61
Serum aldosterone, pg/ml	31 (15; 51)	38 (18; 52)	18 (14; 34)	48 (30; 123)	0.01

CKD – chronic kidney disease; CACS – coronary artery calcium score; AU – Agatston units; DM – diabetes mellitus; BMI – body mass index; SBP – systolic blood pressure; DBP – diastolic blood pressure; TC – total cholesterol; eGFR – estimated glomerular filtration rate

The AUC for age was 0.75 (95% CI = 0.62–0.88) when predicting a CACS > 0 AU (Table 3). The AUC for age (0.80 [0.67–0.93]) was higher than that for aldosterone (0.72 [0.56–0.88]) when predicting CACS > 100 AU, but the difference of the AUCs was not significant ($p=0.39$) (Figure 1, Table 2). The addition of aldosterone on top of age in the prediction of CACS > 100 AU had led to a 10% improvement of the mean Brier score (from 0.16 to 0.14), but non-significant change in the AUC (0.83 [0.70–0.95]). The AUC of the model with age and aldosterone in the prediction of CACS > 100 AU was neither different from the AUC for the model with age alone ($p=0.36$), nor it was different from the model with aldosterone alone ($p=0.16$) (Figure 1, Table 2). According to our data the optimal cut-off point for age for the prediction of CACS > 0 AU was 57 years (sensitivity = 57%, specificity = 90%). For the prediction of CACS > 100 AU the optimal cut-off point for serum aldosterone was 83 pg/ml (sensitivity = 46%, specificity = 90%), for age it was 57 years (sensitivity = 86%, specificity = 76%).

Discussion

Although the coronary artery calcium score can significantly improve cardiovascular risk stratification (Osawa et al., 2016; De Lemos et al., 2017), it may not be

Table 2 – Odds ratios for the prediction of CACS > 0 AU and CACS > 100 AU

	CACS > 0 AU		CACS > 100 AU	
	OR (95% CI)	p-value	OR (95% CI)	p-value
Univariate models				
Age (years)	1.14 (1.04–1.27)	0.01	1.22 (1.08–1.43)	0.01
Female sex (yes/no)	0.59 (0.14–2.07)	0.43	0.98 (0.27–4.09)	0.97
Smoking (yes/no)	1.09 (0.19–8.42)	0.92	0.52 (0.03–3.67)	0.58
DM (yes/no)	2.89 (0.65–20.43)	0.20	1.82 (0.41–7.28)	0.40
BMI (kg/m ²)	1.07 (0.99–1.17)	0.10	1.02 (0.94–1.10)	0.68
SBP (mm Hg)	1.00 (0.97–1.04)	0.86	1.01 (0.98–1.05)	0.41
DBP (mm Hg)	1.00 (0.94–1.05)	0.88	0.99 (0.93–1.05)	0.81
TC (mmol/l)	0.84 (0.48–1.44)	0.52	0.75 (0.39–1.37)	0.37
eGFR (ml/min)	0.04 (0.00–1.12)	0.07	0.50 (0.02–14.86)	0.68
Serum aldosterone (10 pg/ml)	1.02 (0.92–1.16)	0.68	1.18 (1.05–1.35)	0.01
Multivariate model				
Age (years)	–	–	1.20 (1.06–1.41)	0.01
Serum aldosterone (10 pg/ml)	–	–	1.16 (1.02–1.34)	0.03

CACS – coronary artery calcium score; AU – Agatston units; OR – odds ratio; CI – confidence interval; DM – diabetes mellitus; BMI – body mass index; SBP – systolic blood pressure; DBP – diastolic blood pressure; TC – total cholesterol; eGFR – estimated glomerular filtration rate

Table 3 – Estimations of accuracy, distinguishing ability and calibration of the models for prediction CACS > 0 AU and CACS > 100 AU

		Mean Brier score	AUC (CI)	H-L test
CACS > 0 AU	Age	0.20	0.75 (0.62–0.89)	–
	Age	0.16	0.80 (0.67–0.93)	–
CACS > 100 AU	Aldosterone	0.16	0.72 (0.56–0.88)	0.67
	Age + aldosterone	0.14	0.83 (0.70–0.95)	0.81

CACS – coronary artery calcium score; AU – Agatston units; AUC – area under the curve; CI – confidence interval; H-L test – Hosmer-Lemeshow goodness-of-fit test (p-value). P-values for the comparison of the AUCs using method by DeLong et al. (1988): age vs. aldosterone – p=0.39; age vs. age + aldosterone – p=0.36; aldosterone vs. age + aldosterone – p=0.16

affordable for low and middle income countries (Mancia et al., 2013; Zhao et al., 2014). Therefore, a cheaper measure, such as serum aldosterone, to predict the coronary artery calcium score is needed. Findings of this single-center study from Ukraine indicate that aldosterone could predict CACS > 100 AU in patients with CKD. However, aldosterone was not a better predictor than age alone.

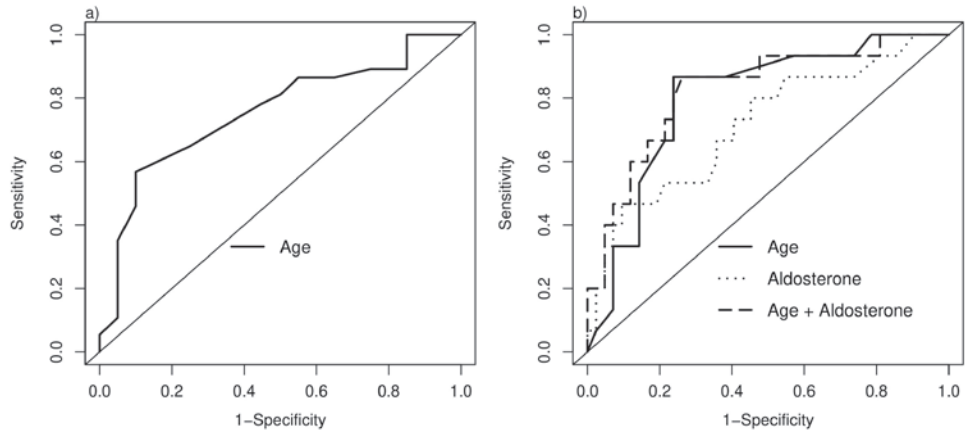


Figure 1 – Receiver operating characteristic curves for the prediction of CACS (coronary artery calcium score) > 0 AU (Agatston units) (a) and CACS > 100 AU (b).

Coronary artery calcium score in the prediction of cardiovascular events

CACS implementation has clear benefits: it is a highly reproducible test, it is non-invasive, fast and simple in performance and its added value to standard cardiovascular risk prediction tools is the greatest among other proposed risk factors (Mancia et al., 2013; Zhao et al., 2014). At the same time, the equipment for CACS may not be available in low and middle income countries, and this equipment requires qualified operators (Zhao et al., 2014). In low resource settings, new diagnostic tools are concentrated in the clinics of big administrative centers, rather than in small clinics (Vedanathan et al., 2014). Governments usually cover only a limited number of investigations, while the fee for the access to a new diagnostic tool may be too high for the majority of the patients (Vedanathan et al., 2014; Zhao et al., 2014). The cost-effectiveness of CACS is a matter of debate (Van Kempen et al., 2011; Mancia et al., 2013; Pletcher, 2016). In the 2013 European Society of Hypertension/European Society of Cardiology Guidelines for the management of arterial hypertension, CACS received the lowest possible grade for cost-effectiveness (Mancia et al., 2013), and there is concern whether it should be recommended for asymptomatic women (Van Kempen et al., 2011; Pletcher, 2016). However, coronary artery calcium scoring in certain populations could allow improvement of outcomes. In asymptomatic individuals, CACS > 100 AU may be regarded as an indication for reclassifying of their cardiovascular risk into a higher grade with the corresponding revision of treatment (Mach et al., 2020). For symptomatic patients, a negative CACS indicates a low probability of obstructive coronary artery disease (Knuuti et al., 2020). Finally, it may be suggested that the interpretation of CACS results for CKD patients should be different from the general population. CACS in CKD patients may be influenced by the calcification

of the medial layer of coronary arteries and, therefore, reflect non-obstructive atherosclerosis (Chen et al., 2017).

Aldosterone in the prediction of cardiovascular events

Aldosterone may be a promising and cheap alternative predictor of cardiovascular events due to the presence of a likely causal relationship between aldosterone and cardiovascular complications (Donderski et al., 2017). The majority of patients with CKD do not die from CKD-related causes of death, but rather die from cardiovascular complications (Thompson et al., 2015). High cardiovascular mortality in CKD patients is related to the rapid development of atherosclerosis, which pathogenesis in CKD is complex (Valdivielso et al., 2019). The development of atherosclerosis in CKD may be influenced by additional (non-classical) cardiovascular risk factors such as low-grade inflammation, mineral and bone disorder and fluid overload (Valdivielso et al., 2019). Aldosterone can be regarded as the factor that participates in all the mentioned pathways (Donderski et al., 2017). However, its measurement may be suggested only in CKD, which is usually accompanied by aldosterone excess or mineralocorticoid receptor activation (Donderski et al., 2017). Unlike other proposed additional markers of cardiovascular events (Osawa et al., 2016; Chen et al., 2018), aldosterone, may be also a treatment target. The involvement of aldosterone in multiple pathways of atherosclerosis progression and availability of aldosterone antagonists (Funder, 2017) provide a good reason for testing aldosterone in routine clinical practice for patients with CKD.

So far it was unclear to what extent aldosterone can be used for cardiovascular risk assessment in patients with CKD. The results of our study now show that aldosterone could predict CACS > 100 AU, but could not predict CACS > 0 AU. In our study the optimal cut-off point for aldosterone in prediction of CACS > 100 AU (83 pg/ml) was found to be close to the threshold for diagnosing high aldosterone in Ukrainian guidelines – 90 pg/ml (Mostovoy and Sidorov, 2016). However, the sensitivity of this optimal cut-off point was 46%, which indicates that more than a half of patients with aldosterone below 83 pg/ml would be falsely classified as having CACS < 100 AU. Therefore, aldosterone measurement may not be recommended in routine clinical practice for prediction of CACS > 100 AU and reassessment of cardiovascular risk in the patients with CKD (Mach et al., 2020).

Moreover, according to results of our study, aldosterone was not a better predictor of CACS than age. In our study age was a significant predictor of both CACS > 100 AU and CACS > 0 AU. Both models for prediction of CACS by age showed that the optimal cut-off point was 57 years. In our study, the optimal cut-off point for age in the prediction of CACS > 100 AU had good sensitivity (86%) and specificity (76%), which allow to consider it for usage in routine clinical practices. The optimal cut-off points for age in our study were close to the age of 55 years, after which changes in treatment may be considered for asymptomatic persons (according

to the 2019 American College of Cardiology/American Heart Association Guideline on the Primary Prevention of Cardiovascular Disease) (Arnett et al., 2019).

Several important remarks needed to be made. First, the population of patients with CKD in Ukraine is much younger compared to other European countries (Kramer et al., 2019). Second, although age is known to be a powerful cardiovascular risk factor (D'Agostino et al., 2008; Piepoli et al., 2016), age alone may not be sufficient for a good discrimination of patients' risk. In the countries that use the same variables for cardiovascular risk stratification (including age), mortality rates differ dramatically (Timmis et al., 2018). Therefore, cardiovascular risk assessment tools that are supposed to have a high predictive value in high income countries may not be generalizable to low-income countries and vice versa. It was hypothesized that aldosterone may improve the prognostic ability of age-based models for cardiovascular risk stratification. However, our study shows that aldosterone neither was better than age in the prediction of CACS, nor did it improve the prediction of CACS by age in CKD patients in Ukraine.

Strengths and limitations

A main strength of this study is the availability of both data on CACS and aldosterone in patients with CKD from an Eastern European country with high cardiovascular mortality (Timmis et al., 2018) and early development of chronic kidney disease (Kramer et al., 2019). This study also has several limitations. One of the main limitations is the small sample size. Results of this study need to be confirmed in a study with a larger sample and external validation is needed. Simultaneous evaluation of serum renin was not performed, therefore differentiation between primary and secondary causes of aldosterone level elevation was not possible. In addition, data about serum aldosterone prior to the start of ACEi/ARB therapy was missing. Therefore, it was impossible to determine whether aldosterone elevation was related to the start of antihypertensive treatment (the aldosterone "breakthrough" phenomenon). The study sample included patients with CKD, and some of the patient had CKD related to systemic sclerosis (n=13). The pathogenesis of organ damage in systemic sclerosis is unique (includes inflammation, excessive fibrosis and vasculopathy) (Orlandi et al., 2018), which could influence the results of the study. However, patients with systemic sclerosis in our study had a stable course of the disease with controlled inflammation and did not receive methotrexate. Also, there was no significant difference in the distribution of sex, age, eGFR, CACS > 0 AU, and CACS > 100 AU between patients with and without systemic sclerosis.

Conclusion

Findings of our study in a sample of CKD patients from a single center in Ukraine suggest that aldosterone was a significant predictor of CACS > 100 AU, but aldosterone was not a better predictor than age. Our findings need to be confirmed

in a larger external sample. Results of this study may be useful for clinicians, who could use age for the assessment of atherosclerosis progression in CKD patients, when CACS is not available. Our study highlights the need for the development of risk assessment tools tailored to local populations with CKD and to the economic resources of healthcare systems.

References

- Arnett, D. K., Blumenthal, R. S., Albert, M. A., Buroker, A. B., Goldberger, Z. D., Hahn, E. J., Himmelfarb, C. D., Khera, A., Lloyd-Jones, D., McEvoy, J. W., Michos, E. D., Miedema, M. D., Muñoz, D., Smith, S. C., Virani, S. S., Williams, K. A., Yeboah, J., Ziaeian, B. (2019) 2019 ACC/AHA Guideline on the primary prevention of cardiovascular disease: Executive summary: A report of the American College of Cardiology/American Heart Association Task Force on clinical practice guidelines. *Circulation* **140(11)**, e563–e595.
- Chen, J., Budoff, M. J., Reilly, M. P., Yang, W., Rosas, S. E., Rahman, M., Zhang, X., Roy, J. A., Lustigova, E., Nessel, L., Ford, V., Raj, D., Porter, A. C., Soliman, E. Z., Wright, J. T. Jr., Wolf, M., He, J.; CRIC Investigators (2017) Coronary artery calcification and risk of cardiovascular disease and death among patients with chronic kidney disease. *JAMA Cardiol.* **2(6)**, 635–643.
- Chen, S.-C., Huang, J.-C., Su, H.-M., Chiu, Y.-W., Chang, J.-M., Hwang, S.-J., Chen, H.-C. (2018) Prognostic cardiovascular markers in chronic kidney disease. *Kidney Blood Press. Res.* **43(4)**, 1388–1407.
- D’Agostino, R. B., Vasan, R. S., Pencina, M. J., Wolf, P. A., Cobain, M., Massaro, J. M., Kannel, W. B. (2008) General cardiovascular risk profile for use in primary care: The Framingham heart study. *Circulation* **117(6)**, 743–753.
- De Lemos, J. A., Ayers, C. R., Levine, B., DeFilippi, C. R., Wang, T. J., Hundley, W. G., Berry, J. D., Seliger, S. L., McGuire, D. K., Ouyang, P., Drazner, M. H., Budoff, M., Greenland, P., Ballantyne, C. M., Khera, A. (2017) Multimodality strategy for cardiovascular risk assessment: Performance in 2 population-based cohorts. *Circulation* **135(22)**, 2119–2132.
- DeLong, E. R., DeLong, D. M., Clarke-Pearson, D. L. (1988) Comparing the areas under two or more correlated receiver operating characteristic curves: A nonparametric approach. *Biometrics* **44(3)**, 837–845.
- Donderski, R., Stróżecki, P., Sulikowska, B., Grajewska, M., Miśkowiec, I., Stefańska, A., Siódmiak, J., Odrowąż-Sypniewska, G., Manitius, J. (2017) Aldosterone antagonist therapy and its relationship with inflammation, fibrosis, thrombosis, mineral-bone disorder and cardiovascular complications in peritoneal dialysis (PD) patients. *Int. Urol. Nephrol.* **49(10)**, 1867–1873.
- Eknoyan, G., Lameire, N., Echardt, K., Kasiske, B., Wheeler, D. (2013) KDIGO 2012 Clinical Practice Guideline for the evaluation and management of chronic kidney disease. *Kidney Int. Suppl.* **3(1)**, 1–150.
- Firke, S. (2020) *janitor: Simple Tools for Examining and Cleaning Dirty Data* (R package version 1.2.1). Available at: <https://CRAN.R-project.org/package=janitor>
- Funder, J. W. (2017) Spironolactone in cardiovascular disease: An expanding universe? *F1000Res.* **6**, 1738.
- Güder, G., Bauersachs, J., Frantz, S., Weismann, D., Allolio, B., Ertl, G., Angermann, C. E., Störk, S. (2007) Complementary and incremental mortality risk prediction by cortisol and aldosterone in chronic heart failure. *Circulation* **115(13)**, 1754–1761.
- Hayashi, K., Suzuki, T., Sakamaki, Y., Ito, S. (2018) Cardiac hypertrophy in chronic kidney disease – Role of aldosterone and FGF23. *Ren. Replace. Ther.* **4(1)**, 10.
- Judd, E., Calhoun, D. A. (2015) Management of hypertension in CKD: Beyond the guidelines. *Adv. Chronic Kidney Dis.* **22(2)**, 116–122.

- Knuuti, J., Wijns, W., Saraste, A., Capodanno, D., Barbato, E., Funck-Brentano, C., Prescott, E., Storey, R. F., Deaton, C., Cuisset, T., Agewall, S., Dickstein, K., Edvardsen, T., Escaned, J., Gersh, B. J., Svitil, P., Gilard, M., Hasdai, D., Hatala, R., Mahfoud, F., Masip, J., Muneretto, C., Valgimigli, M., Achenbach, S., Bax, J. J.; ESC Scientific Document Group (2020) 2019 ESC Guidelines for the diagnosis and management of chronic coronary syndromes. *Eur. Heart J.* **41(3)**, 407–477.
- Kobayashi, M., Stienen, S., Maaten, J. M., Dickstein, K., Samani, N. J., Lang, C. C., Ng, L. L., Anker, S. D., Metra, M., Preud'homme, G., Duarte, K., Lamiral, Z., Girerd, N., Rossignol, P., Veldhuisen, D. J., Voors, A. A., Zannad, F., Ferreira, J. P. (2020) Clinical determinants and prognostic implications of renin and aldosterone in patients with symptomatic heart failure. *ESC Heart Fail.* **7(3)**, 953–963.
- Kramer, A., Pippias, M., Noordzij, M., Stel, V. S., Andrusev, A. M., Aparicio-Madre, M. I., Arribas Monzón, F. E., Åsberg, A., Barbullushi, M., Beltrán, P., Bonthuis, M., Caskey, F. J., Castro de la Nuez, P., Cernevskis, H., De Meester, J., Finne, P., Golan, E., Heaf, J. G., Hemmelder, M. H., Ioannou, K., Kantaria, N., Komissarov, K., Korejwo, G., Kramar, R., Lassalle, M., Lopot, F., Macário, F., Mackinnon, B., Pálsson, R., Pechter, Ü., Piñera, V. C., Santiuste de Pablos, C., Segarra-Medrano, A., Seyahi, N., Slon Roblero, M. F., Stojceva-Taneva, O., Vazellov, E., Winzeler, R., Ziginiskiene, E., Massy, Z., Jager, K. J. (2019) The European Renal Association – European Dialysis and Transplant Association (ERA-EDTA) Registry Annual Report 2016: A summary. *Clin. Kidney J.* **12(5)**, 702–720.
- Lele, S. R., Keim, J. L., Solymos, P. (2019) *ResourceSelection: Resource Selection (Probability) Functions for Use-Availability Data* (R package version 0.3-5). Available at: <https://CRAN.R-project.org/package=ResourceSelection>
- López-Ratón, M., Rodríguez-Álvarez, M. X., Suárez, C. C., Sampedro, F. G. (2014) OptimalCutpoints: An R package for selecting optimal cutpoints in diagnostic tests. *J. Stat. Softw.* **61(8)**, 1–36.
- Mach, F., Baigent, C., Catapano, A. L., Koskinas, K. C., Casula, M., Badimon, L., Chapman, M. J., De Backer, G. G., Delgado, V., Ference, B. A., Graham, I. M., Halliday, A., Landmesser, U., Mihaylova, B., Pedersen, T. R., Riccardi, G., Richter, D. J., Sabatine, M. S., Taskinen, M. R., Tokgozoglu, L., Wiklund, O.; ESC Scientific Document Group (2020) 2019 ESC/EAS Guidelines for the management of dyslipidaemias: Lipid modification to reduce cardiovascular risk. *Eur. Heart J.* **41(1)**, 111–188.
- Mancia, G., Fagard, R., Narkiewicz, K., Redon, J., Zanchetti, A., Böhm, M., Christiaens, T., Cifkova, R., De Backer, G., Dominiczak, A., Galderisi, M., Grobbee, D. E., Jaarsma, T., Kirchhof, P., Kjeldsen, S. E., Laurent, S., Manolis, A. J., Nilsson, P. M., Ruilope, L. M., Schmieder, R. E., Sirnes, P. A., Sleight, P., Viigimaa, M., Waeber, B., Zannad, F.; Task Force Members (2013) 2013 ESH/ESC guidelines for the management of arterial hypertension: The Task Force for the management of arterial hypertension of the European Society of Hypertension (ESH) and of the European Society of Cardiology (ESC). *Eur. Heart J.* **34(28)**, 2159–2219.
- Matsushita, K., Ballew, S. H., Coresh, J. (2016) Cardiovascular risk prediction in people with CKD. *Curr. Opin. Nephrol. Hypertens.* **25(6)**, 518–523.
- Moran, A. E., Forouzanfar, M. H., Roth, G. A., Mensah, G. A., Ezzati, M., Murray, C. J. L. (2014) Temporal trends in ischemic heart disease mortality in 21 world regions, 1980 to 2010: The Global Burden of Disease 2010 Study. *Circulation* **129(14)**, 1483–1492.
- Mostovoy, Y. M., Sidorov, O. O. (2016) *Laboratory Tests. Normal Values, Interpretation of Changes*. Center DZK. Orange Health Consultants (2018) *Health Care in Ukraine*. Commissioned by the Netherlands Enterprise Agency.
- Orlandi, M., Barsotti, S., Lepri, G., Codullo, V., Battista, M. D., Guiducci, S., Rossa, A. D. (2018) One year in review 2018: Systemic sclerosis. *Clin. Exp. Rheumatol.* **113(4)**, 3–23 (Suppl. 36).
- Osawa, K., Nakanishi, R., Budoff, M. (2016) Coronary artery calcification; report from the Multi-Ethnic Study of Atherosclerosis. *Glob. Heart* **11(3)**, 287–293.

- Piepoli, M. F., Hoes, A. W., Agewall, S., Albus, C., Brotons, C., Catapano, A. L., Cooney, M. T., Corrà, U., Cosyns, B., Deaton, C., Graham, I., Hall, M. S., Hobbs, F. D. R., Løchen, M. L., Löllgen, H., Marques-Vidal, P., Perk, J., Prescott, E., Redon, J., Richter, D., Sattar, N., Smulders, Y., Tiberi, M., van der Worp, H. B., van Dis, I., Verschuren, W. M. M., Binno, S.; ESC Scientific Document Group (2016) 2016 European Guidelines on cardiovascular disease prevention in clinical practice. *Eur. Heart J.* **37(29)**, 2315–2381.
- Pletcher, M. (2016) *When Is Measuring a Coronary Artery Calcium Score Cost Effective?* American College of Cardiology. Available at: <https://www.acc.org/latest-in-cardiology/articles/2016/06/14/09/17/when-is-measuring-a-coronary-artery-calcium-score-cost-effective>
- R Core Team (2020) *R: A Language and Environment for Statistical Computing* (3.6.3) [R]. R Foundation for Statistical Computing. Available at: <https://www.R-project.org/>
- Robin, X., Turck, N., Hainard, A., Tiberti, N., Lisacek, F., Sanchez, J.-C., Müller, M. (2011) pROC: An open-source package for R and S+ to analyze and compare ROC curves. *BMC Bioinformatics* **12(1)**, 77.
- Schrier, R. W. (2010) Aldosterone “escape” vs “breakthrough”. *Nat. Rev. Nephrol.* **6(2)**, 61.
- Sing, T., Sander, O., Beerewinkel, N., Lengauer, T. (2005) ROCr: Visualizing classifier performance in R. *Bioinformatics* **21(20)**, 7881.
- Thompson, S., James, M., Wiebe, N., Hemmelgarn, B., Manns, B., Klarenbach, S., Tonelli, M. (2015) Cause of death in patients with reduced kidney function. *J. Am. Soc. Nephrol.* **26(10)**, 2504–2511.
- Timmis, A., Townsend, N., Gale, C., Grobbee, R., Maniadakis, N., Flather, M., Wilkins, E., Wright, L., Vos, R., Bax, J., Blum, M., Pinto, F., Vardas, P.; ESC Scientific Document Group (2018) European Society of Cardiology: Cardiovascular disease statistics 2017. *Eur. Heart J.* **39(7)**, 508–579.
- Valdivielso, J. M., Rodríguez-Puyol, D., Pascual, J., Barrios, C., Bermúdez-López, M., Sánchez-Niño, M. D., Pérez-Fernández, M., Ortiz, A. (2019) Atherosclerosis in chronic kidney disease: More, less, or just different? *Arterioscler. Thromb. Vasc. Biol.* **39(10)**, 1938–1966.
- Van Kempen, B. J. H., Spronk, S., Koller, M. T., Elias-Smale, S. E., Fleischmann, K. E., Ikram, M. A., Krestin, G. P., Hofman, A., Witteman, J. C. M., Hunink, M. G. M. (2011) Comparative effectiveness and cost-effectiveness of computed tomography screening for coronary artery calcium in asymptomatic individuals. *J. Am. Coll. Cardiol.* **58(16)**, 1690–1701.
- Vedanthan, R., Choi, B. G., Baber, U., Narula, J., Fuster, V. (2014) Bioimaging and subclinical cardiovascular disease in low- and middle-income countries. *J. Cardiovasc. Transl. Res.* **7(8)**, 701–710.
- Whelton, P. K., Carey, R. M., Aronow, W. S., Ovbigele, B., Casey, D. E., Smith, S. C., Collins, K. J., Spencer, C. C., Himmelfarb, C. D., Stafford, R. S., Depalma, S. M., Taler, S. J., Gidding, S., Thomas, R. J., Jamerson, K. A., Williams, K. A., Jones, D. W., Williamson, J. D., Maclaughlin, E. J., Muntner, P., Ovbigele, B., Smith, S. C., Spencer, C. C., Stafford, R. S., Taler, S. J., Thomas, R. J., Williams, K. A., Williamson, J. D., Wright, J. T. (2018) 2017 ACC/AHA/AAPA/ABC/ACPM/AGS/APhA/ASH/ASPC/NMA/PCNA Guideline for the prevention, detection, evaluation, and management of high blood pressure in adults: Executive summary: A report of the American College of Cardiology/American Heart Association Task Force on clinical practice guidelines. *Hypertension* **71(6)**, 1269–1324.
- Williams, B., Mancia, G., Spiering, W., Agabiti Rosei, E., Azizi, M., Burnier, M., Clement, D., Coca, A., de Simone, G., Dominiczak, A., Kahan, T., Mahfoud, F., Redon, J., Ruilope, L., Zanchetti, A., Kerins, M., Kjeldsen, S. E., Kreutz, R., Laurent, S., Lip, G. Y. H., McManus, R., Narkiewicz, K., Ruschitzka, F., Schmieder, R. E., Shlyakhto, E., Tsioufis, C., Aboyans, V., Desormais, I.; ESC Scientific Document Group (2018) 2018 ESC/ESH Guidelines for the management of arterial hypertension. *Eur. Heart J.* **39(33)**, 3021–3104.
- Zhao, Y., Malik, S., Wong, N. D. (2014) Evidence for coronary artery calcification screening in the early detection of coronary artery disease and implications of screening in developing countries. *Glob. Heart* **9(4)**, 399.

The Role of Demographic and Clinical Characteristics in Distinguishing Testicular Torsion from Torsion of the Appendix Testis: A Single-center Retrospective Study

**Zlatan Zvizdic¹, Amila Aganovic², Emir Milisic¹, Asmir Jonuzi¹,
Denisa Zvizdic³, Semir Vranic⁴**

¹Clinic of Pediatric Surgery, University Clinical Center Sarajevo, Sarajevo, Bosnia and Herzegovina;

²Ingolstadt Hospital, Ingolstadt, Germany;

³Eye Clinic, University Clinical Center Sarajevo, Sarajevo, Bosnia and Herzegovina;

⁴College of Medicine, QU Health, Qatar University, Doha, Qatar

Received September 13, 2022; Accepted August 17, 2023.

Key words: Acute scrotum – Testicular torsion – Torsion of the appendix testis – Children

Abstract: The acute scrotum (AS) in the pediatric population is a medical emergency. AS is usually caused by testicular torsion (TT) and torsion of the appendix testis (TAT). The current study explored which demographic and clinical characteristics can help distinguish between TT and TAT. We analyzed all children ≤ 16 years who underwent surgical exploration for AS. The patients were divided into Group 1/TT and Group 2/TAT. Ninety patients were included in the study (24 with TT and 66 with TAT). The peak incidence of TT was significantly higher than in the TAT group ($p < 0.001$). Scrotal pain was more prevalent in the TAT group ($p = 0.02$), whereas systemic signs (nausea/vomiting and abdominal pain) affected more frequently the TT patients ($p = 0.003$ and $p < 0.001$, respectively). The duration of symptoms was significantly longer in the TAT group ($p < 0.001$). The duration of symptoms in the TT cohort significantly impacted the testicular salvage ($p = 0.008$). Color Doppler ultrasound (CDUS) findings of absent/decreased testicular blood flow in the affected testis strongly favored the diagnosis of TT ($p < 0.001$). The older age, shorter duration of symptoms, systemic signs, and CDUS findings can help distinguish between the two most common acute scrotum causes.

Mailing Address: Assoc. Prof. Semir Vranic, MD., PhD., College of Medicine, QU Health, Qatar University, PO Box 2713, Doha, Qatar; Phone: +974 4403 7873; e-mails: semir.vranic@gmail.com, svranic@qu.edu.qa

<https://doi.org/10.14712/23362936.2023.20>

© 2023 The Authors. This is an open-access article distributed under the terms of the Creative Commons Attribution License (<http://creativecommons.org/licenses/by/4.0>).

Introduction

In childhood or adolescence, the acute scrotum (AS) is a medical emergency characterized by acute scrotal pain with or without swelling and erythema (Gatti and Murphy, 2008). The most common pathologies encountered in the broad spectrum of pediatric AS are torsion of the appendix testis (TAT), testicular torsion (TT), and epididymo-orchitis (EO). The most important differential diagnosis for AS is TT, which accounts for up to 25% of acute scrotal disease in the pediatric population (Lemini et al., 2016). Testicular torsion (Figure 1A) can occur at any age but usually occurs in young males, with a bimodal incidence in the pediatric population: during the first year of life and between the ages of 13 and 16 (Pogorelic et al., 2016).

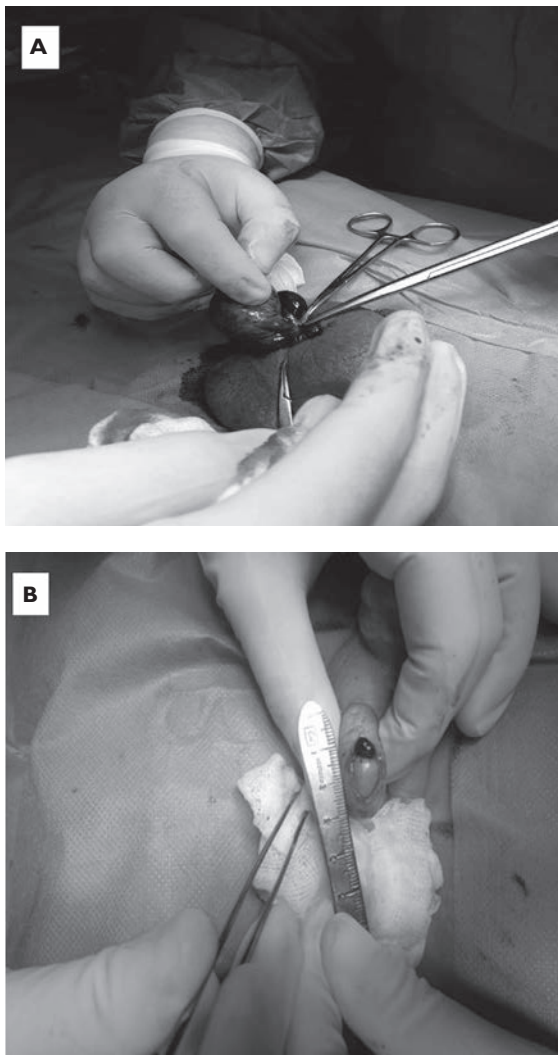


Figure 1A and B – Intraoperative images of a testicular torsion of a 12-year-old boy (A) and a torsion of the appendix testis of a 7-year-old boy (B).

In contrast, the most frequently detected pathology during scrotal exploration is TAT (Figure 1B), representing 54–71% of the operative diagnosis of AS (Mushtaq et al., 2003; Hart et al., 2016; Lala et al., 2019). TAT makes up 95% of torsed appendices (Vijayaraghavan, 2006).

Clinical distinction between TT and TAT is frequently tricky but critical because timely assessment and intervention in TT cases can preserve the affected testicle (Boettcher et al., 2012; Kumar et al., 2020). If treated within 6 hours of the presenting pain, there is a good chance of saving the affected testicle, as 90–100% of testicles will be saved. If treated within 6–12 h, depending on the degree of the torsion, 20–50% of testicles will be saved, and if treated within 12–24 h, only 0–10% of testicles will be saved (Pogorelic et al., 2021).

Various studies explored the differentiation of TT from TAT (Ciftci et al., 2004; Fujita et al., 2017; Tanaka et al., 2020). However, differential diagnosis of AS, particularly TT, remains challenging and shows a considerable risk of misdiagnosis (Ciftci et al., 2004).

The present study analyzed the pediatric cohort of TT and TAT and explored the impact of baseline demographic and clinical characteristics on differential causes of AS.

Material and Methods

We conducted a retrospective study using a cohort of pediatric patients presenting with AS who underwent scrotal exploration at the University Clinical Center Sarajevo, Bosnia and Herzegovina, between 2012 and 2016. Data were obtained from the medical records. We divided the patients into two groups according to the operative findings: Group 1 or TT group and Group 2 or TAT group and compared baseline demographic and clinical characteristics between them. The patients with TT were divided into two subgroups according to testicular viability and the type of treatment: orchidectomy and orchidopexy groups.

The primary outcome of the study was to explore the difference between testicular torsion and torsion of the appendix testicles based on their baseline demographic and clinical characteristics. The secondary outcome was determining the association between symptom duration and degree of torsion with treatment outcome (orchidectomy vs. orchidopexy) in boys and adolescents with testicular torsion.

Inclusion criteria for the study were confirmed diagnosis of TT or TAT and age below 16 years. Those with other causes of AS and those with incomplete or missing data were excluded from the study.

The following demographic and clinical characteristics were recorded: age, laterality (right/left), presenting symptoms (scrotal pain, erythema of the scrotal skin, swelling, nausea/vomiting, abdominal pain, and fever), duration of symptoms, seasonality, history of scrotal trauma, and color Doppler ultrasound (CDUS). Patients' age was categorized into five groups: <1 year, 1–3, 4–6, 7–11, and 12–16 years.

All patients underwent testicular ultrasonography with CDUS before surgery. The access for surgical exploration of the testis in all cases was through the midline

scrotal incision. TT was defined as twisting the spermatic cord and its contents with resultant ischemia due to compromised blood flow to the testicle. TAT was defined as twisting and ischemia of the testicular appendage located on the superior pole of the testicle between the testis and epididymis.

All medical records were de-identified and pseudo-anonymized for the current study. The study was approved by the local institutional review board (IRB) (Ethical Committee of the Clinical Center, University of Sarajevo, 0901-2-678/18). The IRB waived informed consent due to the retrospective nature of the study.

Statistical analysis

Mean and median were used to measure central tendency, standard deviation, and range as dispersion measures for continuous variables. The values of categorical variables were presented as numbers or percentages. The Kolmogorov-Smirnov test tested the normality of data distribution for each variable. Chi-square and Fisher's exact tests were used to explore the differences between the categorical variables. P-values < 0.05 were considered significant. All statistical assays were performed using the Statistical Package for the Social Sciences (SPSS) IBM Version 26 (SPSS) (UNICOM Systems, Inc.).

Results

The baseline demographic and clinical characteristics of the two pediatric cohorts are presented in Table 1.

Ninety-eight pediatric patients with AS were identified in the period 2012–2016. Eight patients were excluded from the study as they had other pathologies (e.g., EO, n=4) or incomplete clinical histories (n=4). Thus, 90 patients with TT and TAT met the inclusion criteria and constituted the final cohort.

Twenty-four TT cases (26.6%) (Group 1) and 66 (73.4%) TAT cases (Group 2) were seen during the study period. Patients with TT in this study were significantly older (13.5 ± 2.6 years [range, ten days – 15.8 years]) than those with TAT (9.5 ± 2.8 years [range 0.7–14.7 years]) ($p < 0.001$).

Although TT and TAT affected children of different ages, significant differences in both groups were observed. Thus, the peak incidence of TT was in the age of 12–16 years (75%), whereas the peak of TAT was in the age group of 7–11 years (57%) ($p < 0.001$ for both calculations).

There was no statistically significant difference between the two groups in laterality ($p = 0.28$). However, left-sided scrotal involvement was more common in TT cases (66%), whereas TAT cases had no significant difference in affected sides. We found that right-sided TT increases in adolescent patients: left-side TT involvement was recorded in 100% of patients under 12 years. In comparison, the incidence on that side dropped to 55.6% in patients aged ≥ 12 .

Scrotal pain, erythema of the scrotal skin, and scrotal swelling were the most common clinical symptoms in both observed groups (Table 1). Interestingly, scrotal

Table 1 – Baseline demographic, clinical characteristics and ultrasonography findings of patients with testicular torsion and torsion of the appendix testis

Variable	Testicular torsion	Torsion of the appendix testis	P-value
Demographic characteristics of the cohort			
Patients (n=90)	24 (26.6%)	66 (73.4%)	
Age (year; median ± SD)	13.5 ± 2.6	9.5 ± 2.8*	<0.001
<1 year	2 (8.3%)	1 (1.5%)	<0.001
1–3 years	1 (4.2%)	5 (7.7%)	
4–6 years	2 (8.3%)	6 (9.2%)	
7–11 years	1 (4.2%)	37 (57%)	
12–16 years	18 (75%)	16 (24.6%)	
Laterality (n %)			0.28
Right side	8 (33.3%)	33 (50%)	
Left side	16 (66.6%)	32 (48.5%)	
Both sides	0 (0%)	1 (1.5%)	
History of trauma			0.50
Yes	2 (8.3%)	11 (16.7%)	
No	22 (91.7%)	55 (83.3%)	
Presenting clinical symptoms			
Scrotal pain (n %)	20 (83.3%)	65 (98.5%)	0.02
Erythema (n %)	20 (83.3%)	51 (77.3%)	0.77
Swelling (n %)	13 (54.2%)	44 (66.6%)	0.33
Nausea/vomiting (n %)	7 (29.2%)	3 (4.5%)	0.003
Abdominal pain (n %)	6 (25%)	0 (0%)	<0.001
Fever (n %)	2 (8.3%)	0 (0%)	0.07
Duration of symptoms mean: 24 hours, median: 48 hours (range, 30 minutes – 480 hours)			
≤6 hours	9 (37.5%)	7 (10.6%)	<0.001
6–12 hours	0 (0%)	4 (6%)	
12–24 hours	7 (29.2%)	5 (7.5%)	
>24 hours	8 (33.3%)	50 (75.7%)	
Season			0.31
Spring	4 (16.6%)	18 (27.2%)	
Summer	8 (33.3%)	11 (16.7%)	
Autumn	7 (29.2%)	18 (27.2%)	
Winter	5 (21%)	19 (28.7%)	
Color Doppler ultrasound findings			
Absent/decreased flow	23 (96%)	5 (7.5%)	<0.001
Increased/normal flow	1 (4%)	61 (92.5%)	

Only significant variable values are bolded. *Age is missing for one patient in this category. SD – standard deviation

Table 2 – The duration of symptoms was significantly associated with the treatment options ($p=0.008$, Fisher's exact test). Similar results (77.5% vs. 37.5%) were obtained when the variable duration of symptoms was dichotomized by the median value (12 hours) ($p=0.038$, Fisher's exact test)

Patients with testicular torsion (n=24)		Treatment		Total
		orchidectomy	orchidopexy	
Duration of symptoms	<42 hours*	4 (25.0%)	12 (75.0%)	16 (100%)
	>42 hours	7 (87.5%)	1 (12.5%)	8 (100%)
Total		11 (46.0%)	13 (54.0%)	24 (100%)

*the mean value dichotomized the variable

pain (without recorded accurate localization of tenderness and its intensity) was statistically more present in TAT patients ($p=0.02$). In contrast, nausea/vomiting and abdominal pain occurred more frequently among the TT patients ($p=0.003$ and $p<0.001$, respectively). Notably, fever and abdominal pain did not affect TAT patients (Table 1).

The mean duration of symptoms for the entire cohort was 63.3 hours (range 30 minutes to 480 hours) with a median of 48 hours. The mean duration of symptoms was significantly shorter in the TT group (42 hours, range, 1–336 hours with a median of 12 hours) than in the TAT group (71 hours, range, 1–480 hours with a median of 48 hours) ($p<0.001$).

Among twenty-four patients with TT, 11 cases (46%) had undergone orchidectomy, and 13 cases (54%) had orchidopexy (Table 2). The duration of symptoms significantly impacted the treatment outcome (orchidectomy vs. orchidopexy, $p=0.008$) (Table 2).

There was no significant difference in the seasons of onset between TT patients and those with TAT ($p=0.31$). The lowest TT cases (21%) were recorded during the winter, whereas the largest TAT cases (28.7%) were recorded during the same season.

Most cases (91.7% of TT and 83.3% of TAT cases) had spontaneous torsion, whereas the remaining 8.3% of TT cases and 16.3% of TT cases were trauma-related. However, the difference was not statistically significant ($p=0.50$).

Ultrasonographically, the two diseases presented strikingly different. Thus, twenty-three patients with TT (96%) and only five patients with TAT (7.5%) showed absent or decreased testicular blood flow in the affected testes, whereas 61 (92.5%) patients with TAT and only 1 (4%) patient with TT showed increased or normal testicular blood flow in the affected testes (Table 1). CDUS findings of absent or decreased testicular blood flow in the affected testes significantly correlated with TT's presence ($p<0.001$). In contrast, CDUS findings of increased or normal blood flow significantly correlated with the presence of TAT ($p<0.001$).

Discussion

It is well documented that TAT is the most common cause of AS in children who underwent scrotal exploration (Murphy et al., 2006). Emergency scrotal exploration is the standard management means, as no other investigation can confidently exclude TT from the differential diagnosis of AS (Cavusoglu et al., 2005). Our results for the occurrence of TT and TAT are in line with the previous studies (Van Glabeke et al., 1999; McAndrew et al., 2002; Mushtaq et al., 2003; Cavusoglu et al., 2005; Murphy et al., 2006; Yang et al., 2011). Of pediatric patients with AS who underwent emergency surgery, TT is the cause of 17–72% of cases (Van Glabeke et al., 1999; Mushtaq et al., 2003; Cavusoglu et al., 2005; Yang et al., 2011). In our study, TT occurred in ~27% of cases, whereas TAT affected 73% of the AS patients. Like other studies (Ciftci et al., 2004), the patients with TT were the eldest, and their presentation was the earliest compared with the TAT patients.

Consistent with previous studies, our findings of 24 TT patients indicate that this condition occurs more frequently on the left side (Marulaiah et al., 2010; Mukendi et al., 2020). This could be anatomically related to the greater length of the left spermatic cord, which is more prone to twisting (Williamson, 1976). Data in the literature on the association between age and laterality of TT are scarce. Our finding that right-sided TT increases in adolescent patients is consistent with the study conducted by Mukendi et al. (2020). Further studies on a larger sample are necessary to determine the clinical significance of this association.

A history of nausea/vomiting and abdominal pain, as markers of a systemic response to an ischemic event in the body secondary to celiac ganglion stimulation, strongly suggest TT. However, they are absent in more than two-thirds of patients. Similar results have been reported in other studies (Hegarty et al., 2001; Srinivasan et al., 2011). Furthermore, a series of children with TT who presented with abdominal pain without testicular pain were also reported (Pogorelic et al., 2019; Wang and Mo, 2019).

The presence of only abdominal pain or other nonspecific symptoms (nausea, vomiting or urinary symptoms) may delay the diagnosis and treatment with an increased incidence of testicular loss. In our study, only 2/24 (8.3%) of patients with TT had nonspecific symptoms without testicular pain, which is in line with previous studies by Pogorelic et al. (2019) and Wang and Mo (2019). Both patients from our cohort were misdiagnosed as having abdominal diseases. Later surgical exploration revealed that both testicles had necrotized because of the ischemia time, and consequently, an orchidectomy was performed.

We believe that the higher frequency of scrotal pain in patients with TAT could be explained by the lack of registration of the exact localization of pain and the initial presentation of a larger number of patients with advanced local scrotal findings.

Our previous study showed that the duration of symptoms is the most crucial predictor of testicular salvage following TT in children (Zvizdic et al., 2021). In the present study, the duration of symptoms was significantly different between

the two groups. Like another study (Fujita et al., 2017), our patients with TT had a significantly shorter time to presentation than patients with TAT. This could be explained by the more extensive symptoms caused by TT compared with TAT symptoms, leading to an earlier visit to the doctor.

In our cohort, we found that the laterality of TT to the right side increases in adolescence. We noted that more than half of adolescent boys aged ≥ 12 presented with right-sided TT. Documented data in the literature on the association between age and laterality of TT are very scarce. The relationship between age and laterality of TT was investigated in only one study conducted in South Africa, which included 308 patients from 10 years old and above (Mukendi et al., 2020). They found that boys aged ≥ 16 years are 1.5 times more likely to present with right-sided TT than those < 16 years of age, though the difference was not significant (Mukendi et al., 2020). Further studies are needed to elucidate this possible association between older adolescent age and right-sided TT.

The seasonal influence on TT or TAT is contradictory in the current literature. While some studies have found a link between cold weather and TT and TAT (Lyronis et al., 2009; Molokwu et al., 2020), other studies failed to provide this evidence (Cost et al., 2011). Our study has not found a positive association between cold weather and TT.

Although most TT and TAT cases develop spontaneously, the causes of TT and TAT may be trauma-related (sports or physical activity) in $\sim 5\%$ of cases (Ringdahl and Teague, 2006). History of trauma was present in 8.3% of TT cases and 16.7% of TAT cases. Our study did not reveal a significant difference in the history of trauma between the examined groups.

CDUS has substantially improved patients' clinical assessment with AS, determining TT's presence and the extent and reducing the unnecessary exploration rate (Lam et al., 2005; Sung et al., 2012). On sonography, the torsed testis may be enlarged and appear hypoechoic, but sometimes it can appear normal, particularly in the first few hours (Sung et al., 2012). In the evaluation of AS, CDUS has a sensitivity of $\sim 64\text{--}100\%$ and a specificity of $97\text{--}100\%$, showing reduced or absent blood flow to the testis as a highly specific finding in most TT patients (Chmelnik et al., 2010). However, false-negative and false-positive Doppler evaluations in the diagnosis of TT have been reported in the literature. Our study's data further support the excellent clinical utility of CDUS in differentiating between TT and TAT.

Due to the common practice at our institution that scrotal exploration is considered the procedure of choice for acute scrotum, a reasonably large number of scrotal explorations of the acute scrotum during the study period were operatively diagnosed as torsion of testicular appendages. Some other studies have supported this approach. According to Murphy et al. (2006), prompt surgical intervention in all patients with AS can minimize testicular loss. Surgical treatment of twisted appendages is safe, allowing accurate diagnosis and pain relief with minimal morbidity (Tanaka et al., 2020). However, as a positive consequence of the results

of this study, we believe that this dogmatic attitude will be replaced with a more conservative approach to patients with TAT in our local setting.

There are several limitations to our study. First, it is a retrospective observational study; second, it comprises a smaller number of patients with TT; and third, the study was conducted in a single institution, limiting its generalizability. The present study also lacks some essential clinical data, such as a lack of precise localization of scrotal pain.

In conclusion, distinguishing TT from other acute scrotal pathology, including TAT, is crucial for timely surgical intervention and preservation of testes affected by AS. Older age, nausea/vomiting, abdominal pain, shorter duration of symptoms, and CDUS findings of absent or decreased testicular blood flow in the affected testis can distinguish between TT and TAT.

This article was previously accepted by another journal. After that, the authors withdrew it because of unacceptable post-editing of the manuscript by its editorial office.

References

- Boettcher, M., Bergholz, R., Krebs, T. F., Wenke, K., Aronson, D. C. (2012) Clinical predictors of testicular torsion in children. *Urology* **79(3)**, 670–674.
- Cavusoglu, Y. H., Karaman, A., Karaman, I., Erdogan, D., Aslan, M. K., Varlikli, O., Cakmak, O. (2005) Acute scrotum – Etiology and management. *Indian J. Pediatr.* **72(3)**, 201–203.
- Chmelnik, M., Schenk, J. P., Hinz, U., Holland-Cunz, S., Gunther, P. (2010) Testicular torsion: Sonomorphological appearance as a predictor for testicular viability and outcome in neonates and children. *Pediatr. Surg. Int.* **26(3)**, 281–286.
- Ciftci, A. O., Senocak, M. E., Tanyel, F. C., Buyukpamukcu, N. (2004) Clinical predictors for differential diagnosis of acute scrotum. *Eur. J. Pediatr. Surg.* **14(5)**, 333–338.
- Cost, N. G., Bush, N. C., Barber, T. D., Huang, R., Baker, L. A. (2011) Pediatric testicular torsion: Demographics of national orchiopexy versus orchiectomy rates. *J. Urol.* **185**, 2459–2463 (Suppl. 6).
- Fujita, N., Tambo, M., Okegawa, T., Higashihara, E., Nutahara, K. (2017) Distinguishing testicular torsion from torsion of the appendix testis by clinical features and signs in patients with acute scrotum. *Res. Rep. Urol.* **9**, 169–174.
- Gatti, J. M., Murphy, J. P. (2008) Acute testicular disorders. *Pediatr. Rev.* **29(7)**, 235–241.
- Hart, J., Pastore, G., Jones, M., Barker, A., Khosa, J., Samnakay, N. (2016) Chronic orchalgia after surgical exploration for acute scrotal pain in children. *J. Pediatr. Urol.* **12(3)**, 168.e1–168.e6.
- Hegarty, P. K., Walsh, E., Corcoran, M. O. (2001) Exploration of the acute scrotum: A retrospective analysis of 100 consecutive cases. *Ir. J. Med. Sci.* **170(3)**, 181–182.
- Kumar, V., Matai, P., Prabhu, S. P., Sundeeep, P. T. (2020) Testicular loss in children due to incorrect early diagnosis of torsion. *Clin. Pediatr. (Phila.)* **59(4–5)**, 436–438.
- Lala, S., Price, N., Upadhyay, V. (2019) Re-presentations and recurrent events following initial management of the acute paediatric scrotum: A 5-year review. *ANZ J. Surg.* **89(4)**, E117–E121.
- Lam, W. W., Yap, T. L., Jacobsen, A. S., Teo, H. J. (2005) Colour Doppler ultrasonography replacing surgical exploration for acute scrotum: Myth or reality? *Pediatr. Radiol.* **35(6)**, 597–600.
- Lemini, R., Guana, R., Tommasoni, N., Mussa, A., Di Rosa, G., Schleaf, J. (2016) Predictivity of clinical findings and Doppler ultrasound in pediatric acute scrotum. *Urol. J.* **13(4)**, 2779–2783.

- Lyronis, I. D., Ploumis, N., Vlahakis, I., Charissis, G. (2009) Acute scrotum – Etiology, clinical presentation and seasonal variation. *Indian J. Pediatr.* **76(4)**, 407–410.
- Maruliah, M., Gilhotra, A., Moore, L., Boucaut, H., Goh, D. W. (2010) Testicular and paratesticular pathology in children: A 12-year histopathological review. *World J. Surg.* **34(5)**, 969–974.
- McAndrew, H. F., Pemberton, R., Kikiros, C. S., Gollow, I. (2002) The incidence and investigation of acute scrotal problems in children. *Pediatr. Surg. Int.* **18(5–6)**, 435–437.
- Molokwu, C. N., Ndoumbe, J. K., Goodman, C. M. (2020) Cold weather increases the risk of scrotal torsion events: Results of an ecological study of acute scrotal pain in Scotland over 25 years. *Sci. Rep.* **10(1)**, 17958.
- Mukendi, A. M., Kruger, D., Haffejee, M. (2020) Characteristics and management of testicular torsion in patients admitted to the Urology Department at Chris Hani Baragwanath Academic Hospital. *Afr. J. Urol.* **26**, 34.
- Murphy, F. L., Fletcher, L., Pease, P. (2006) Early scrotal exploration in all cases is the investigation and intervention of choice in the acute paediatric scrotum. *Pediatr. Surg. Int.* **22(5)**, 413–416.
- Mushtaq, I., Fung, M., Glasson, M. J. (2003) Retrospective review of paediatric patients with acute scrotum. *ANZ J. Surg.* **73(1–2)**, 55–58.
- Pogorelic, Z., Mustapic, K., Jukic, M., Todoric, J., Mrkic, I., Messtrovic, J., Juric, I., Furlan, D. (2016) Management of acute scrotum in children: A 25-year single center experience on 558 pediatric patients. *Can. J. Urol.* **23(6)**, 8594–8601.
- Pogorelic, Z., Neumann, C., Jukic, M. (2019) An unusual presentation of testicular torsion in children: A single-centre retrospective study. *Can. J. Urol.* **26(6)**, 10026–10032.
- Pogorelic, Z., Milanovic, K., Versic, A. B., Pasini, M., Divkovic, D., Pavlovic, O., Lucev, J., Zufic, V. (2021) Is there an increased incidence of orchiectomy in pediatric patients with acute testicular torsion during COVID-19 pandemic? A retrospective multicenter study. *J. Pediatr. Urol.* **17(4)**, 479.e1–479.e6.
- Ringdahl, E., Teague, L. (2006) Testicular torsion. *Am. Fam. Physician* **74(10)**, 1739–1743.
- Srinivasan, A., Cinman, N., Feber, K. M., Gitlin, J., Palmer, L. S. (2011) History and physical examination findings predictive of testicular torsion: An attempt to promote clinical diagnosis by house staff. *J. Pediatr. Urol.* **7(4)**, 470–474.
- Sung, E. K., Setty, B. N., Castro-Aragon, I. (2012) Sonography of the pediatric scrotum: Emphasis on the Ts – Torsion, trauma, and tumors. *AJR Am. J. Roentgenol.* **198(5)**, 996–1003.
- Tanaka, K., Ogasawara, Y., Nikai, K., Yamada, S., Fujiwara, K., Okazaki, T. (2020) Acute scrotum and testicular torsion in children: A retrospective study in a single institution. *J. Pediatr. Urol.* **16(1)**, 55–60.
- Van Glabeke, E., Khairouni, A., Larroquet, M., Audry, G., Gruner, M. (1999) Acute scrotal pain in children: Results of 543 surgical explorations. *Pediatr. Surg. Int.* **15(5–6)**, 353–357.
- Vijayaraghavan, S. B. (2006) Sonographic differential diagnosis of acute scrotum: Real-time whirlpool sign, a key sign of torsion. *J. Ultrasound Med.* **25(5)**, 563–574.
- Wang, F., Mo, Z. (2019) Clinical evaluation of testicular torsion presenting with acute abdominal pain in young males. *Asian J. Urol.* **6(4)**, 368–372.
- Williamson, R. C. (1976) Torsion of the testis and allied conditions. *Br. J. Surg.* **63(6)**, 465–476.
- Yang, C., Song, B., Tan, J., Liu, X., Wei, G. H. (2011) Testicular torsion in children: A 20-year retrospective study in a single institution. *ScientificWorldJournal* **11**, 362–368.
- Zvzidic, Z., Aganovic, A., Milisic, E., Jonuzi, A., Zvzidic, D., Vranic, S. (2021) Duration of symptoms is the only predictor of testicular salvage following testicular torsion in children: A case-control study. *Am. J. Emerg. Med.* **41**, 197–200.

Rehabilitation of Dentofacial Asymmetry Secondary to Unilateral Temporomandibular Joint Ankylosis with Dual Distraction and Fixed Orthodontics – Stability at Three-year Follow-up

**Harpreet Singh¹, Sonal Mishra², Dhirendra Srivastava²,
Poonam Sharma¹, Lokesh Chandra², Pranav Kapoor¹,
Raj Kumar Maurya³**

¹Department of Orthodontics and Dentofacial Orthopedics, ESIC Dental College and Hospital, New Delhi, India;

²Department of Oral and Maxillofacial Surgery, ESIC Dental College and Hospital, New Delhi, India;

³Department of Orthodontics, Central Government Dental Unit, Dehradun, India

Received November 27, 2022; Accepted August 17, 2023.

Key words: Dual distraction – One-stage approach – Orthodontics – Stability – Temporary anchorage device – Unilateral TMJ ankylosis

Abstract: Optimal rehabilitation of asymmetric dentofacial deformity secondary to unilateral temporomandibular joint (TMJ) ankylosis is often a challenge. The purpose of this case series is to present an insight into esthetic, occlusal and functional rehabilitation of two patients with varying degree of asymmetric Class II dentofacial deformities secondary to long-standing unilateral TMJ ankylosis. The patients were treated with one-stage surgical protocol employing simultaneous dual distraction technique along with interpositional arthroplasty. Dual distraction technique entailed the simultaneous use of two distractors which allowed for proper control of proximal condylar segment during the course of distraction and lowering the risk of ankylosis recurrence. Thereafter, comprehensive fixed orthodontic mechanotherapy involving the use of temporary anchorage devices was instituted to align and level the compensated dentition. Post-treatment records showed significant improvements in skeletal disharmony and functional stability with good functional occlusion. At the three-year follow-up, the morphological and functionally acceptable results

Mailing Address: Dr. Sonal Mishra, 7/105 A, Shayanika Apartments, Flat No. 101, Tilak Nagar Crossing Street, Swaroop Nagar, Kanpur 208002, Uttar Pradesh, India; e-mail: sonal.816@gmail.com

<https://doi.org/10.14712/23362936.2023.21>

© 2023 The Authors. This is an open-access article distributed under the terms of the Creative Commons Attribution License (<http://creativecommons.org/licenses/by/4.0>).

were reasonably well-maintained, with no signs of relapse. Through the two cases reported here, we would like to highlight that one-stage concurrent arthroplasty and dual distraction technique is a safe, stable, and reliable approach for surgical and functional rehabilitation of an adult asymmetric dentofacial deformity secondary to unilateral TMJ ankylosis. Meticulously executed comprehensive orthodontic manipulations involving use of acrylic bite-blocks, elastic traction, and temporary skeletal anchorage device play a crucial role in enhancing the final occlusal outcomes.

Introduction

In spite being one of the most prevalent and disfiguring craniofacial anomaly, asymmetric dentofacial deformity due to unilateral temporomandibular joint (TMJ) ankylosis often presents a complex therapeutic challenge (Zhu et al., 2013). Increased severity of muscular atrophy with laterognathism and retrognathism due to prolonged duration of associated hypomobility further compounds the challenging treatment process (Motta et al., 2007). Additionally, it becomes challenging to correct facial asymmetry among these patients by maintaining balance of optimum craniofacial health and cost-economic aspects to achieve satisfactory treatment goals (Zhu et al., 2013; De Roo et al., 2016).

Numerous treatment techniques, such as ramus osteotomy, high condylectomy, coronoidectomy, gap arthroplasty, interpositional gap arthroplasty, reconstruction of the joint using autogenous grafts, alloplastic materials or vascularised flaps, distraction osteogenesis, early mobilization, and aggressive physiotherapy, have been widely employed for the management of TMJ ankylosis and associated asymmetric skeletal deformities (De Roo et al., 2016).

One-stage surgery involving simultaneous gap arthroplasty and distraction osteogenesis has proven to be a viable option in the treatment of TMJ ankylosis and coexisting severe micrognathia in aptly selected cases (Dean and Alamillos, 1999; Yu et al., 2009; Giraddi et al., 2016; Sharma et al., 2016). Even so, an issue of concern to the surgeon is the potential for encroachment on the gap (arthroplasty) by the proximal segment (Srivastava et al., 2019). Moreover, the management of malocclusion after distraction osteogenesis is also fraught with challenges and is often not documented to a satisfactory degree in the literature.

The purpose of this case series is to present an insight into esthetic, occlusal and functional rehabilitation of two patients with varying degree of asymmetric Class II dentofacial deformities secondary to long-standing unilateral TMJ ankylosis. The patients were treated with one-stage surgical protocol employing simultaneous dual distraction technique along with interpositional arthroplasty. The long-term followed-up occlusal outcomes are detailed in which postdistraction orthodontic treatment following single-step simultaneous dual distraction and interpositional arthroplasty helped align and level the compensated dentition. Furthermore, the merits of dual distraction technique and factors governing stability of treatment results are also discussed.

Case report

Case 1

A 21-year-old adult male presented seeking treatment for facial asymmetry and chewing difficulties with reduced mouth-opening (Figure 1). He had a history of facial trauma due to fall at the age of 5 years.

On extraoral examination, the patient exhibited facial asymmetry involving the lower third of the face, with lateral deviation of the mandibular symphysis towards the left, a severely retrognathic mandible and limited interincisal opening of 10 mm.

Intraorally, an asymmetric sagittal occlusal relationship was observed: Class I molar and canine relations on the right side and Class II occlusion on the left side. Overjet

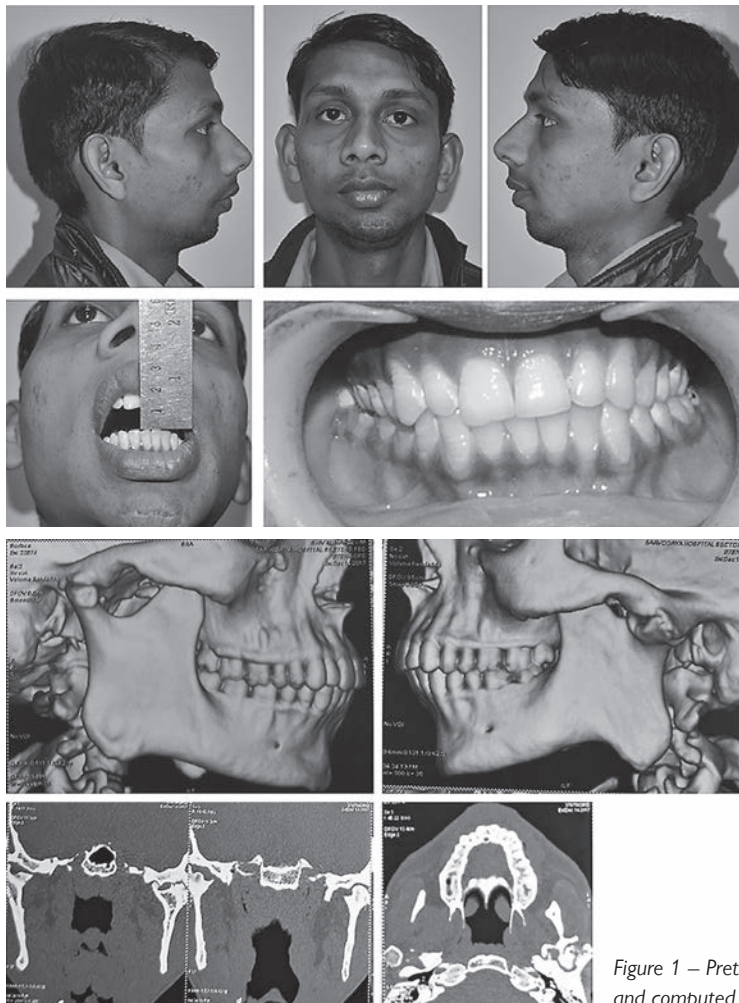


Figure 1 – Pretreatment photographs and computed tomography images.

and overbite were 3 mm and 4 mm, respectively. Mild crowding was noted in lower arch. The occlusal plane canted slightly superior on the left side and the mandibular dentoalveolar midline was deviated toward the left by 4.5 mm in relation to upper dentoalveolar midline. Pretreatment non contrast computed tomographic (NCCT) images revealed a bony ankylotic mass on the medial aspect of left TMJ, and a deformed condylar head, glenoid fossa and zygomatic arch on the right side (Figure 1).

The patient was diagnosed with an asymmetric Class II dentofacial deformity (with mandibular laterognathism and retrognathism) caused by unilateral TMJ ankylosis.

The treatment goals were to improve the diminished mouth opening by mobilizing the TMJ on the left side, improve the asymmetric facial appearance and mandibular position, and establish a normal intermaxillary relationship with a Class I molar occlusion.

Considering the history of ankylosis and long-standing severity of preoperative mouth opening limitation and low self-esteem caused by associated mandibular deformity, simultaneous execution of gap arthroplasty and dual distraction osteogenesis were contemplated to obtain adequate mouth-opening range (35 mm) and restoration of facial symmetry with stable jaw form and function. Thereafter, postdistraction orthodontic treatment was planned for levelling and aligning the dentition over the respective alveolar bases, guiding the selective eruption of teeth, correction of cross-bite and transverse inter-occlusal disharmony.

Treatment progress

The active treatment comprised of surgical phase involving simultaneous interpositional arthroplasty and dual distraction in phase 1 of treatment, accompanied by fixed orthodontic mechanotherapy in phase 2.

Initially, in a one-stage operation under general anaesthesia, interpositional arthroplasty with temporalis myofascial flap was performed to release left TMJ ankylosis (Figure 2). Concomitantly, in accordance with the protocol of Srivastava et al. (2019), two custom-fabricated extraoral monofocal/univector distractors were affixed at two different predetermined locations on the left side. Distractor A, with its vector oriented parallel to posterior border of the ramus, was used to maintain the gap created after removal of the ankylotic segment and, if indicated, also to increase the gap following activation. Another distractor B, positioned obliquely, was utilized to increase the ramus and body's vertical and the horizontal dimensions of the ramus and body, respectively, thus facilitating correction of the mandibular asymmetry (Figure 3). Following the completion of distractor B's distraction phase, distractor A was removed, and active physical therapy was initiated. During the consolidation phase, occlusal acrylic splints and elastics were used as internal fixators to counteract the vertical downward pull by supra-omohyoid group of muscles, mould the callus and obtain occlusal guidance. Following the radiographic appearance of the cortical outline on the callus during consolidation, distractor B was removed.

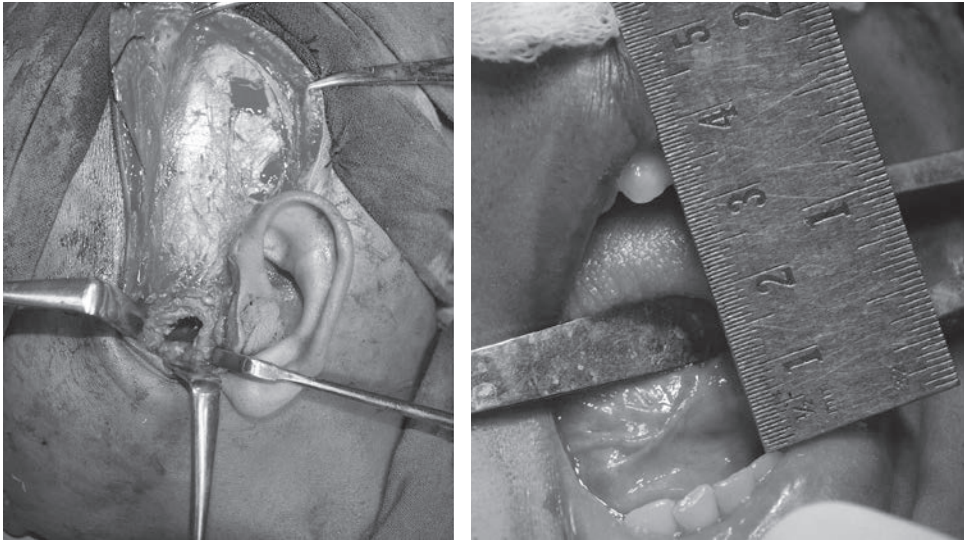


Figure 2 – Intraoperative photograph showing increased mouth opening achieved after arthroplasty.



Figure 3 – Interdistraction photographs showing dual distraction and radiographs taken during consolidation phase after distraction.

A total of 12 mm of distraction was performed at a rate of 0.5 mm twice a day, followed by a 12-week consolidation phase. Post-distraction, mandibular symmetry was restored along with discernible reduction in facial convexity. Desired overcorrection of the mandibular midline was achieved with the appearance of Class III incisal relationship and reverse overjet of 2 mm (Figure 4).

At 3 months postdistraction, mandibular right central incisor was extracted and full fixed 0.022×0.028-inch preadjusted Edgewise appliances were placed in both arches in phase 2 of treatment. Alignment and levelling were performed with

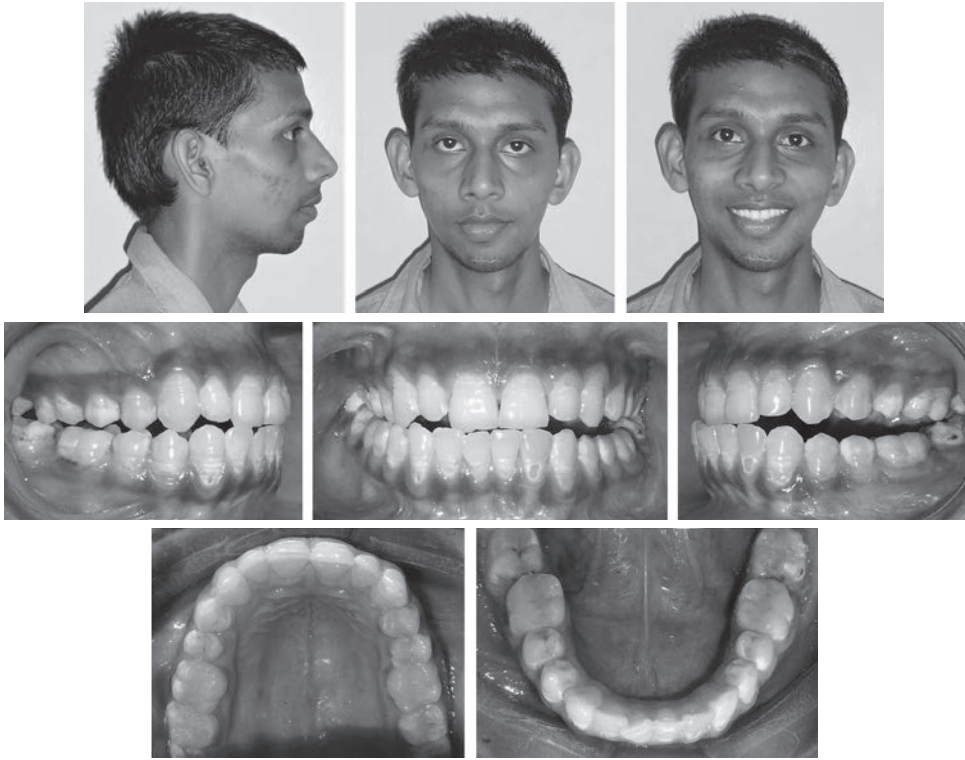


Figure 4 – Postdistraction extraoral and intraoral photographs demonstrating improved facial symmetry and appearance of incisal Class III relationship, posterior open bite on the left and crossbite on the right side.

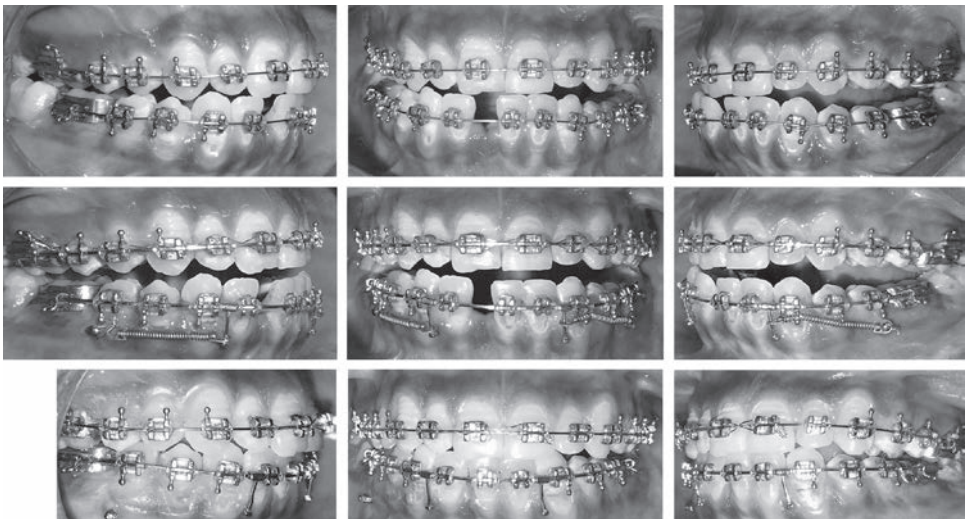


Figure 5 – Treatment progress photographs demonstrating levelling, aligning and miniscrew supported retraction of mandibular incisors during postdistraction orthodontic phase.

0.016-inch nickel-titanium (NiTi) and 0.017×0.025-inch superelastic NiTi wires. The lower incisors were retracted on a 0.019×0.025-in continuous stainless-steel (SS) wire using direct anchorage from temporary anchorage devices (TADs) i.e., mini-implants (6.0 mm long, 1.6 mm in diameter; Absoanchor – Dentos, Deagu, South Korea) inserted bilaterally into the interradicular attached gingiva between the mandibular second premolars and the first molars. 0.014-inch SS wires were used during detailing and settling phases (Figure 5). The overall treatment time including

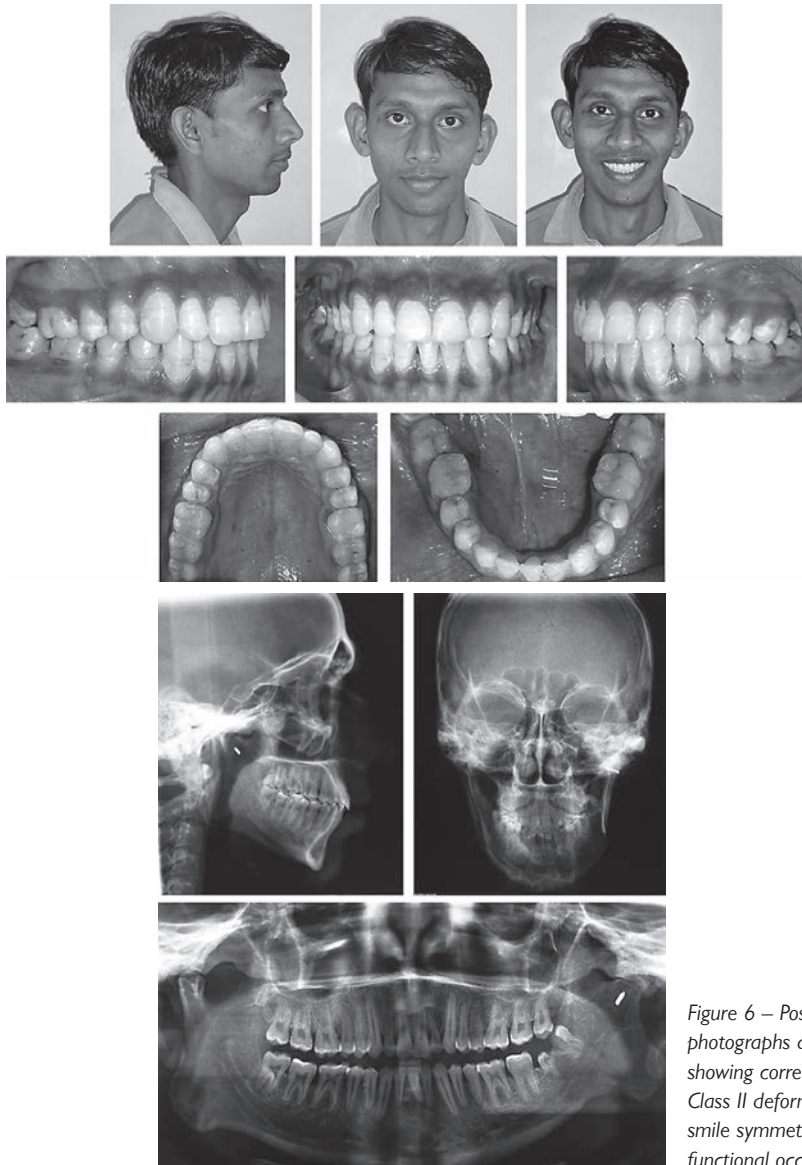


Figure 6 – Posttreatment photographs and radiographs showing corrected asymmetric Class II deformity with restored smile symmetry and Class I functional occlusion.



Figure 7 – Three-year follow-up extraoral and intraoral photographs depicting well-maintained stable results.

distraction osteogenesis (DO) was 20 months. After debonding, circumferential Hawley-type retainers were delivered for full-time wear for one year.

Treatment results

Post-treatment records showed significant improvements in facial aesthetics and profile, elimination of facial asymmetry, along with establishment of normal overjet, overbite and Class I canine-guided functional occlusion (Figure 6). The maxillary dentoalveolar midline coincided with the middle of the mandibular central incisor, without any aesthetic compromise. Panoramic radiograph demonstrated satisfactory root parallelism and no evidence of apical root resorption. After three years, the occlusion remained stable with well-maintained harmonious facial balance (Figure 7).

Case 2

The patient was a 24-year-old female with chief complaints of asymmetrical appearance, backwardly positioned chin and limited mouth opening. She exhibited inferiority complex with very low self-esteem. Her medical records revealed history of trauma to the mandible in childhood. Extraoral clinical examination revealed severe facial asymmetry with mandibular laterognathism to the left side and marked deficiency in the lower third of the face with severe mandibular retrognathism. The chin projection was inadequate, mimicking a bird face deformity. Facial atrophy was

observed on the right side of the chin. The maximum mouth opening was 11 mm due to the bony ankylosis of left TMJ. Intraorally, she exhibited a Class I malocclusion on the right and Class II on the left. Mandibular dentoalveolar midline deviation of 5 mm to the left side was observed (Figure 8).



Figure 8 – Pretreatment extraoral and intraoral photographs showing severe facial asymmetry with bird face deformity, limited mouth opening and malocclusion.

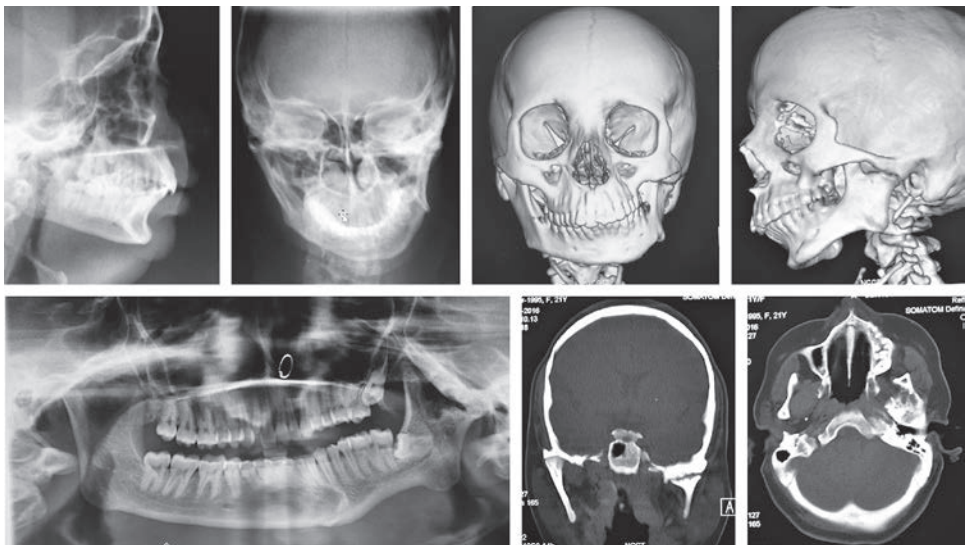


Figure 9 – Pretreatment radiographs and computed tomography images. Figure 9C (top row, third figure) is reprinted from *Journal of Oral and Maxillofacial Surgery*, 77/12, Dhirendra Srivastava, Payal Luthra, Sonal Mishra, Lokesh Chandra, Sarang Sharma, Harpreet Singh, Technique of Dual Distraction for Correction of Unilateral Temporomandibular Joint Ankylosis with Facial Asymmetry: A Case Series, 2555.e1–2555.e12. Copyright (2019), with permission from Elsevier.

Lateral cephalogram exhibited an obvious skeletal Class II relationship with severe mandibular retrusion. Dental compensations were observed in maxillary and mandibular dentitions. Postero-anterior cephalogram showed significant facial asymmetry with deviation of the chin point to the left side by 7 mm relative to the facial midline. The disparity in ramus sizes between the left and right sides, as well as impacted maxillary and mandibular left third molars, were evident on panoramic radiograph. NCCT of TMJ revealed deformed, flattened and mediolaterally widened left condylar process with irregular articular surface and reduced joint space, indicative of bony ankylosis of left TMJ (Figure 9).

Treatment objectives were to restore the joint function, correct the asymmetric retrognathic mandibular and chin deformity caused by left TMJ ankylosis, enhance her facial appearance and profile, and establish acceptable facial harmony. Orthodontic objectives included stabilization of post-surgical outcomes, harmonization of upper and lower arch forms, establishment of normal overjet, overbite and a stable functional occlusion.

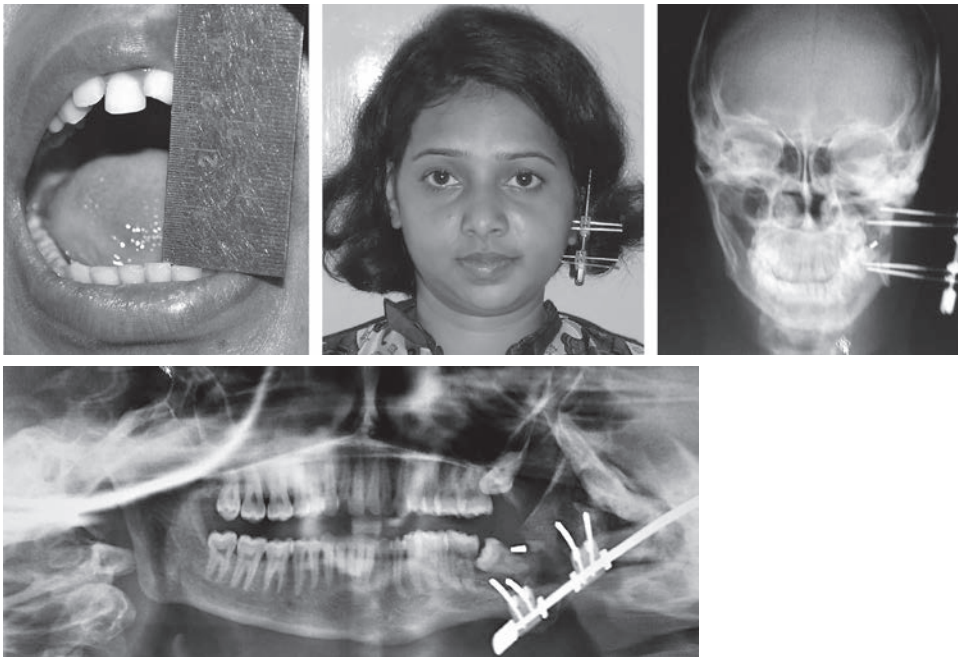


Figure 10 – Photographs showing improved mouth opening following arthroplasty, corrected mandibular asymmetry and radiographs during consolidation phase. Figure 10C (top row, third figure) is reprinted from *Journal of Oral and Maxillofacial Surgery*, 77/12, Dhirendra Srivastava, Payal Luthra, Sonal Mishra, Lokesh Chandra, Sarang Sharma, Harpreet Singh, *Technique of Dual Distraction for Correction of Unilateral Temporomandibular Joint Ankylosis with Facial Asymmetry: A Case Series*, 2555.e1–2555.e12. Copyright (2019), with permission from Elsevier.



Figure 11 – Postdistraction extraoral and intraoral photographs demonstrating improved facial symmetry, profile esthetics and appearance of Class III incisal relationship, left posterior open bite and right posterior cross bite. Figure 11B, D, E, F (top row middle figure; middle row all figures) is reprinted from *Journal of Oral and Maxillofacial Surgery*, 77/12, Dhirendra Srivastava, Payal Luthra, Sonal Mishra, Lokesh Chandra, Sarang Sharma, Harpreet Singh, *Technique of Dual Distraction for Correction of Unilateral Temporomandibular Joint Ankylosis with Facial Asymmetry: A Case Series*, 2555.e1–2555.e12. Copyright (2019), with permission from Elsevier.

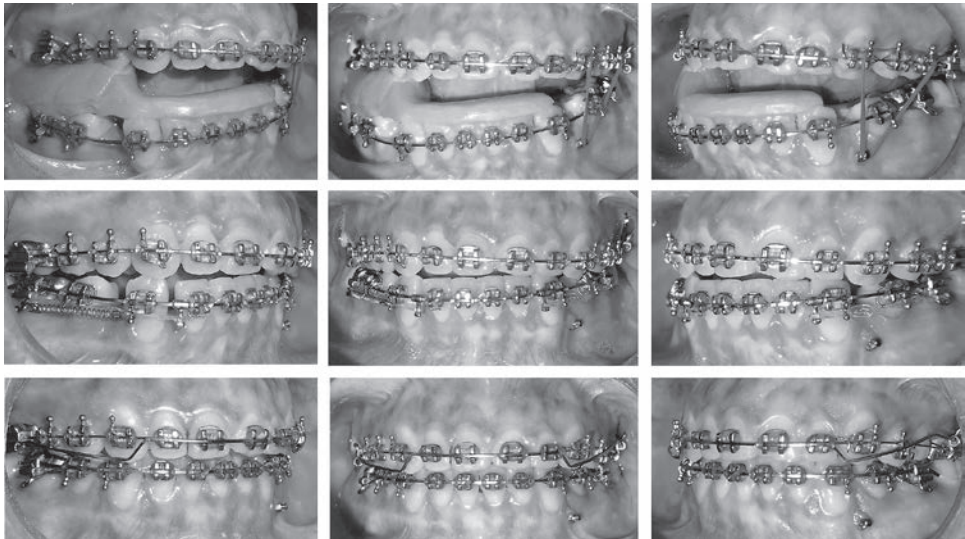


Figure 12 – Treatment progress photographs showing aligning of arches, and utilization of acrylic bite-block, elastic traction, and a temporary skeletal anchorage device for levelling of the cant of maxillary occlusal plane.

Treatment progress

At the outset, interpositional arthroplasty for release of TMJ ankylosis and establishment of adequate mouth-opening range, along with dual distraction for correction of asymmetric Class II deformity were performed simultaneously as single-step surgical procedures.

After achieving the desired ramal and mandibular lengthening, the distraction devices were maintained for 5 months until cortical outline was visible in

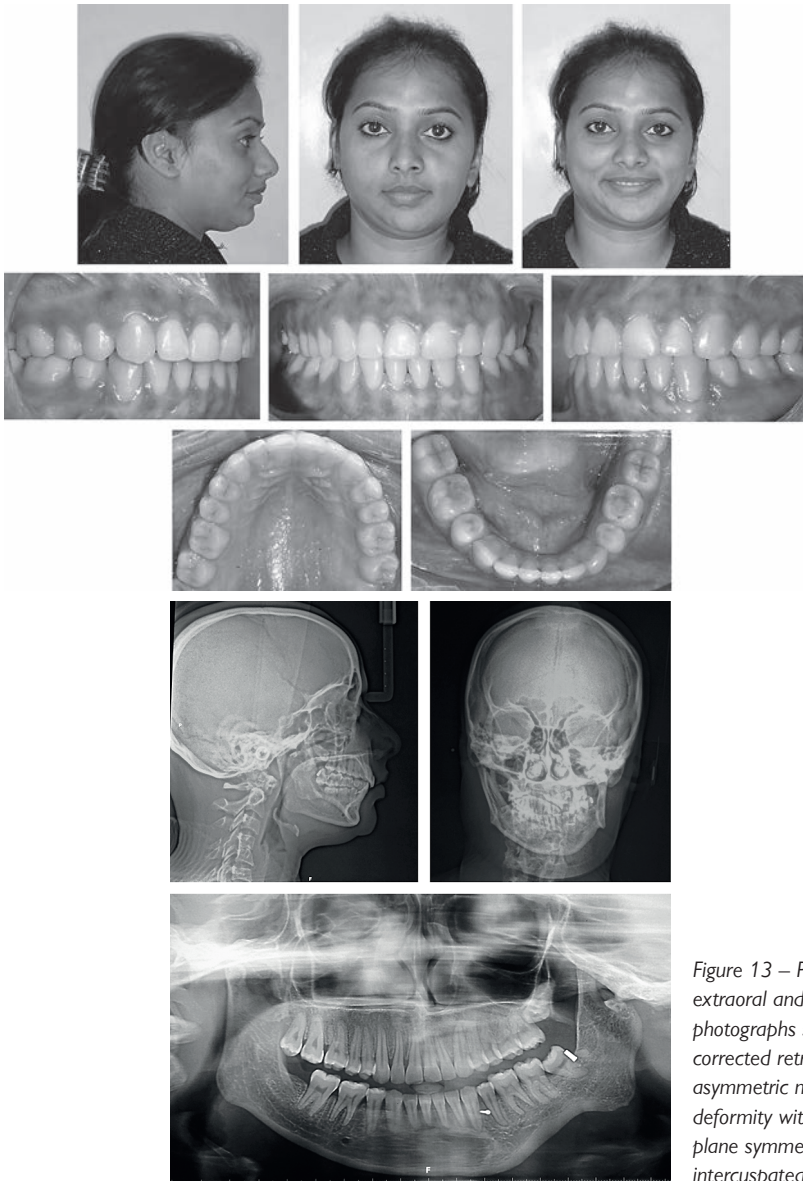


Figure 13 – Posttreatment extraoral and intraoral photographs showing corrected retrognathic and asymmetric mandibular deformity with restored occlusal plane symmetry and well-intercusated occlusion.

radiographs. A total of 13 mm of distraction was performed at a rate of 0.5 mm twice a day, accompanied by consolidation period of 16 weeks. Post-distraction, the mandibular retrusion considerably reduced and significant improvements in facial appearance were achieved (Figure 10).

However, intraorally, transient malocclusion developed with reverse overjet of 4 mm, posterior open bite on the elongated side and a crossbite on the contralateral side (Figure 11). Post-distraction orthodontic treatment was instituted following extractions of mandibular right and left first premolars and placement of 0.22×0.28-inch fixed appliances. Dental impressions were taken, and a lingual-arch supported acrylic bite-block covering the incisal edges of mandibular anterior teeth was cemented in the lower arch. To facilitate quick en-masse posterior levelling of the maxillary occlusal plane, sectional wires were hinged between the left canine and first molar, and vertical traction using elastics was applied by a mandibular miniscrew to maxillary left buccal segment. Following correction of the cant of maxillary occlusal plane, maxillary arch was stabilized using continuous 0.019×0.025-inch SS wire; and retraction of mandibular incisors progressed using continuous 0.019×0.025-inch SS wires (Figure 12).

After the removal of appliances, conventional maxillary Hawley retainer and a bonded 4-to-4 mandibular lingual retainer along with circumferential mandibular



Figure 14 – Three-year follow-up extraoral and intraoral photographs demonstrating stability of achieved results.

Hawley retainer were used for full-time retention for 6 months and then at night only for another 6 months.

Treatment results

Following 19 months of active treatment (including dual distraction), significantly improved facial symmetry and stable skeletal position with a well-settled symmetric functional occlusion was established (Figure 13). The upper dental midline coincided with the middle of the mandibular left central incisor, which did not cause any esthetic compromise to the patient. Three-year posttreatment records confirmed the stability of frontal and profile esthetics along with a tight functional occlusion (Figure 14).

Discussion

Facial asymmetry negatively impacts a patient's orofacial, psychosocial, and nutritional development by bringing forth inadequacies of a morphologic, aesthetic and stomatognathic nature. A tailor-made approach with treatment objectives determined by the patients' concerns and clinical diagnosis including malocclusion, dental compensations and concomitant sagittal and/or vertical jaw imbalance is therefore deemed most essential (Cheong and Lo, 2011).

For adults with severe asymmetric hypoplastic mandibular deformities, DO has proven to be a safe versatile technique with predictable and stable treatment results when compared to traditional bilateral sagittal split osteotomies (Al-Moraissi and Ellis, 2015). Additionally, gradual adaptation of the soft-tissue components to changes in mandibular length throughout the course of the distraction and consolidation periods represent the beneficial effects of the distraction forces on the surrounding soft tissues (distraction histogenesis) (Schreuder et al., 2007).

Dual distraction technique involving the placement of two distractors obviates the requirement for a second surgical procedure. The distractor A can be activated to increase the gap created by arthroplasty if it is deemed less than satisfactory. Patients with short ramus height, wherein increasing the gap by further bone removal could risk perforation into the middle cranial fossa (superiorly) or predispose injury to the inferior alveolar neurovascular bundle (inferiorly), may specially benefit from dual distraction approach (Srivastava et al., 2019).

Two distractors arguably allow for proper segment control by avoiding the upward and medial movement of the proximal bony segment as well as lowering the potential for impingement of the gap that was created by the arthroplasty, thus lowering the risk of recurrence of ankylosis (Srivastava et al., 2019). Oblique positioning of distractor B with angular osteotomy permits simultaneous elongation of both the mandibular ramus and corpus, thus enabling correction of mandibular asymmetry, eliminating the need of second surgery, and giving it an advantage over differential vertical and horizontal distraction.

Moulding of the generate at the end of the active period of distraction by intermaxillary elastic traction involving the use of acrylic bite-blocks and Erich arch bar helped counteract the vertical downward pull of supra-omohyoid group of muscles, close the anterior open bite and prevent inadvertent excessive increase in the mandibular plane angle. After distraction consolidation, intensive orthodontic treatment in both patients necessitated/entailed alignment and levelling of the compensated dentition over alveolar bone, establishment of symmetry within occlusal relationships between the maxillary and mandibular arches, correction of transverse maxillomandibular disharmony and controlled vertical closure of the unilateral posterior open bite (Hanson and Melugin, 1999). While performing dental decompensations, mandibular incisors were retracted taking into account the symphysis and alveolar housing's anatomical boundaries.

It has been observed that apart from mandibular deviation, the abnormal mandibular growth associated with TMJ ankylosis usually results in restricted downward maxillary growth on the affected side (Trahar et al., 2003). The resultant effect is canting of occlusal plane and decreased facial height on the affected side. Usually, additional surgery such as LeFort I osteotomy combined with bone grafts is necessitated to correct the maxillary occlusal cant and restore the normal vertical maxillary height on the affected side (Obwegeser, 1988; Molina, 1999). However, in Case 2, quick en-masse correction of the canted maxillary occlusal plane was achieved by camouflage orthodontic treatment involving the use of acrylic splint, elastic traction and miniscrew anchorage devices. Interocclusal gap created on the left side was used for selective extrusion of the maxillary left posterior dentition and alveolar process.

From a biological and biomechanical perspective, miniscrews have gained popularity for management of wide spectrum of discrepancies because forces can be applied directly from the bone-borne anchor unit. By offering the advantages of maintaining the integrity of the mandibular occlusal plane, reducing anchorage burden, preserving stability and optimizing time duration (Amm, 2012), utilization of TADs also provides biological, therapeutic and psychological advantages, as discernible in our case. Additionally, the complexity and potential risks associated with LeFort 1 osteotomy such as intraoperative and postoperative complications in terms of hemorrhage, pain, swelling, nerve injury, and infection were altogether obviated (Sousa and Turrini, 2012).

To further improve the lower one-third facial esthetics in Case 2, sliding genioplasty for centring of chin accompanied by volume augmentation on right side of face using medpore alloplastic reconstruction/fat graft, if required thereafter, was proposed as a secondary procedure. However, the patient refused to undergo another surgical intervention.

Postoperatively, the recovery period was uneventful in both patients with no detection of any relapse and neurosensory deficit. A major concerning factor commonly associated with the usage of extraoral distractor is the possibility of skin

scarring. In these circumstances, placement of the pins within the submandibular fold with minimum soft tissue strain and by squeezing the cheek skin between the thumb and index finger before inserting the second pin (to allow for stretching) helps reduce the length of the traction scar. Minor point-like external skin scarring following secondary healing did not result in esthetic compromise in present cases.

One-stage treatment, often requiring intermaxillary fixation limits the use of intensive mouth opening exercises, thereby increasing the risk of relapse (Zhu et al., 2013). Although the process of dual distraction involving concurrent fixation of gap arthroplasty avoids the need for intermaxillary fixation, early and aggressive postoperative mouth opening exercises cannot be performed owing to physical interference with the distraction process (with likelihood of disruption of callus). However, passive mouth opening exercises and regular physiological masticatory function are sufficient to preserve the achieved mouth opening during the distraction period, as observed in both patients. Following completion of consolidation period, aggressive physiotherapy exercises were employed to maintain functional integrity and prevent recurrence. In accordance with the patient-centred outcome, one-stage treatment protocol facilitating simultaneous correction of ankylosis, and facial deformities helped obviate the need for a second major surgery and provide more immediate resolution of the patients' chief complaints, thus uplifting their self-esteem. At 3-year follow-up review, both patients maintained satisfactory mouth opening, function, and esthetic appearance.

Stability considerations

A systematic review of the stability and the effects of mandibular DO on hard and soft tissues found variables such as high gonial angle and Jarabak ratio to be correlated with an increased tendency for significant skeletal relapse, but without significantly worsening the overall treatment results (Rossini et al., 2016). Considerable reduction in overjet at long-term follow-up has also been reported to support the long-term effectiveness of DO (Rossini et al., 2016), as was discernible in present cases.

Factors governing the stability of the surgical results included: effective surgical release of ankylosis, establishment of adequate mouth-opening range, improved control of the distraction vectors by employing two extraoral distractors and adequate consolidation phase. Above all, early institution of passive mouth opening and closing exercises during the distraction phase of distractor B, accompanied by active isometric and isotonic physiotherapeutic regimen (following removal of distractor A and completion of the distraction phase of distractor B) intensively for up to 2 years along with close follow-ups, also played a crucial role in achieving stable successful outcomes in terms of restoring physiological TMJ function and preventing recurrence of ankylosis. Occlusal acrylic splints and stable muscular forces also aid in preventing relapse and ensuring stability in peri-distraction phase (Chugh et al.,

2021). Postdistraction orthodontic manipulations involving elimination of occlusal compensations, adequate levelling and alignment of dental arches, restoration of proper overjet and occlusion, correction of transverse discrepancy by proper arch coordination, appropriate first and third order control and extended period of rigid retention protocol, combined altogether, contributed to long term stability of the occlusal results.

Conclusion

Correction of asymmetric dentofacial deformities present a complex therapeutic scenario to plan and accomplish. The optimal skeletal and functional enhancements along with harmonious esthetic outcomes demonstrate that one-stage concurrent arthroplasty and dual distraction osteogenesis is a safe, stable, and reliable approach for surgical rehabilitation of an adult asymmetric dentofacial deformity secondary to unilateral TMJ ankylosis. Comprehensive fixed orthodontic mechanotherapy which includes the use of acrylic bite-blocks, elastic traction, and temporary skeletal anchorage device is critical in the management of specific malocclusion caused by distraction osteogenesis. More research is warranted to determine the treatment's long-term efficacy and underlying remodelling processes.

References

- Al-Moraissi, E. A., Ellis, E. 3rd (2015) Bilateral sagittal split ramus osteotomy versus distraction osteogenesis for advancement of the retrognathic mandible. *J. Oral Maxillofac. Surg.* **73**, 1564–1574.
- Amm, E. W. (2012) Three-year follow-up of a patient with hemifacial microsomia treated with distraction osteogenesis, temporary anchorage devices, and orthodontics. *Am. J. Orthod. Dentofacial Orthop.* **142**, 115–128.
- Cheong, Y. W., Lo, L. J. (2011) Facial asymmetry: Etiology, evaluation, and management. *Chang Gung Med. J.* **34**, 341–351.
- Chugh, A., Mehrotra, D., Yadav, P. K. (2021) A systematic review on the outcome of distraction osteogenesis in TMJ ankylosis. *J. Oral Biol. Craniofac. Res.* **11**, 581–595.
- Dean, A., Alamillos, F. (1999) Mandibular distraction in temporomandibular joint ankylosis. *Plast. Reconstr. Surg.* **104**, 2021–2031.
- De Roo, N., Van Doorne, L., Troch, A., Vermeersch, H., Brusselaers, N. (2016) Quantifying the outcome of surgical treatment of temporomandibular joint ankylosis: A systematic review and meta-analysis. *J. Craniomaxillofac. Surg.* **44**, 6–15.
- Girardi, G. B., Arora, K., Sai Anusha, A. J. (2016) Distraction osteogenesis in the treatment of temporomandibular joint ankylosis with mandibular micrognathia. *Ann. Maxillofac. Surg.* **6**, 68–74.
- Hanson, P. R., Melugin, M. B. (1999) Orthodontic management of the patient undergoing mandibular distraction osteogenesis. *Semin. Orthod.* **5**, 25–34.
- Molina, F. (1999) Combined maxillary and mandibular distraction osteogenesis. *Semin. Orthod.* **5**, 41–45.
- Motta, A., Louro, R. S., Medeiros, P. J., Capelli, J. Jr. (2007) Orthodontic and surgical treatment of a patient with an ankylosed temporomandibular joint. *Am. J. Orthod. Dentofacial Orthop.* **131**, 785–796.
- Obwegeser, H. L. (1988) Variations of a standard approach for correction of the bird-face deformity. *J. Craniomaxillofac. Surg.* **16**, 247–265.
- Rossini, G., Vinci, B., Rizzo, R., Pinho, T. M. D., Deregibus, A. (2016) Mandibular distraction osteogenesis:

- A systematic review of stability and the effects on hard and soft tissues. *Int. J. Oral Maxillofac. Surg.* **45**, 1438–1444.
- Schreuder, W. H., Jansma, J., Bierman, M. W., Vissink, A. (2007) Distraction osteogenesis versus bilateral sagittal split osteotomy for advancement of the retrognathic mandible: A review of the literature. *Int. J. Oral Maxillofac. Surg.* **36**, 103–110.
- Sharma, A., Paeng, J. Y., Yamada, T., Kwon, T. G. (2016) Simultaneous gap arthroplasty and intraoral distraction and secondary contouring surgery for unilateral temporomandibular joint ankyloses. *Maxillofac. Plast. Reconstr. Surg.* **38**, 12.
- Sousa, C. S., Turrini, R. N. (2012) Complications in orthognathic surgery: A comprehensive review. *J. Oral Maxillofac. Surg. Med. Pathol.* **24**, 67–74.
- Srivastava, D., Luthra, P., Mishra, S., Chandra, L., Sharma, S., Singh, H. (2019) Technique of dual distraction for correction of unilateral temporomandibular joint ankylosis with facial asymmetry: A case series. *J. Oral Maxillofac. Surg.* **77**, 2555.e1–2555.e12.
- Trahar, M., Sheffield, R., Kawamoto, H., Lee, H. F., Ting, K. (2003) Cephalometric evaluation of the craniofacial complex in patients treated with an intraoral distraction osteogenesis device: A preliminary report. *Am. J. Orthod. Dentofacial Orthop.* **124**, 639–650.
- Yu, H., Shen, G., Zhang, S., Wang, X. (2009) Gap arthroplasty combined with distraction osteogenesis in the treatment of unilateral ankylosis of the temporomandibular joint and micrognathia. *Br. J. Oral Maxillofac. Surg.* **47**, 200–204.
- Zhu, S., Wang, D., Yin, Q., Hu, J. (2013) Treatment guidelines for temporomandibular joint ankylosis with secondary dentofacial deformities in adults. *J. Craniomaxillofac. Surg.* **41**, e117–e127.

Vaping Associated Acute Eosinophilic Pneumonia: A Clinical and Radiologic Mimicker of COVID-19

**Alyssa Bonnier¹, Anum Nida², Woon Hean Chong³,
Santu Saha⁴, Biplab K. Saha⁵**

¹Department of Critical Care Nursing, Goldfarb School of Nursing, Barnes Jewish College, Saint Louis, USA;

²Department of Medicine, Ozarks Medical Center, West Plains, USA;

³Department of Intensive Care Medicine, Ng Teng Fong General Hospital, National University Health System, Singapore City, Singapore;

⁴Department of Medicine, Saha Clinic, Lohagara, Narail, Bangladesh;

⁵Department of Pulmonary, Critical Care and Sleep Medicine, University of Florida, Gainesville, USA

Received October 27, 2022; Accepted August 17, 2023.

Key words: Vaping – Lung injury – Acute eosinophilic pneumonia – AEP – Smoking

Abstract: Acute eosinophilic pneumonia (AEP) is a rare cause of respiratory failure. It is primarily a disease of smokers, either a new smoker or an existing one with a recent increase in cigarette consumption. Other risk factors include toxic gas exposure, inhalational illicit drugs, and smoking marijuana. AEP has also been reported in patients with e-cigarette or vaping associated lung injury (EVALI). We present the case of a 20-year-old male who presented to the hospital with acute respiratory failure. The patient has been vaping heavily for the past three months and started smoking three days before presenting to the emergency department. He was hypertensive, tachycardic, tachypneic, and required high-flow nasal cannula to maintain SpO₂ > 92%. His condition deteriorated in the first 24 hours following hospitalization requiring noninvasive positive pressure ventilation. Bronchoalveolar lavage revealed an eosinophil count of 36%. Bronchoalveolar lavage (BAL) cytology revealed lipid-laden macrophages. He was diagnosed with AEP due to EVALI, and the patient was treated with high dose corticosteroid with subsequent improvement. Before the bronchoscopic evaluation, the clinical and radiologic findings were

Mailing Address: Biplab K. Saha, MD., FCCP, Division of Pulmonary, Critical Care and Sleep Medicine, Medical Sciences Building, Room #M-452, University of Florida, 1600 SW Archer Road, Gainesville, FL 32608, USA; e-mails: spanophilic@yahoo.com, biplab.saha@medicine.ufl.edu

<https://doi.org/10.14712/23362936.2023.22>

© 2023 The Authors. This is an open-access article distributed under the terms of the Creative Commons Attribution License (<http://creativecommons.org/licenses/by/4.0>).

consistent with COVID-19, and the patient was tested twice for SARS-CoV-2 PCR. In the appropriate clinical setting, AEP should be considered in the differential diagnoses of community-acquired pneumonia, acute respiratory distress syndrome (ARDS), and COVID-19, especially in this pandemic era.

Introduction

Acute eosinophilic pneumonia (AEP) is a rare and possibly under-diagnosed etiology of acute respiratory failure that can resemble community-acquired pneumonia, acute respiratory distress syndrome (ARDS), and coronavirus disease 2019 (COVID-19). AEP is characterized by an acute onset of febrile illness with hypoxemic respiratory failure, radiologic chest infiltrate, and >25% eosinophil on bronchoalveolar lavage (BAL) in the absence of any known etiologies of pulmonary eosinophilia (Philit et al., 2002). Although often referred to as idiopathic AEP, several major risk factors are frequently present in patients with AEP. AEP is primarily a disease of smokers, either a new smoker (sometimes after quitting for a period and then resuming) or an existing one with a recent increase in cigarette consumption (De Giacomo et al., 2018). However, AEP has also been reported in patients with exposure to toxic gas (Hirai et al., 2000; Philit et al., 2002), inhaled recreational drugs (McCormick and Nelson, 2007), marijuana (Liebling and Siu, 2013), aroma therapy with essential oil (Kodama et al., 2022), and even in patients with COVID-19 (Murao et al., 2020). Immediately before the COVID-19 pandemic, there was an epidemic of electronic cigarette or vaping associated lung injury (EVALI) in young adults across the United States (Werner et al., 2020). AEP in the setting of EVALI has been reported in a small number of these patients (Arter et al., 2019; Wolf and Richards, 2020). We present the case of a young man with AEP in the setting of combined e-cigarette use and smoking that mimicked COVID-19.

Case report

A 20-year-old young male presented to the hospital with low-grade fever, cough, yellow sputum, wheezing, and dyspnea for three days. He reported generalized fatigue, poor appetite, weight loss, malaise, night sweats, and chills. The patient was initially dyspneic with exertion, which progressed rapidly to resting dyspnea, prompting the emergency department (ED) visit. He had a past medical history of hypertension that was diagnosed at the age of 15. A workup for secondary causes of hypertension was negative. His regular home medication included lisinopril, which he has not been taking for two months. The patient recently lost his father and started using nicotine containing vaping products over the past three months. Due to a higher stress level, the patient started vaping heavily in the past week or so. Additionally, he started smoking combustible cigarettes three days before his symptom onset. He had no known respiratory disease or family history of respiratory illness. He denied any drug use, recent travel, sick contacts, personal history of tuberculosis, or exposure to a patient with tuberculosis. He had no

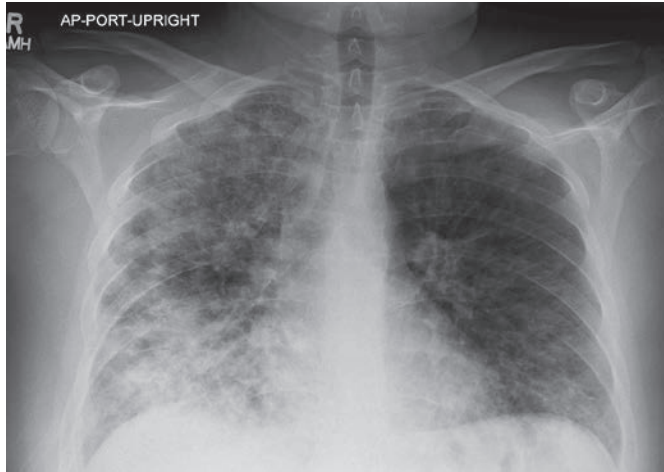


Figure 1 – Chest X-ray showing diffuse bilateral infiltrate. The opacities are both alveolar and interstitial.

pets at home and gave no history of hot tub use or use of feathered pillows. The patient lived in Histoplasma endemic rural United States. He was vaccinated against COVID-19 with two doses of mRNA vaccines.

In the ED, his vital signs were as follows: blood pressure 153/85 mm Hg, pulse 128 beats per minute, temperature 36.8 °C, respiratory rate 28 breaths per minute, and SpO₂ 78% on room air, requiring high flow nasal cannula to achieve SpO₂ > 92%. Physical examination revealed a young man in moderate distress. Chest auscultation was significant for crackles at bilateral lung bases without wheezing or rhonchi. There was no rash, clubbing, peripheral edema, or hepatosplenomegaly. The laboratory workup showed leukocytosis of 22,000/μl. The admission peripheral blood absolute eosinophil level was 484 cells/μl (2.2%). There were no electrolyte abnormalities or organ dysfunction. Serum procalcitonin level was normal. The C-reactive protein (CRP) level was elevated at 158.4 mg/l (normal < 10 mg/l).



Figure 2 – Coronal section of the computed tomography of the chest showed ill-defined centrilobular nodularity primarily on the left side and areas of ground glass opacity and consolidation on the right (A). Axial section showing small volume bilateral pleural effusion (B). Axial view demonstrated interlobular septal thickening with ground glass opacity of the secondary pulmonary nodule consistent with “crazy paving pattern”.

A chest X-ray showed diffuse bilateral alveolar opacity involving all lung zones (Figure 1). A computed tomographic angiogram (CTA) of the chest demonstrated bilateral areas of ground glass opacity, consolidation, and “crazy paving pattern” in the right lower lobe (Figure 2). There was also small bilateral pleural effusion but no pulmonary embolism. A bedside echocardiogram showed normal ejection fraction, no valvular abnormalities, and mitral valve E/septal E’ ratio of 6, inconsistent with elevated cardiac filling pressures. Severe acute respiratory syndrome coronavirus 2 (SARS-CoV-2) PCR from the nasopharyngeal (NP) swab was negative. The patient was diagnosed with multilobar pneumonia and started on broad-spectrum antibiotics. Although the SARS-CoV-2 PCR was negative, the chest imaging was concerning for COVID-19, and the patient was started on empiric remdesivir and dexamethasone. As there was also the suspicion of EVALI, the corticosteroid was thought to be the appropriate intervention. The patient was tested a second time for SARS-CoV-2 PCR from another NP specimen, and the study was negative. Due to increasing oxygen requirements, he was admitted to the intensive care unit. His respiratory status worsened over the next 24 hours requiring non-invasive positive pressure ventilation.

A bronchoscopic evaluation showed diffuse airway inflammation and erythema without any active bleeding or mucus impaction. BAL was performed from the medial segment of the right middle lobe. Two 60cc aliquots of saline were instilled and the total fluid return was 45 ml. The fluid was cloudy without any blood tinge. Cell count analysis of the BAL showed 36% eosinophils, 28% lymphocytes, 20% macrophages, 6% neutrophils, and 10% other cells. Cytologic examination of BAL revealed numerous lipid-laden macrophages (LLM) and an increased number of eosinophils (Figure 3). An extensive microbiologic workup, including SARS-CoV-2 PCR was negative. The clinical presentation and BAL findings were consistent with the diagnosis of acute eosinophilic pneumonia. Given the severity of hypoxemia and the necessity of non-invasive positive pressure ventilation, the patient was started on 60 mg of intravenous methylprednisolone every 6 hours with rapid clinical and radiologic improvement within 48 hours (Figure 4). The patient was discharged home

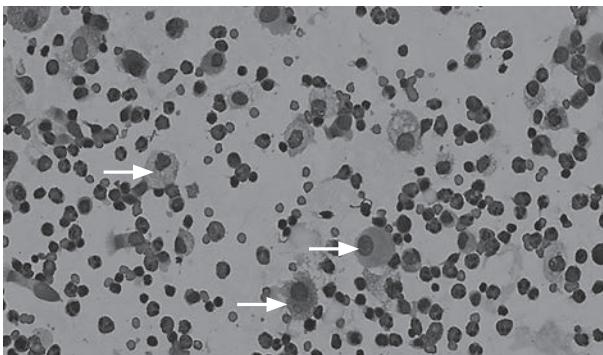


Figure 3 – Cytologic examination of the bronchoalveolar lavage revealed foamy macrophages (arrow) and increased number of eosinophils.

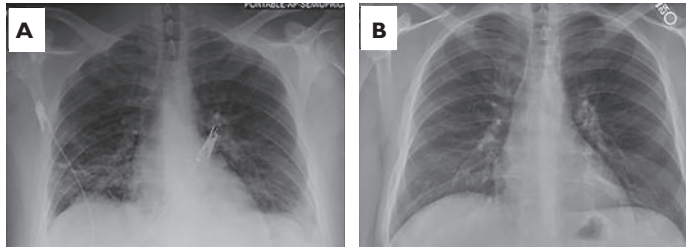


Figure 4 – Chest X-ray 72 hours after initiation of high dose steroid therapy on the day of discharge demonstrated a significant improvement (A). A follow-up X-ray one week after discharge was normal (B).

on 60 mg of prednisone daily (with a tapering plan over the next four weeks) within 72 hours after the initiation of methylprednisolone therapy with minimal oxygen requirement. During outpatient follow-up a week after discharge, he was back to normal without any respiratory complaints. During the course of his illness, the peripheral blood eosinophils reached a peak of 700 cells on day 2.

Discussion

SARS-CoV-2 is the etiologic agent for the COVID-19 pandemic, which has caused more than 6 million deaths worldwide (Saha et al., 2020). Involvement of the lower respiratory tract by SARS-CoV-2 may result in severe COVID-19 requiring hospitalization and intensive care admission. However, the presentation of COVID-19 could be indistinguishable from other respiratory illnesses because of the nonspecificity of the symptoms. Similarly, the radiologic appearance of COVID-19 could also be identical to many other respiratory diseases (Saha et al., 2021). Additionally, false-negative SARS-CoV-2 PCRs are not uncommon, complicating the issue further (Kanji et al., 2021; Saha et al., 2022). Therefore, caution should be practiced to avoid misdiagnosis and provide appropriate patient care.

The use of electronic cigarettes or vaping has become a popular trend among adolescents and teenagers. Unfortunately, the misguided notion that vaping is “safe” has led to nicotine addiction among millions of high school students in the United States (Wang et al., 2020). Starting in August 2019, an epidemic of EVALI has been reported in all states in the US, with a mortality rate of approximately 2.6% (Cherian et al., 2020). Extensive research has suggested the likely culprit is vitamin E acetate in the vaping solution. However, other possible etiologies, including tetrahydrocannabinol (THC), could not be definitively ruled out. The primary histopathologic lesion in EVALI has been acute fibrinous pneumonitis, diffuse alveolar damage (DAD), organizing pneumonia, and bronchiolitis (Butt et al., 2019). Although uncommon, AEP has been reported in a few patients with EVALI during the epidemic in the US and before that (Thota and Latham, 2014; Kamada et al., 2016; Mull et al., 2020; Puebla Neira et al., 2020; Wolf and Richards, 2020; Takigawa et al., 2022; Bonnier et al., 2023).

AEP was first reported in 1989 nearly simultaneously by two independent groups from the United States (Allen et al., 1989; Badesch et al., 1989). The

authors reported a new entity, which, unlike chronic eosinophilic pneumonia, had an acute onset of respiratory symptoms associated with constitutional symptoms, demonstrated diffuse pulmonary involvement on radiologic imaging, and prompt response to systemic corticosteroids (CS). The BAL eosinophil count was elevated (greater than 25%), generally without peripheral eosinophilia. The new entity was considered idiopathic as all known causes of pulmonary eosinophilia were excluded. However, as more cases and small retrospective studies were available, it became clear that most of these patients were smokers (Philit et al., 2002; Shorr et al., 2004; Uchiyama et al., 2008). AEP was reported in patients who were new smokers or resumed smoking after quitting for some time. Also, smokers with a recent increase in cigarette consumption were found to be susceptible. In one of the largest retrospective studies of patients with AEP, 99% of patients were smokers (Rhee et al., 2013). It is important to emphasize that only a minute percent of smokers develop AEP, perhaps highlighting the contribution of one's genetic makeup. Recurrence of AEP following provocation by smoking has been documented in a number of cases (Nakajima et al., 1998). AEP is more prevalent in men than women. There may also be a seasonal variation in the occurrence of AEP, with a higher incidence during the summer months (Yoon et al., 2016).

The exact pathophysiology of AEP is currently unknown. However, it is thought to originate from epithelial and endothelial injury due to inhalational toxins (smoke, vaping products and others). The tissue injury results in the robust expression of interleukin-33 (IL-33), which likely plays the central role in the pathogenesis of AEP (De Giacomo et al., 2018). The IL-33, in turn, causes activation of innate lymphoid cells (ILC)-2 in the airways and dictates a Th2 helper cell-mediated inflammatory response promoting the production of IL-4, IL-5, and IL-13 that is responsible for the recruitment of eosinophils in the lungs. At the same time, neutrophils, alveolar macrophages, and lymphocytes are also recruited by an unknown mechanism and likely contribute to the pathogenesis (Fujimura et al., 1998). High levels of IL-5 in the patients' serum have been reported in patients with AEP (Miki et al., 2002).

There are no specific historical diagnostic clues for AEP, but it is often considered in patients who are new smokers or increased smoking consumption recently. An increasing peripheral blood eosinophil level in hospitalized patients may also prompt the consideration of AEP in differential diagnoses of pneumonia (Jhun et al., 2014). Patients present with fever, cough with or without sputum production, chest pain, and dyspnea. The median duration between onset of smoking (or increased quantity) and AEP has been reported to be 17 days (range 13–26 days) (Rhee et al., 2013). Other studies have shown similar data, with most patients presenting within a month after a change in their smoking behavior (Suzuki and Suda, 2019). In our patient, the duration of smoking onset and symptom onset was only three days, raising the question of whether smoking and vaping could have an additive effect. A previous paper reported the interval between smoking onset and AEP as short as two days (Nakajima et al., 1998).

The diagnostic criteria used for defining AEP have varied among studies. Some authors have included patients with respiratory symptoms for up to one month (Philit et al., 2002; Shorr et al., 2004; Rhee et al., 2013; Jhun et al., 2014; De Giacomo et al., 2017), whereas others have considered one to two weeks (Sine et al., 2018). Some reports have considered fever a crucial component (Philit et al., 2002; Shorr et al., 2004), but others have reported its absence in a significant number of patients (Rhee et al., 2013). The severity of respiratory failure has also varied among studies, with some showing a high rate of respiratory failure requiring mechanical ventilation (Philit et al., 2002; Shorr et al., 2004). In contrast, others have shown many minimally symptomatic patients and a low incidence of intubation (Rhee et al., 2013). AEP likely has a spectrum of presentations that ranges from mild self-limiting illness to respiratory failure resulting in death.

The physical examination findings are nonspecific. Chest auscultation often reveals basilar crackles but could be unrevealing. The radiologic chest imaging typically shows bilateral lung infiltrates, but unilateral involvement may also be seen. Computed tomography (CT) scan of the chest provides a more detailed evaluation. Bronchiolocentric ill-defined centrilobular pulmonary nodule, ground glass opacity, consolidation, bronchovascular bundle thickening, and interlobular septal thickening are seen in patients with AEP (Rhee et al., 2013). Small bilateral pleural effusion is present in nearly two-thirds of patients (Sine et al., 2018). Laboratory evaluation shows leukocytosis with neutrophilia and elevated inflammatory markers, such as CRP and d-dimer. Peripheral eosinophilia may be present in a minority of patients at the time of presentation or develop within the next few days (Jhun et al., 2014).

Bronchoscopy plays a crucial role in the diagnosis of AEP. A BAL eosinophil level greater than 25% is necessary to make the definitive diagnosis. A bronchoscopy could also rule out other causes of pulmonary eosinophilia. We identified lipid-laden macrophages (LLM) on the cytologic evaluation from BAL. LLM or foamy macrophages have been reported in patients with EVALI (Maddock et al., 2019), and some authors have suggested LLM as a marker for EVALI (Guerrini et al., 2020). However, LLM could be seen in a multitude of disease processes including in otherwise healthy smokers (Ghosh et al., 2021). Deposition of lipid particles in the alveolar macrophages (AM) represent improper cycling of the surfactants by the AM. Inhalation of an oil-based compound, as seen in lipoid pneumonia, is another etiology of LLM on BAL (Chieng et al., 2022). The histopathologic examination of the lungs shows eosinophilic infiltration of pulmonary parenchyma and interstitial tissue, eosinophilic abscesses, nonnecrotizing perivascular inflammation, and sometimes diffuse alveolar damage (De Giacomo et al., 2018). Hyperplasia of the interstitial lymphocytes, type-2 alveolar epithelial cells, and intraalveolar organizing exudates are also seen.

Treatment with systemic corticosteroid (CS) is highly effective in AEP. Patients show clinical and radiographic improvement within 48–72 hours. The absence

of improvement within this time frame may point toward a different diagnosis. Patients with respiratory failure requiring intubation typically receive high dose CS (methylprednisolone 60 to 125 mg every 6 hours), whereas less sick individuals could be treated with 40–60 mg of prednisone daily. The CS is typically tapered over 4–8 weeks, but a 2-week course is equally effective (Rhee et al., 2013). No prospective studies have compared different dosing of CS in patients with AEP. Nevertheless, the prognosis is generally good. The presence of peripheral eosinophilia may suggest a more benign disease course (Jhun et al., 2014).

We have reported the case of AEP in a young male likely caused by vaping with a possible contribution from new-onset smoking. The diagnosis was confirmed by bronchoscopic evaluation showing BAL eosinophil > 25% and the absence of any microbiologic cause of pulmonary eosinophilia. The clinical and radiologic manifestations were initially concerning for COVID-19, but an accurate diagnosis was eventually reached after careful evaluation. Therefore, AEP should be considered in the differential diagnoses of community-acquired pneumonia, ARDS, and suspected COVID-19, especially in the presence of risk factors and developing peripheral eosinophilia.

References

- Allen, J. N., Pacht, E. R., Gadek, J. E., Davis, W. B. (1989) Acute eosinophilic pneumonia as a reversible cause of noninfectious respiratory failure. *N. Engl. J. Med.* **321(9)**, 569–574.
- Arter, Z. L., Wiggins, A., Hudspath, C., Kisling, A., Hostler, D. C., Hostler, J. M. (2019) Acute eosinophilic pneumonia following electronic cigarette use. *Respir. Med. Case Rep.* **27**, 100825.
- Badesch, D. B., King, T. E., Schwarz, M. I. (1989) Acute eosinophilic pneumonia: A hypersensitivity phenomenon? *Am. Rev. Respir. Dis.* **139(1)**, 249–252.
- Bonnier, A., Saha, S., Shkolnik, B., Saha, B. K. (2023) A comparative analysis of acute eosinophilic pneumonia associated with smoking and vaping. *Am. J. Med. Sci.* **365(3)**, 315–317.
- Butt, Y. M., Smith, M. L., Tazelaar, H. D., Vaszar, L. T., Swanson, K. L., Cecchini, M. J., Boland, J. M., Bois, M. C., Boyum, J. H., Froemming, A. T., Khor, A., Mira-Avendano, I., Patel, A., Larsen, B. T. (2019) Pathology of vaping-associated lung injury. *N. Engl. J. Med.* **381(18)**, 1780–1781.
- Cherian, S. V., Kumar, A., Estrada-Y-Martin, R. M. (2020) E-cigarette or vaping product-associated lung injury: A review. *Am. J. Med.* **133(6)**, 657–663.
- Chiang, H. C., Ibrahim, A., Chong, W. H., Freed, H., Fabian, T., Saha, B., Foulke, L., Chopra, A. (2022) Lipoid pneumonia. *Am. J. Med. Sci.* **363(5)**, 452–455.
- De Giacomi, F., Decker, P. A., Vassallo, R., Ryu, J. H. (2017) Acute eosinophilic pneumonia: Correlation of clinical characteristics with underlying cause. *Chest* **152(2)**, 379–385.
- De Giacomi, F., Vassallo, R., Yi, E. S., Ryu, J. H. (2018) Acute eosinophilic pneumonia. Causes, diagnosis, and management. *Am. J. Respir. Crit. Care Med.* **197(6)**, 728–736.
- Fujimura, M., Yasui, M., Shinagawa, S., Nomura, M., Matsuda, T. (1998) Bronchoalveolar lavage cell findings in three types of eosinophilic pneumonia: Acute, chronic and drug-induced eosinophilic pneumonia. *Respir. Med.* **92(5)**, 743–749.
- Ghosh, A., Ahmad, S., Coakley, R. D., Sassano, M. F., Alexis, N. E., Tarran, R. (2021) Lipid-laden macrophages are not unique to patients with e-cigarette or vaping product use-associated lung injury. *Am. J. Respir. Crit. Care Med.* **203(8)**, 1030–1033.

- Guerrini, V., Panettieri, R. A., Gennaro, M. L. (2020) Lipid-laden macrophages as biomarkers of vaping-associated lung injury. *Lancet Respir. Med.* **8(2)**, e6.
- Hirai, K., Yamazaki, Y., Okada, K., Furuta, S., Kubo, K. (2000) Acute eosinophilic pneumonia associated with smoke from fireworks. *Intern. Med.* **39(5)**, 401–403.
- Jhun, B. W., Kim, S. J., Kim, K., Lee, J. E. (2014) Clinical implications of initial peripheral eosinophilia in acute eosinophilic pneumonia. *Respirology* **19(7)**, 1059–1065.
- Kamada, T., Yamashita, Y., Tomioka, H. (2016) Acute eosinophilic pneumonia following heat-not-burn cigarette smoking. *Respirol. Case Rep.* **4(6)**, e00190.
- Kanji, J. N., Zelyas, N., MacDonald, C., Pabbaraju, K., Khan, M. N., Prasad, A., Hu, J., Diggle, M., Berenger, B. M., Tipples, G. (2021) False negative rate of COVID-19 PCR testing: A discordant testing analysis. *Viol. J.* **18(1)**, 13.
- Kodama, T., Watanabe, T., Mataka, N., Kanoh, S., Kichikawa, Y. (2022) Acute eosinophilic pneumonia following aromatherapy with essential oil. *Respir. Med. Case Rep.* **37**, 101657.
- Liebling, P. D., Siu, S. (2013) A novel cause of eosinophilic pneumonia: Recreational marijuana exposure. *J. Bronchology Interv. Pulmonol.* **20(2)**, 183–185.
- Maddock, S. D., Cirulis, M. M., Callahan, S. J., Keenan, L. M., Pirozzi, C. S., Raman, S. M., Aberegg, S. K. (2019) Pulmonary lipid-laden macrophages and vaping. *N. Engl. J. Med.* **381(15)**, 1488–1489.
- McCormick, M., Nelson, T. (2007) Cocaine-induced fatal acute eosinophilic pneumonia: A case report. *WMJ* **106(2)**, 92–95.
- Miki, K., Miki, M., Okano, Y., Nakamura, Y., Ogushi, F., Ohtsuki, Y., Nakayama, T. (2002) Cigarette smoke-induced acute eosinophilic pneumonia accompanied with neutrophilia in the blood. *Intern. Med.* **41(11)**, 993–996.
- Mull, E. S., Erdem, G., Nicol, K., Adler, B., Shell, R. (2020) Eosinophilic pneumonia and lymphadenopathy associated with vaping and tetrahydrocannabinol use. *Pediatrics* **145(4)**, e20193007.
- Murao, K., Saito, A., Kuronuma, K., Fujiya, Y., Takahashi, S., Chiba, H. (2020) Acute eosinophilic pneumonia accompanied with COVID-19: A case report. *Respirol. Case Rep.* **8(9)**, e00683.
- Nakajima, M., Manabe, T., Niki, Y., Matsushima, T. (1998) Cigarette smoke-induced acute eosinophilic pneumonia. *Radiology* **207(3)**, 829–831.
- Philit, F., Etienne-Mastroianni, B., Parrot, A., Guérin, C., Robert, D., Cordier, J.-F. (2002) Idiopathic acute eosinophilic pneumonia: A study of 22 patients. *Am. J. Respir. Crit. Care Med.* **166(9)**, 1235–1239.
- Puebla Neira, D., Tamba, S., Bhasin, V., Nawgiri, R., Duarte, A. G. (2020) Discordant bilateral bronchoalveolar lavage findings in a patient with acute eosinophilic pneumonia associated with counterfeit tetrahydrocannabinol oil vaping. *Respir. Med. Case Rep.* **29**, 101015.
- Rhee, C. K., Min, K. H., Yim, N. Y., Lee, J. E., Lee, N. R., Chung, M. P., Jeon, K. (2013) Clinical characteristics and corticosteroid treatment of acute eosinophilic pneumonia. *Eur. Respir. J.* **41(2)**, 402–409.
- Saha, B. K., Bonnier, A., Chong, W. (2020) Antimalarials as antivirals for COVID-19: Believe it or not! *Am. J. Med. Sci.* **360(6)**, 618–630.
- Saha, B. K., Chong, W. H., Austin, A., Kathuria, R., Datar, P., Shkolnik, B., Beegle, S., Chopra, A. (2021) Pleural abnormalities in COVID-19: A narrative review. *J. Thorac. Dis.* **13(7)**, 4484–4499.
- Saha, B. K., Saha, S., Chong, W. H., Beegle, S. (2022) Indications, clinical utility, and safety of bronchoscopy in COVID-19. *Respir. Care* **67(2)**, 241–251.
- Shorr, A. F., Scoville, S. L., Cersovsky, S. B., Shanks, G. D., Ockenhouse, C. F., Smoak, B. L., Carr, W. W., Petrucci, B. P. (2004) Acute eosinophilic pneumonia among US Military personnel deployed in or near Iraq. *JAMA* **292(24)**, 2997–3005.
- Sine, C. R., Hiles, P. D., Scoville, S. L., Haynes, R. L., Allan, P. F., Franks, T. J., Morris, M. J., Osborn, E. C. (2018) Acute eosinophilic pneumonia in the deployed military setting. *Respir. Med.* **137**, 123–128.

- Suzuki, Y., Suda, T. (2019) Eosinophilic pneumonia: A review of the previous literature, causes, diagnosis, and management. *Allergol. Int.* **68(4)**, 413–419.
- Takigawa, Y., Sato, K., Inoue, A., Nagae, M., Inoue, T., Onishi, K., Mitsumune, S., Watanabe, H., Kudo, K., Sato, A., Fujiwara, K., Shibayama, T. (2022) Acute eosinophilic pneumonia caused by nicotine-free vaping in an adolescent patient: A case report. *Respirol. Case Rep.* **10(6)**, e0961.
- Thota, D., Latham, E. (2014) Case report of electronic cigarettes possibly associated with eosinophilic pneumonitis in a previously healthy active-duty sailor. *J. Emerg. Med.* **47(1)**, 15–17.
- Uchiyama, H., Suda, T., Nakamura, Y., Shirai, M., Gemma, H., Shirai, T., Toyoshima, M., Imokawa, S., Yasuda, K., Ida, M., Nakano, Y., Inui, N., Sato, J., Hayakawa, H., Chida, K. (2008) Alterations in smoking habits are associated with acute eosinophilic pneumonia. *Chest* **133(5)**, 1174–1180.
- Wang, T. W., Neff, L. J., Park-Lee, E., Ren, C., Cullen, K. A., King, B. A. (2020) E-cigarette use among middle and high school students – United States, 2020. *MMWR Morb. Mortal. Wkly Rep.* **69(37)**, 1310–1312.
- Werner, A. K., Koumans, E. H., Chatham-Stephens, K., Salvatore, P. P., Armatas, C., Byers, P., Clark, C. R., Ghinai, I., Holzbauer, S. M., Navarette, K. A., Danielson, M. L., Ellington, S., Moritz, E. D., Petersen, E. E., Kiernan, E. A., Baldwin, G. T., Briss, P., Jones, C. M., King, B. A., Krishnasamy, V., Rose, D. A., Reagan-Steiner, S.; Lung Injury Response Mortality Working Group (2020) Hospitalizations and deaths associated with EVALI. *N. Engl. J. Med.* **382(17)**, 1589–1598.
- Wolf, M., Richards, J. (2020) Acute eosinophilic pneumonia due to vaping-associated lung injury. *J. Crit. Care Med.* **6(4)**, 259–262.
- Yoon, C., Kim, S. J., Kim, K., Lee, J. E., Jhun, B. W. (2016) Clinical characteristics and factors influencing the occurrence of acute eosinophilic pneumonia in Korean military personnel. *J. Korean Med. Sci.* **31(2)**, 247–253.

Osteomyelitis and Thrombosis in a Newborn with Group A Streptococcus Infection

Georgios Mitsiakos, Dimitra Gialamprinou, Christos Tsakalidis, Evgenia Babatseva, Maria Lithoxopoulou, Elisavet Diamanti

2nd Neonatal Department and Neonatal Intensive Care Unit, Aristotle University of Thessaloniki, “Papageorgiou” General Hospital of Thessaloniki, Thessaloniki, Greece

Received July 7, 2022; Accepted August 17, 2023.

Key words: Osteomyelitis – Thrombosis – Neonate – *Streptococcus*

Abstract: Neonatal osteomyelitis (OM), although exceptionally rare, has been linked to detrimental sequel, as diagnosis in the early stages is challenging and any delay in treatment can lead to disturbance in skeletal growth. In pediatric OM the most commonly grown bacteria is *Staphylococcus aureus* followed by group A *Streptococcus* (GAS). Notwithstanding, sepsis-induced coagulopathy is a well-known entity in children and adults, still sepsis-associated thrombosis is sparsely observed. we present a case of a newborn with GAS associated OM and thrombosis. A term neonate on the 11th day of life was referred to our NICU due to right (R) lower limb edema, cyanosis and core temperature up to 39 °C. Late onset sepsis was suspected and started on vancomycin and amikacin. A colour Doppler scan showed thrombosis of the R common femoral vein. The neonate started on iv unfractionated heparin. Ampicillin was added given positive for GAS blood culture. An MRI on the 5th day of admission, showed evidence of thrombosis resolution. On the 14th day of admission, a bone Tc99 scan showed evidence of OM of R femur. Antibiotic treatment switched to amoxicillin per os. The management was restricted to anticoagulant therapy with low molecular weight heparin for 3 months and antibiotic therapy for 6 months without surgery intervention and the patient recovered and discharged at 42 days of age. Early diagnosis and treatment of neonatal osteomyelitis can prevent bone destruction. Sepsis-associated thrombosis is barely observed during osteomyelitis, yet it should be considered as an emerged case requiring prompt treatment.

Mailing Address: Assoc. Prof. Georgios Mitsiakos, MD., PhD., 2nd Neonatal Department and Neonatal Intensive Care Unit, Aristotle University of Thessaloniki, “Papageorgiou” General Hospital of Thessaloniki, Ring Road, Nea Efkarpia, PC 56403, Thessaloniki, Greece; Phone: +30 231 332 33 54; e-mail: mitsiakos@auth.gr

<https://doi.org/10.14712/23362936.2023.23>

© 2023 The Authors. This is an open-access article distributed under the terms of the Creative Commons Attribution License (<http://creativecommons.org/licenses/by/4.0>).

Introduction

The prevalence of osteomyelitis (OM) in neonates ranges from 1–3 cases for every 1,000 hospitalized subjects (Frederiksen et al., 1993). From a pathophysiological aspect, the presence of transphyseal vessels crossing the growth plate makes possible the spread of infection from metaphysis to epiphysis. Osteomyelitis in neonates is challenging to diagnose in early stages and, although not frequent, can potentially lead to joint destruction and growth failure. The most common cause of OM is *Staphylococcus aureus* followed by maternal vaginal pathogens (Ilharreborde, 2015). In neonates very few cases of OM attributed to group A *Streptococcus* (GAS) have been described (Berberian et al., 2010). The invasive type of GAS infection is linked to the M-protein mediated activation of the clotting cascade (Ben Nasr et al., 1995). Vascular thrombosis as purpura fulminans is a well-recognized clinical feature of coagulopathy dysregulation provoked by generalized GAS infection (González-Abad and Alonso Sanz, 2020).

Regarding coagulopathy in the neonatal period, hemostasis following developmental age-related maturation pattern is widely stressed for thromboembolic events (Andrew, 1995). Thromboembolism in hospitalized neonates ranges from 2.4 to 6.8 events per 1,000 admissions (van Elteren et al., 2011). Particularly, venous thrombosis represents 50% of thromboembolic events, and deep venous thrombosis mostly comes as a complication of central line insertion while neonatal thrombosis is strongly correlated with sepsis (Monagle et al., 2012).

However, neonatal OM from GAS combined with deep vein thrombosis as a sequel of GAS-associated invasive disease has not been reported so far. We report a case of neonatal OM in parallel with thrombosis of the affected limb caused by GAS in a term female newborn.

Case report

A female neonate on the 11th day of life was referred to our NICU (Neonatal Intensive Care Unit) from a secondary hospital facility due to right (R) lower limb edema, cyanosis and core temperature up to 39 °C. A 2-day course of agitation and reduced oral intake had preceded the referral. Reduced spontaneous movement of the right (R) lower limb and pain in diaper changes were also reported. No clinical signs of upper respiratory tract infection were noted. This was a term neonate delivered from a multigravida 24-years-old mother at 40 weeks postmenstrual age with caesarean section due to breech position of the baby. Birth weight was 3,760 g and somatometric features were within normal range.

During admission, physical examination revealed paleness, mottled skin and irritability, rectal temperature of 39 °C. She weighed 3,850 g. Clinical evidence of right lower limb swelling combined with erythematous appearance of skin which was painful on palpation with markedly reduced spontaneous movements of femur, raised the suspicion of deep vein thrombosis (Figure 1A). She was hemodynamic stable without need for cardiovascular or respiratory support. Laboratory



Figure 1A – Swelling and discoloration of right lower limb indicative of thrombosis on admission (at 11th day of life); 1B – remission of right lower limb swelling after 48 h of heparin treatment.

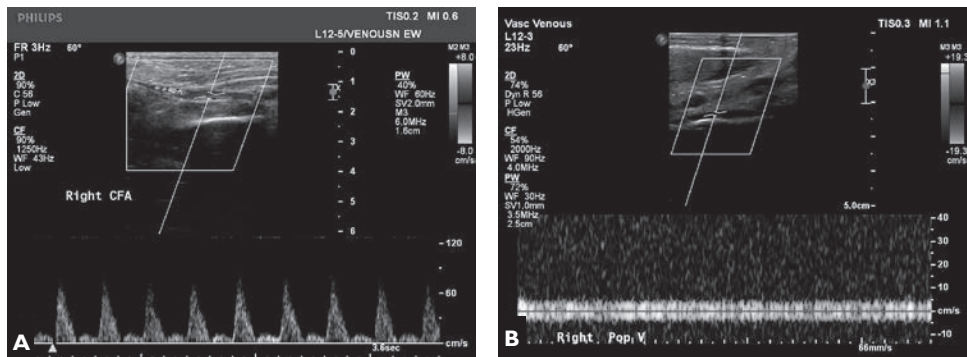


Figure 2A and B – Colour Doppler ultrasound scan of right leg showed thrombosis of right common femoral vein (CFV) with unobstructed arterial flow on admission.

examination showed a hemoglobin of 12.5 g/dl, thrombocytes were $146 \times 10^9/l$, leukocytes were $5.88 \times 10^9/l$ with an absolute neutrophil count of $2.96 \times 10^9/l$ and C-reactive protein was 21.8 mg/dl. Urine sediment and cerebrospinal fluid analyses were negative for pathogens isolation. Screening for coagulation disorders was unremarkable. Sepsis screen was obtained, a late onset sepsis was suspected and was commenced on vancomycin and amikacin as well as sedation with fentanyl. Brain ultrasound including Doppler scan was performed, without evidence of hemorrhage or infarction. Joint vascular and radiology team also performed a colour Doppler scan of R leg that showed thrombosis of R common femoral vein (CFV) with unobstructed arterial flow (Figure 2A and B). The neonate was immensely started, as per our NICU protocol, on iv unfractionated heparin with a loading dose of 75 mg/kg and maintenance dose of 28 mg/kg/hour for 4 hours. The

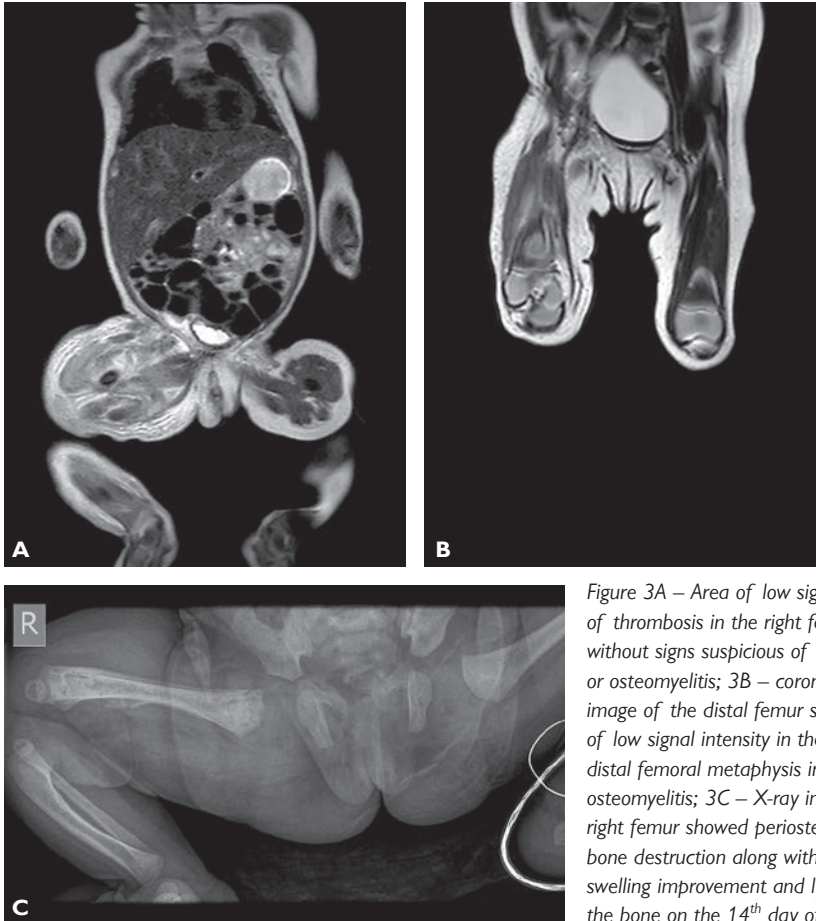


Figure 3A – Area of low signal in the site of thrombosis in the right femoral lumen, without signs suspicious of bone malignancy or osteomyelitis; 3B – coronal T1-weighted image of the distal femur shows an area of low signal intensity in the right medial distal femoral metaphysis indicative of osteomyelitis; 3C – X-ray imaging of the right femur showed periosteal reaction and bone destruction along with deep soft tissue swelling improvement and lytic changes in the bone on the 14th day of admission.

efficacy of heparin was evaluated with activated partial thromboplastin time (APTT), international normalized ratio (INR), anti-Xa in the end of the aforementioned course of intravenous heparin. The switch to low molecular weight heparin (LMWH) enoxaparin (150 mg/kg/dose subcutaneously) was guided by conventional laboratory scan. Antibiotic treatment was adjusted to ampicillin, vancomycin, amikacin given positive for *Streptococcus pyogenes* (group A) blood culture at the admission sample. On the 3rd day of admission, 48 hours post heparin infusion, there was noted clinical improvement in terms of edema reduction and decrease in R leg discoloration as well as lessening in pain (Figure 1B). The colour Doppler ultrasound showed reduction of the thrombus and blood flow improvement. An MRI (magnetic resonance imaging) R lower limb was performed on the 5th day of admission, showing evidence of gradual improvement in the site of thrombosis, without signs suspicious of bone malignancy (Figure 3A). On the 14th day of

admission, due to localized pain in the proximal part of R femur, a bone Tc99 scan was performed, which showed evidence of osteomyelitis of R femur. Similar findings indicative of osteomyelitis were detected on MRI (Figure 3B). Simultaneously, an X-ray imaging of the femur revealed periosteal reaction, bone destruction and soft tissue improvement while there were no pathological findings on X-ray at disease onset (Figure 3C). Orthopedic consultation was performed, and antibiotic treatment switched to amoxicillin per os after a 4-weeks intravenous course. The overall antibiotic treatment lasted for a 6 week course.

Evaluation of the family for *Streptococcus* colonization or infection was performed and nasal, rectal and vaginal samples were obtained. *Streptococcus pyogenes* was not confirmed in the isolates.

The management restricted to anticoagulant therapy with LMWH for 3 months (1-month therapeutic dose and 2-months prophylactic dose) and antibiotic therapy alone without surgery intervention and the patient recovered and discharged at 42 days of age. There were no profound complications and no recurrence for both bone damages or impaired movement and thrombosis with a mean follow up period of 12 and 6 months respectively. Labours for the evaluation of coagulation disturbances remained consistently negative for a time period of 6 months.

Discussion

In our patient GAS was isolated in blood culture, although this specific pathogen has been only described in very few cases of neonatal OM, with good response to 4-weeks intravenous vancomycin, ampicillin and amikacin and 2-weeks oral amoxicillin treatment (Frederiksen et al., 1993; Berberian et al., 2010; Ilharreborde, 2015). In our case, late onset sepsis was initially considered as the cause of the patient's clinical presentation, thus the neonate was initially started on vancomycin and amikacin. The most frequently isolated pathogen in neonates diagnosed with OM is *methicillin-resistant Staphylococcus aureus* (MRSA) followed by *Streptococcus group B* and gram-negative pathogens as part of maternal flora and breach delivery has been strongly proposed as risk factor which predisposes subjects for osteomyelitis in the neonatal period (Sarlangue et al., 2007). Based on the above, Castellazzi et al. (2016) recently suggested that, when neonatal OM is suspected, empirical antibiotic treatment with antistaphylococcal penicillin or vancomycin combined with amikacin should be opted as first choice. There is wide discussion in the management of pediatric OM, with some researchers suggesting a short-term intravenous treatment switched thereafter to oral agents in non-complicated cases, for an overall course of 3–6 weeks (Dartnell et al., 2012). However, the safety and efficacy of this approach in neonates has not been proven yet (Castellazzi et al., 2016). Our patient was initially treated as late-onset sepsis although she should have been treated for a community acquired infection. The antibiotic scheme with vancomycin and amikacin was driven by the improvement of inflammatory markers within 48 hours from the start of the above regimens.

Typically changes in X-ray may be present approximately 7–10 days after the disease onset while MRI imaging may play a role in the diagnosis in early stages (Blickman et al., 2004). Bone ultrasound (u/s) is a promising diagnostic tool in specialists with experience. The mean time of diagnosis is reported at 12–14 days after disease onset (Zhan et al., 2019). Our patient's diagnosis was set at 14 day of disease progress by bone Tc99 scan and confirmed by MRI and X-ray findings.

Group A Streptococcus has been reported as the second more frequent bacterial cause of OM in children. The invasive form of GAS-associated infection causes coagulation disorders mostly linked to plasminogen and kininogen activation, for this reason is also associated with episodes of vascular thrombosis (Ben Nasr et al., 1995). Soluble M-protein and its serotypes by using immunoregulatory properties activate equally the tissue factor, contact system and platelets (Shannon et al., 2007). This protein mediated activation of clotting factors and cells results in a stable fibrin structure which entraps bacteria and eliminates infection spread. GAS as a major immunomodulator leads to dysregulation of the coagulation system enhancing its invasive nature and presenting as purpura fulminans (González-Abad and Alonso Sanz, 2020). Sepsis-induced coagulopathy and immunothrombosis in the context of bacteria spread elimination is a well-established knowledge in both children and adults but scarcely investigated in neonates. Aberrations in the activation of coagulation cascade may lead in disturbances like disseminated intravascular coagulation with thrombosis or bleeding. Limited cases of thrombosis during osteomyelitis have been reported in the neonatal period. Moreover, it is a unique report of the deep vein thrombosis manifestation in GAS-associated neonatal osteomyelitis.

Neonatal venous thrombosis mostly is observed in hospitalized neonates while signs and symptoms are linked with thrombosis location. Premature infants are more prone to venous thrombosis accounted for 71% of the overall incidence. The underlying sickness and intensive care unit handlings are responsible for differences in timing thrombosis occurrence between term and preterm neonates (Saracco et al., 2016). In a German registry thrombosis was more commonly detected at 11th or 12th day of life than at birth mainly for premature neonates (Nowak-Göttl et al., 1997). Similarly, in our patient the diagnosis was placed on 12th day of life. Moreover, the presence of thrombosis at the admission was misleading for the final diagnosis. Ultrasonography is the most common imaging modality widely used to diagnose venous thrombosis (Male et al., 2003). An ultrasonography and a confirmatory MRI scan were performed to our patient.

There is a paucity of data regarding evidence based on clinical trials in treatment of neonatal thrombosis which is largely based on consensus guidelines. According to American College of Chest Physicians' guidelines treatment include unfractionated heparin and low molecular weight heparin and the administered doses are much higher to reach therapeutic targets compared to older children regarding the developmental hemostasis in neonates (Andrew, 1995; van Elteren et al., 2011;

Monagle et al., 2012). Duration of treatment varies from 3 months for thrombosis related to underlying disease to 6 months for idiopathic thrombosis (Monagle et al., 2012). Recent literature has introduced a new generation anticoagulant, rivaroxaban, for neonatal venous thrombosis. Its use is considered to secure non-recurrence of thrombosis, thrombus elimination and reduction of bleeding risk compared to standard heparin and vitamin K antagonists (Male et al., 2020). In our patient therapeutic levels of LMWH achieved with enhanced doses under monitoring with aPTT and anti-Xa levels. By simultaneously monitoring the maximum of safety and efficacy of heparin administration was achieved.

Conclusion

It follows that although osteomyelitis in neonates is rare it should be considered along with reduction in limb movement. Early diagnosis and treatment can prevent bone destruction and impairment of bone growth. *Group A Streptococcus*-associated osteomyelitis is equally rare and a potential risk factor for deep venous thrombosis development which in turn could be life threatening without prompt treatment.

References

- Andrew, M. (1995) Developmental hemostasis: Relevance to hemostatic problems during childhood. *Semin. Thromb. Hemost.* **21(4)**, 341–356.
- Ben Nasr, A. B., Herwald, H., Müller-Esterl, W., Björck, L. (1995) Human kininogens interact with M protein, a bacterial surface protein and virulence determinant. *Biochem. J.* **305(Pt 1)**, 173–180.
- Berberian, G., Firpo, V., Soto, A., Lopez Mañan, J., Torroija, C., Castro, G., Polanuer, P., Espinola, C., Piñeiro, J. L., Rosanova, M. T. (2010) Osteoarthritis in the neonate: Risk factors and outcome. *Braz. J. Infect. Dis.* **14(4)**, 413–418.
- Blickman, J. G., van Die, C. E., de Rooy, J. W. J. (2004) Current imaging concepts in pediatric osteomyelitis. *Eur. Radiol.* **14**, L55–L64 (Suppl. 4).
- Castellazzi, L., Mantero, M., Esposito, S. (2016) Update on the management of pediatric acute osteomyelitis and septic arthritis. *Int. J. Mol. Sci.* **17(6)**, 855.
- Dartnell, J., Ramachandran, M., Katchburian, M. (2012) Haematogenous acute and subacute paediatric osteomyelitis: A systematic review of the literature. *J. Bone Joint Surg. Br.* **94(5)**, 584–595.
- Frederiksen, B., Christiansen, P., Knudsen, F. U. (1993) Acute osteomyelitis and septic arthritis in the neonate, risk factors and outcome. *Eur. J. Pediatr.* **152(7)**, 577–580.
- González-Abad, M. J., Alonso Sanz, M. (2020) Invasive *Streptococcus pyogenes* infections (2011–2018): EMM-type and clinical presentation. *An. Pediatr. (Engl. Ed.)* **92(6)**, 351–358. (in Spanish)
- Ilharreborde, B. (2015) Sequelae of pediatric osteoarticular infection. *Orthop. Traumatol. Surg. Res.* **101**, S129–S137 (Suppl. 1).
- Male, C., Kuhle, S., Mitchell, L. (2003) Diagnosis of venous thromboembolism in children. *Semin. Thromb. Hemost.* **29(4)**, 377–390.
- Male, C., Lensing, A. W. A., Palumbo, J. S., Kumar, R., Nurmeev, I., Hege, K., Bonnet, D., Connor, P., Hooimeijer, H. L., Torres, M., Chan, A. K. C., Kenet, G., Holzhauer, S., Santamaría, A., Amedro, P., Chalmers, E., Simioni, P., Bhat, R. V., Yee, D. L., Lvova, O., Beyer-Westendorf, J., Biss, T. T., Martinelli, I., Saracco, P., Peters, M., Kállay, K., Gauger, C. A., Massicotte, M. P., Young, G., Pap, A. F., Majumder, M., Smith, W. T., Heubach, J. F., Berkowitz, S. D., Thelen, K., Kubitzka, D., Crowther, M., Prins, M. H.,

- Monagle, P.; EINSTEIN-Jr Phase 3 Investigators (2020) Rivaroxaban compared with standard anticoagulants for the treatment of acute venous thromboembolism in children: A randomised, controlled, phase 3 trial. *Lancet Haematol.* **7(1)**, e18–e27.
- Monagle, P., Chan, A. K. C., Goldenberg, N. A., Ichord, R. N., Journeycake, J. M., Nowak-Göttl, U., Vesely, S. K. (2012) Antithrombotic therapy in neonates and children: Antithrombotic Therapy and Prevention of Thrombosis, 9th ed.: American College of Chest Physicians Evidence-Based Clinical Practice Guidelines. *Chest* **141**, e737S–e801S (Suppl. 2).
- Nowak-Göttl, U., von Kries, R., Göbel, U. (1997) Neonatal symptomatic thromboembolism in Germany: Two year survey. *Arch. Dis. Child. Fetal Neonatal Ed.* **76(3)**, F163–F167.
- Saracco, P., Bagna, R., Gentilomo, C., Magarotto, M., Viano, A., Magnetti, F., Giordano, P., Luciani, M., Molinari, A. C., Suppiej, A., Ramenghi, L. A., Simioni, P.; Neonatal Working Group of Registro Italiano Trombosi Infantili (RITI) (2016) Clinical data of neonatal systemic thrombosis. *J. Pediatr.* **171**, 60-6.e1.
- Sarlangue, J., Castella, C., Pontailleur, J., Chateil, J. F. (2007) Neonatal infections of the bones and joints. *Arch. Pediatr.* **14**, S108–S112 (Suppl. 2). (in French)
- Shannon, O., Hertzén, E., Norrby-Teglund, A., Mörgelin, M., Sjöbring, U., Björck, L. (2007) Severe streptococcal infection is associated with M protein-induced platelet activation and thrombus formation. *Mol. Microbiol.* **65(5)**, 1147–1157.
- van Elteren, H. A., Veldt, H. S., Te Pas, A. B., Roest, A. A. W., Smiers, F. J., Kollen, W. J., Sramek, A., Walther, F. J., Lopriore, E. (2011) Management and outcome in 32 neonates with thrombotic events. *Int. J. Pediatr.* **2011**, 217564.
- Zhan, C., Zhou, B., Du, J., Chen, L. (2019) Clinical analysis of 17 cases of neonatal osteomyelitis: A retrospective study. *Medicine (Baltimore)* **98(2)**, e14129.

Successful Treatment of Detachment of the Incision after Al-Ghorab Procedure: A Case Report and Review of Literature

Rifat Burak Ergül¹, Mehmet Akif Ramazanoğlu², Murat Sambel², Sinan Akşit², Murat Dursun¹, Ateş Kadioğlu^{1,2}

¹Department of Urology, Istanbul Faculty of Medicine, Istanbul University, Istanbul, Turkey;

²Department of Urology, Section of Andrology, Istanbul Faculty of Medicine, Istanbul University, Istanbul, Turkey

Received December 31, 2022; Accepted August 17, 2023.

Key words: Al-Ghorab procedure – Priapism – Shunt surgery – Wound infection

Abstract: Al-Ghorab procedure is known as open distal shunt for the treatment of ischemic priapism. In the literature, no information in terms of complications is available in three of fourteen studies. In the remaining eleven studies, complications occurred in five studies only. Here we present a case report describing successful treatment of detachment of the incision after Al-Ghorab procedure.

Mailing Address: Rifat Burak Ergül, MD., Department of Urology, Istanbul Faculty of Medicine, Istanbul University, Topkapi Neighbourhood, Turgut Özal Street No. 118, 34093 Fatih, Istanbul, Turkey; Phone: +90 212 414 20 00; Fax: +90 212 635 85 22; e-mail: rifat-ergul@hotmail.com

<https://doi.org/10.14712/23362936.2023.24>

© 2023 The Authors. This is an open-access article distributed under the terms of the Creative Commons Attribution License (<http://creativecommons.org/licenses/by/4.0>).

Introduction

Priapism is defined as a prolonged penile erection lasting longer than four hours unrelated to sexual interest or stimulation. The incidence of priapism is 0.9/100,000 per year (Eland et al., 2001). Priapism is categorised as *ischemic* (low flow), *stuttering* (recurrent) and *non-ischemic* (high flow).

Ischemic priapism accounts for 95% of the priapism cases and if not treated accordingly, leads within few hours to irreversible changes resulting in permanent erectile dysfunction. First line therapy is intracavernosal aspiration \pm irrigation with 0.9% saline, eventually in combination with pharmacological agents. Penile shunt surgery (PSS) and implantation of a penile prosthesis (IPP) are indicated as a second-line treatment. Types of shunt surgeries are percutaneous distal (corpora-glandular), open distal (corpora-glandular), open proximal (corpora-spongiosal), peno-scrotal decompression and corpora-venous anastomoses/shunts.

Open distal (corpora-glandular) shunt is known as Al-Ghorab procedure and was modified by Burnett. Briefly, Al-Ghorab procedure is 1–2 centimetre (cm) long transverse incision approximately 1 cm distally from the dorsal coronal margin of the glans penis. The distal end parts of the tunica albuginea underneath

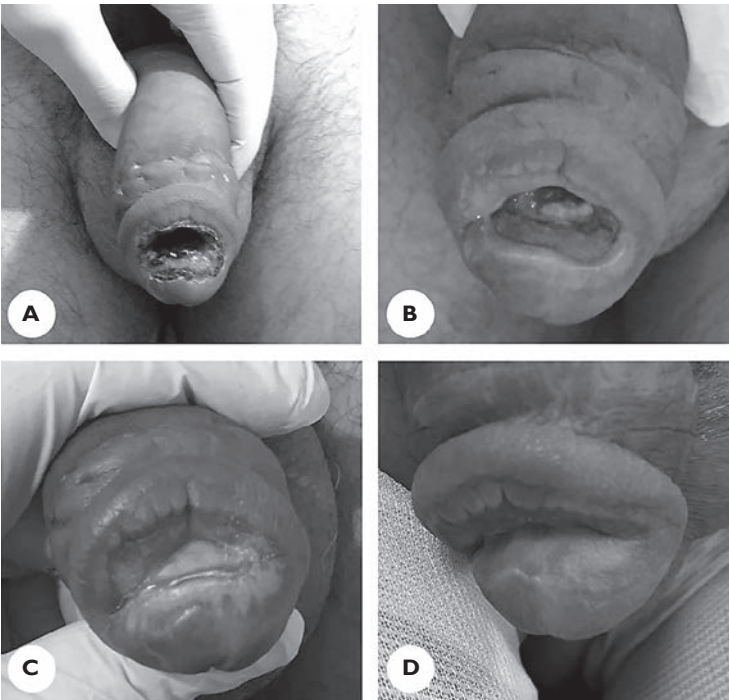


Figure 1 – A) Detachment of the incision on the glans; B) follow-up on the 15th day; C) follow-up on the fourth month; D) local finding before glansplasty.

the incision are excised bilaterally and a corpora-glandular shunt is created (Burnett's modification instead of tunica albuginea excision uses Hegar dilators to create communication between the corpora cavernosa and the glans). The penis is manually compressed from proximal to distal and the accumulated blood in corpora cavernosa is completely drained until fresh blood is obtained. The operation is completed by using 3/0 absorbable sutures to close the skin incision (Muller, 2016).

Case report

A 48-year-old patient without any comorbidity presented for an episode of priapism (after intracavernosal injection of papaverine hydrochloride) lasting for more than 48 hours to an emergency clinic in Iran, where he underwent cavernosal aspiration and saline irrigation with sympathomimetic agent. The priapism episode persisted, and he underwent Al-Ghorab procedure as described above.

Subsequently, the patient was evaluated on the sixth postoperative day at our outpatient clinic after Al-Ghorab procedure. On physical examination detachment of the incision on the glans and foul-smelling discharge were noticed (Figure 1A).

The amoxicillin/clavulanic acid 1,000 mg was administered immediately. After the antibiotic treatment the infection at the detachment side ceased and the patient was scheduled for glans approximation procedure six months after the surgery (Figure 1B and C).

The patient returned six months later from Iran and underwent a glansplasty operation (Figure 1D). The fibrotic tissue at the edges of the wound was removed and the wings of the glans were approximated by means of two-layer fashion. The first layer was approximated by using 4/0 polyglycolic acid and the skin by 4/0 rapid-polyglycolic acid. The histopathological examination of fibrotic tissue revealed fibrosis with inflammatory infiltration. No complications were seen at the postoperative follow-up (Figure 2A).

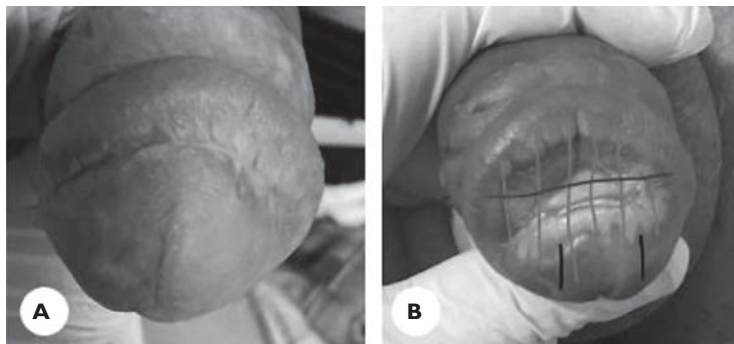


Figure 2 – A) Postoperative second month; B) light grey lines: arteries, dark grey line: Al-Ghorab incision, black line: T-shunt incision.

Table 1 – Studies with Al-Ghorab procedure

	Type of surgery	Number of patients	Number of patients with complications	Type of complications
Ercole et al. (1981)	Al-Ghorab	7	NR	
Segal et al. (2013)	modified Al-Ghorab	10	2	1: wound infection, penile necrosis, urethrocutaneous fistula
Burnett and Pierorazio (2009)	modified Al-Ghorab	3	0	
Teo et al. (2021)	Al-Ghorab	1	0	
Afriansyah et al. (2017)	modified Al-Ghorab	1	NR	
Sekerci et al. (2015)	Al-Ghorab	1	0	
Paladino et al. (2014)	Al-Ghorab	1	1	necrosis distal to the incision, dorsal glandular urethrocutaneous fistula, meatal stenosis
Ford-Glanton et al. (2014)	modified Al-Ghorab	1	1	necrosis, abscess, gangrene
De Stefani et al. (2001)	Al-Ghorab	1	1	urethrocutaneous fistula
Lian et al. (2010)	modified Al-Ghorab	12	0	
Shiraishi and Matsuyama (2013)	modified Al-Ghorab	2	0	
Zheng et al. (2013)	1: Al-Ghorab 2: Al-Ghorab + Grayhack-shunt	1 1	0 1	0 urethral fistula
Nixon et al. (2003)	Al-Ghorab	18	NR	
Ugwumba et al. (2016)	Al-Ghorab	15	0	

NR – not reported

Discussion

Al-Ghorab procedure is one of the shunt surgeries performed as the second line treatment of ischemic priapism. Wound infections, cavernositis, penile skin necrosis, urethrocutaneous fistula, and urethral stricture can develop after Al-Ghorab procedure. There are 14 studies evaluating Al-Ghorab or modified Al-Ghorab

procedure in the literature. In three of fourteen studies, no information in terms of complications is available. In the remaining eleven studies, complications occurred in five of them only (Table 1).

Segal et al. (2013) examined 10 cases treated with modified Al-Ghorab shunt procedure. Wound infection and penile skin necrosis were encountered in two patients after the surgery and one of them developed urethrocutaneous fistula (Segal et al., 2013). The causes of priapism in these two patients were idiopathic and intracavernosal injection of trimix. The patients were treated with surgical debridement.

Paladino et al. (2014) reported necrosis and urethrocutaneous fistula due to Al-Ghorab procedure in a patient who was on valproic acid, clonazepam, haloperidol and levomepromazine for the treatment of schizophrenia. An inadvertent injury of the glandular urethra occurred during the Al-Ghorab procedure. In the follow-up of the patient, necrosis occurred in the distal part of the incision and the patient developed dorsal glandular urethrocutaneous fistula and meatal stenosis on the 14th day after catheter removal. Johanson urethroplasty was performed to treat the fistula.

Ford-Glanton et al. (2014) reported a case of priapism with diabetes mellitus, arterial hypertension, hepatitis C and hyperlipidaemia. The patient complained of fever on admission to the hospital. Leukocytosis ($27,200 \times 10^9/l$) was detected in the blood count. The patient underwent Al-Ghorab procedure and antibiotic treatment for ten days with cephalexin. On the 21st day of the follow-up, thick scar tissue was observed in the glans penis and the wound was considered to have healed properly. However, on the 30th day, the patient presented with complete glans necrosis. After MR (magnetic resonance) imaging, an abscess of approximately 14 cm length was detected spreading to both corpora cavernosa and an emergency distal penectomy was performed. Unlike this case, the patient in our report was on antibiotic treatment for four weeks and he developed no additional penile pathology except wound dehiscence.

De Stefani et al. (2001) reported a case with priapism which was initially treated with Winter procedure. Because of the persistence of priapism episode, Al-Ghorab procedure was performed. The patient developed high flow priapism postoperatively which was treated with the embolization of the cavernosal arteries. Few days later, small, darkened spot appeared on the skin of the glans. Meatal stenosis and urethrocutaneous fistula developed one month later. The fistula was treated with three-layer microsurgical technique and stenosis was managed with self-dilation.

Zheng et al. (2013) reported a urethral fistula in a patient with a priapism episode caused by risperidone. Winter, Al-Ghorab and Grayhack-shunt operations were performed as the surgical treatment of the priapism episode. The urethrocutaneous fistula, which appeared in the early period, closed spontaneously seven months postoperatively.

Al-Ghorab procedure is one of the distal shunts used in the treatment of ischemic priapism with high success rate (80–100%) since 1970s. However, the distal deep arteries which run longitudinally on the glans can be damaged by the transverse incision in this procedure which is subject to complications related to ischemia (Juskiewenski et al., 1982). Wound infection, glans necrosis and gangrene are more likely to occur in Al-Ghorab procedure which can compromise the branches of the deep dorsal artery. Therefore, procedures such as T-shunt, in which an incision parallel to the course of arteries is performed, should be preferred to prevent possible complications (Figure 2B).

Conclusion

Al-Ghorab procedure has a lot of complications such as wound infections, glans necrosis etc. Based on the anatomic localisation of the arteries, T-shunt procedure should be preferred as a management of ischemic priapism not responding to less invasive therapeutic modalities.

References

- Afriansyah, A., Yuri, P., Hutasoit, Y. I. (2017) Intracorporeal dilatation plus Al-Ghorab corporoglandular shunt for salvage management of prolonged ischemic priapism. *Urol. Case Rep.* **12**, 11–13.
- Burnett, A. L., Pierorazio, P. M. (2009) Corporal “snake” maneuver: Corporoglandular shunt surgical modification for ischemic priapism. *J. Sex. Med.* **6**, 1171–1176.
- De Stefani, S., Savoca, G., Ciampalini, S., Stener, S., Gattuccio, I., Belgrano, E. (2001) Urethrocuteaneous fistula as a severe complication of treatment for priapism. *BJU Int.* **88**, 642–643.
- Eland, I. A., van der Lei, J., Stricker, B. H., Sturkenboom, M. J. (2001) Incidence of priapism in the general population. *Urology* **57**, 970–972.
- Ercole, C. J., Pontes, J. E., Pierce, J. M. Jr. (1981) Changing surgical concepts in the treatment of priapism. *J. Urol.* **125**, 210–211.
- Ford-Glanton, B. S., Patel, P., Siddiqui, S. (2014) Penile gangrene with abscess formation after modified Al-Ghorab shunt for idiopathic ischemic priapism. *Case Rep. Urol.* **2014**, 705417.
- Juskiewenski, S., Vaysse, P., Moscovici, J., Hammoudi, S., Bouissou, E. (1982) A study of the arterial blood supply to the penis. *Anat. Clin.* **4**, 101–107.
- Lian, W., Lv, J., Cui, W., Jin, Z., Liu, T., Li, W., Yuan, Y., Xin, Z. (2010) Al-Ghorab shunt plus intracavernous tunneling for prolonged ischemic priapism. *J. Androl.* **31**, 466–471.
- Muller, A. (2016) Al-Ghorab shunt for priapism. *J. Sex. Med.* **13**, 1279–1284.
- Nixon, R. G., O’Connor, J. L., Milam, D. F. (2003) Efficacy of shunt surgery for refractory low flow priapism: A report on the incidence of failed detumescence and erectile dysfunction. *J. Urol.* **170**, 883–886.
- Paladino, J. R. Jr., Wroclawski, M., Den Julio, A., Teixeira, G. K., Glina, S., Lima Pompeo, A. C. (2014) Urethrocuteaneous fistula post-Al-Ghorab shunt. *Can. Urol. Assoc. J.* **8**, E570–E571.
- Segal, R. L., Readal, N., Pierorazio, P. M., Burnett, A. L., Bivalacqua, T. J. (2013) Corporal Burnett “Snake” surgical maneuver for the treatment of ischemic priapism: Long-term followup. *J. Urol.* **189**, 1025–1029.
- Sekerci, C. A., Akbal, C., Sener, T. E., Sahan, A., Sahin, B., Baltacioglu, F., Simsek, F. (2015) Resistant pediatric priapism: A real challenge for the urologist. *Can. Urol. Assoc. J.* **9**, E562–E564.
- Shiraishi, K., Matsuyama, H. (2013) Salvage management of prolonged ischemic priapism: Al-Ghorab shunt plus cavernous tunneling with blunt cavernosotomy. *J. Sex. Med.* **10**, 599–602.

- Teo, J. S. M., Lee, H. J., Yuen, J. S. P. (2021) Perioperative anticoagulation and open distal corpora cavernosa shunt in the management of a case of stuttering idiopathic persistent childhood ischaemic priapism. *Asian J. Urol.* **8**, 436–439.
- Ugwumba, F. O., Ekwedigwe, H. C., Echetafu, K. N., Okoh, A. D., Nnabugwu, I., Ugwuudu, E. S. (2016) Ischemic priapism in South-East Nigeria: Presentation, management challenges, and aftermath issues. *Niger. J. Clin. Pract.* **19**, 207–211.
- Zheng, D. C., Yao, H. J., Zhang, K., Xu, M. X., Chen, Q., Chen, Y. B., Cai, Z. K., Lu, M. J., Wang, Z. (2013) Unsatisfactory outcomes of prolonged ischemic priapism without early surgical shunts: Our clinical experience and a review of the literature. *Asian J. Androl.* **15**, 75–78.

Use of a Questionnaire for Evaluation of Surgical Treatment of Masseter Muscle Hypertrophy: A Case Report

**Luiza Roberta Bin, Mateus Diego Pavelski,
Ana Carolina Fraga Fernandes, Eleanor Álvaro Garbin Junior**

Oral and Maxillofacial Surgery, State University of Western Paraná, Cascavel, Brazil

Received February 15, 2023; Accepted August 17, 2023.

Key words: Masseter muscle – Muscle hypertrophy – Myotomy

Abstract: Masseter hypertrophy (MH) is an uncommon natural condition that affects the facial contour. The etiology is debatable, and complaints are usually cosmetic in nature. The diagnosis is essentially clinical and aided by imaging tests. Treatment is still controversial. The literature is relatively scarce in relation to information on MH, particularly in the evaluation of outcomes. Through questionnaires, the progress was observed in the evaluation of the outcomes of aesthetic procedures. Thus, the purpose of this paper is to apply a Facelift Outcome Evaluation (FOE) questionnaire to evaluate the outcomes of surgical treatment in a case of MH. A 23-year-old male presented to the clinic complaining of bullying due to his facial aesthetics. Clinical and imaging evaluation was performed, with the creation of surgical guides. The patient answered the FOE questionnaire pre- and postoperatively, with results of 12.5 and 100.00 respectively. This subjectively shows the success of the treatment. We suggest that a questionnaire applied exclusively to masseter hypertrophy should be developed, as well as studies for the development of muscle volume measurement protocols, aiming at a more specific evaluation of the surgical outcomes.

Mailing Address: Luiza Roberta Bin, DDS., Oral and Maxillofacial Surgery, State University of Western Paraná, 1619 Universitaria – Universitario, Cascavel, Paraná, 85819-110, Brazil; e-mail: luizarbin@protonmail.com

Introduction

Masseter hypertrophy (MH) is an uncommon natural condition that affects the facial contour (Oliveira et al., 2004; Pereira et al., 2006; Tabrizi et al., 2010; Özkan et al., 2012; Andreishchev et al., 2014; Simão et al., 2014; Trento et al., 2017; Ayhan et al., 2018; Almkhtar and Fabi, 2019) and which may also be referred to as square face syndrome (Rispoli et al., 2008; Özkan et al., 2012; Andreishchev et al., 2014; Trento et al., 2017). Because the masseter muscle plays a key role in facial aesthetics (Xu and Yu, 2013), patients may suffer from psychological issues due to their facial appearance (Tabrizi et al., 2010; Özkan et al., 2012; Ayhan et al., 2018). MH is more common between 20 and 40 years of age, with no difference between genders (Oliveira et al., 2004; Pereira et al., 2006; Bravo et al., 2016; Almkhtar and Fabi, 2019), being more present among Asians and less among Caucasians (Rispoli et al., 2008; Bravo et al., 2016). The etiology is discussed as involving masticatory habits, bruxism, and mandibular retrusion (Oliveira et al., 2004; Pereira et al., 2006; Pary and Pary, 2011; Simão et al., 2014; Almkhtar and Fabi, 2019). It is accepted that, because the masseteric musculature is inserted in the angle of the mandible, it may cause an overdevelopment of this region, due to muscle strength (Rispoli et al., 2008; Pary and Pary, 2011; Andreishchev et al., 2014; Trento et al., 2017; Ayhan et al., 2018). Generally, the patient's complaint is aesthetic (Pereira et al., 2006; Rispoli et al., 2008; Trento et al., 2017; Ayhan et al., 2018), due to asymmetry, when unilateral, or due to a very wide face, when bilateral (Pary and Pary, 2011; Trento et al., 2017; Anehosur et al., 2020). The bilateral condition is more common (Kim and Kameyama, 1992). Unilateral hypertrophy is mainly since 78% of the population has one preferred side in mastication (Almkhtar and Fabi, 2019). Despite being considered an asymptomatic condition, it may be related to bruxism, pain, or functional disorders (Oliveira et al., 2004; Bravo et al., 2016; Ayhan et al., 2018; Almkhtar and Fabi, 2019; Anehosur et al., 2020). The diagnosis is essentially clinical and supported by imaging tests (Pereira et al., 2006; Simão et al., 2014; Trento et al., 2017), such as ultrasonography, computed tomography (CT), three-dimensional reconstruction, and magnetic resonance imaging (Oliveira et al., 2004; Ayhan et al., 2018; Almkhtar and Fabi, 2019; Anehosur et al., 2020). The differential diagnosis involves vascular or glandular tumours and inflammatory diseases, such as myositis ossificans (Rispoli et al., 2008; Özkan et al., 2012; Simão et al., 2014; Trento et al., 2017; Ayhan et al., 2018), which should be considered especially when there is facial asymmetry (Ayhan et al., 2018).

Treatment is controversial (Tabrizi et al., 2010; Özkan et al., 2012; Ayhan et al., 2018) and encompasses two approaches: conservative (Oliveira et al., 2004; Pereira et al., 2006; Kühl et al., 2013; Simão et al., 2014; Bravo et al., 2016; Ayhan et al., 2018; Almkhtar and Fabi, 2019) and surgical (Oliveira et al., 2004; Pereira et al., 2006; Kühl et al., 2013; Trento et al., 2017; Ayhan et al., 2018). Conservative treatment is based on the creation of muscle relaxant plates and the use of muscle relaxants, although they are not as effective (Pereira et al., 2006; Pary and Pary,

2011; Almkhatar and Fabi, 2019). The infiltration of botulinum toxin type A in the medial portion of the muscle – the region with the greatest ramification of the masseteric nerve – can be a safe alternative, as it minimizes muscle contraction by preventing the release of acetylcholine in the synaptic cleft, decreasing muscle activity (Bravo et al., 2016; Almkhatar and Fabi, 2019), being first described in 1994 by Moore and Wood and Smyth (Xu and Yu, 2013; Almkhatar and Fabi, 2019). Nevertheless, it is not a definitive treatment option, as muscle function returns after 3–6 months following application (Pary and Pary, 2011; Bravo et al., 2016; Almkhatar and Fabi, 2019). Surgical treatment was first described by Gurney in 1947 and was based on partial removal of the masseter muscle through an extraoral approach (Kim and Kameyama, 1992; Oliveira et al., 2004; Kim et al., 2005; Rispoli et al., 2008; Tabrizi et al., 2010; Andreishchev et al., 2014; Trento et al., 2017). Wood suggested the resection of the mandibular angle, without manipulation of the masseter, by intraoral access (Tabrizi et al., 2010; Özkan et al., 2012; Ayhan et al., 2018). In 1949, Adams proposed associating partial muscle resection with resection of the mandibular angle (Kim and Kameyama, 1992; Oliveira et al., 2004; Rispoli et al., 2008; Andreishchev et al., 2014). Given the fact that the goal of the treatment is to achieve the aesthetic result, the intraoral access was introduced, avoiding scars and/or nerve damage in the marginal branch of the facial nerve (Andreishchev et al., 2014; Trento et al., 2017; Almkhatar and Fabi, 2019), being described by Converse in 1951 (Kim and Kameyama, 1992; Kim et al., 2005; Andreishchev et al., 2014; Trento et al., 2017). Surgical management is relatively simple, albeit with variable results (Kim et al., 2005). Finally, there is no consensus on which option would be the most suitable for the treatment of MH (Rispoli et al., 2008; Tabrizi et al., 2010; Pary and Pary, 2011; Almkhatar and Fabi, 2019).

The literature is relatively scarce in relation to information on MH (Pary and Pary, 2011; Trento et al., 2017), mainly in the form of evaluation of outcomes (Furlani, 2015). Greater objectivity is needed in the evaluation of outcomes of aesthetic treatments, in which this parameter is subjective (Furlani, 2015). Through questionnaires, an evolution has been observed in the evaluation of the outcomes of these procedures (Furlani, 2015). Questionnaires provide the feedback from patients, which indicate positive or negative outcomes and the degree of the result (Hajcak et al., 2006).

Therefore, the purpose of this paper is to apply a Facelift Outcome Evaluation (FOE) questionnaire to evaluate the outcomes of surgical treatment in a case of MH.

Case report

A 23-year-old male patient was admitted to the oral and maxillofacial surgery department for complaining about his aesthetic appearance and facial width, precisely in the region of the mandibular angles. He reported being the victim of bullying and ridicule for his facial appearance. During physical examination, it was

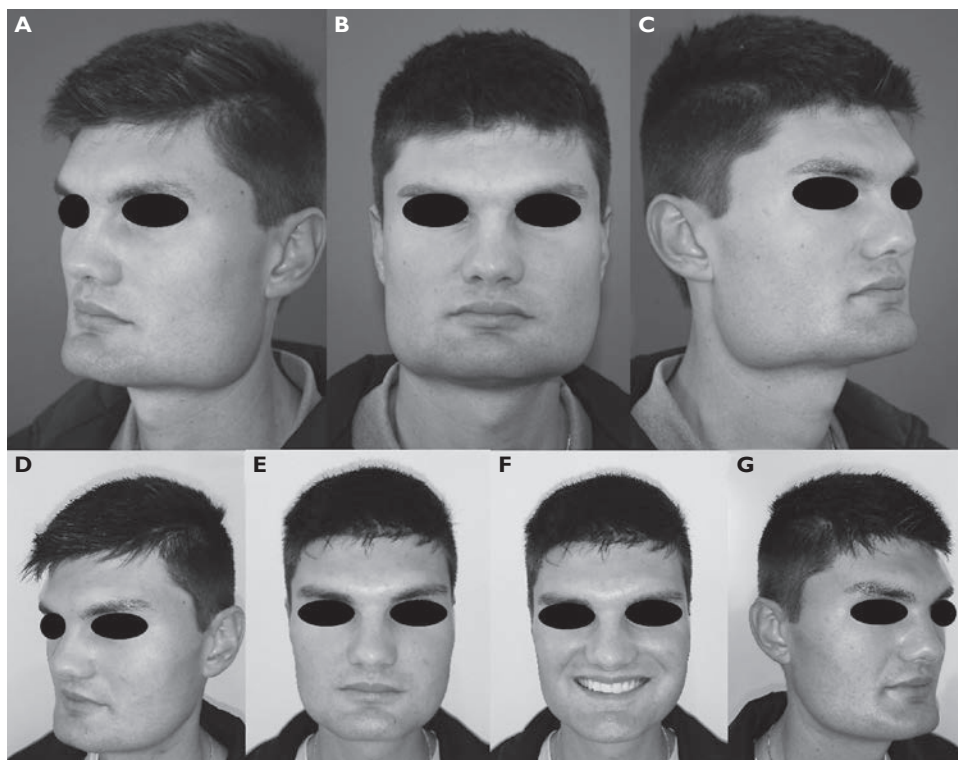


Figure 1 – A) Initial clinical appearance of the patient in $\frac{3}{4}$ left view; B) initial clinical appearance of the patient in frontal view; C) initial clinical appearance of the patient in $\frac{3}{4}$ right view; D) postoperative at 6 months clinical appearance of the patient in $\frac{3}{4}$ left view; E) postoperative at 6 months clinical appearance of the patient in frontal view; F) postoperative at 6 months clinical appearance in smiling frontal view; G) postoperative at 6 months clinical appearance of the patient in $\frac{3}{4}$ right view.

observed that the patient had a slightly class II bite, with acceptable occlusion, absence of excessive tooth wear, and bilateral masseteric swelling (Figure 1A–C). He denied having deleterious or parafunctional habits. In this context, complementary imaging tests were requested to diagnose the swelling.

Panoramic radiography showed a prominent mandibular angle without bone abnormality (Figure 2). On computed tomography of the face, a prominent muscle and bone position was observed in the mandibular angle, also without bone alterations (Figure 3A–C). The diagnosis of masseter hypertrophy was concluded through a combination of clinical and imaging evaluation. Subsequently, following the application of the FOE questionnaire according to the formula $\text{sum of responses}/16 \times 100$, the result $2/16 \times 100 = 12.5$ was found.

The patient was instructed as to conservative treatment option, such as interocclusal device and application of botulinum toxin, in an attempt to reduce

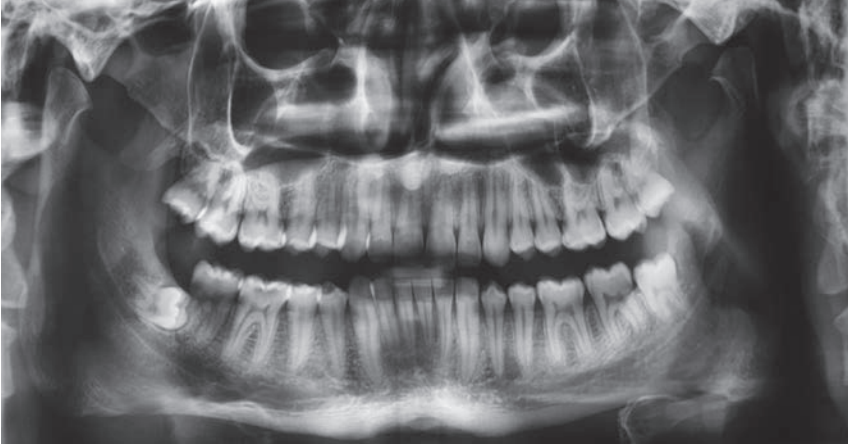


Figure 2 – Initial panoramic radiograph.

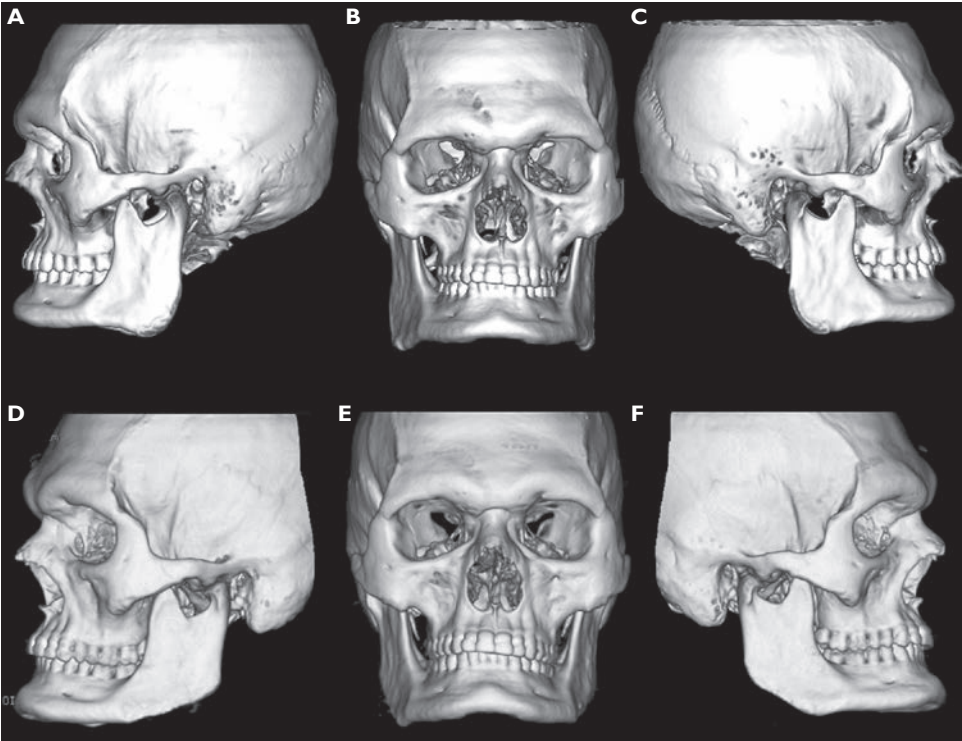


Figure 3 – A) Initial computed tomography in 3D reconstruction of the patient in $\frac{3}{4}$ left view; B) initial computed tomography in 3D reconstruction of the patient in frontal view; C) initial computed tomography in 3D reconstruction of the patient in $\frac{3}{4}$ right view; D) postoperative computed tomography in 3D reconstruction of the patient in $\frac{3}{4}$ left view; E) postoperative computed tomography in 3D reconstruction of the patient in frontal view; F) postoperative computed tomography in 3D reconstruction of the patient in $\frac{3}{4}$ right view.

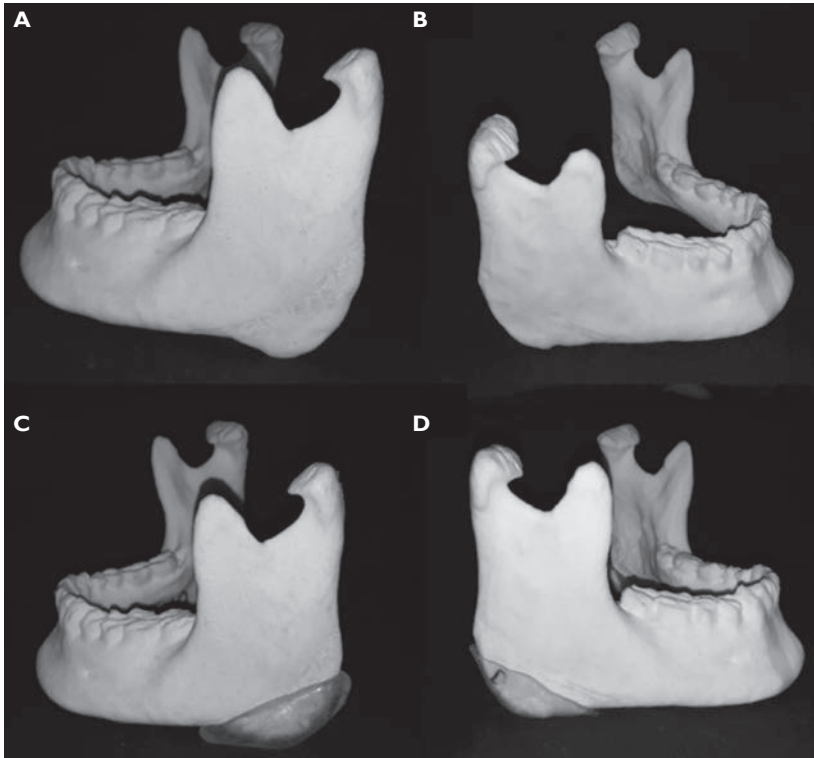


Figure 4 – A) 3D printed model in ¾ left view; B) 3D printed model in ¾ right view; C) left cutting guide positioned in the 3D printed model; D) right cutting guide positioned in the 3D printed model.

muscle strength and cause atrophy of the masseter muscle. Another alternative would be the orthognathic surgery to improve the facial appearance and zygomatic osteotomy. However, the patient chose the mandibular recontour osteotomy and masseter muscle myotomy.

For the surgical planning, a 3D stereolithographic model was made based on computed tomography scan, and osteotomy guides were made with acrylic resin (Figure 4). The procedure was performed under general anesthesia, through a bilateral submandibular access. The regions of the mandibular angles were exposed, and the superficial and deep layers of the masseter muscle were careful dissected. Mandibular osteotomies were performed in the mandibular angle according to the proper position of surgical guides, using a piezoelectric surgery device and 72-fissure burr and grinding burr to smooth the osteotomy edges (Figure 5A–D). For the myotomy, an electrocautery was used during tissue cutting and partial removal of the muscle layer, aiming to minimize bleeding, followed by suturing in layers and dressing (Figure 5E and F).

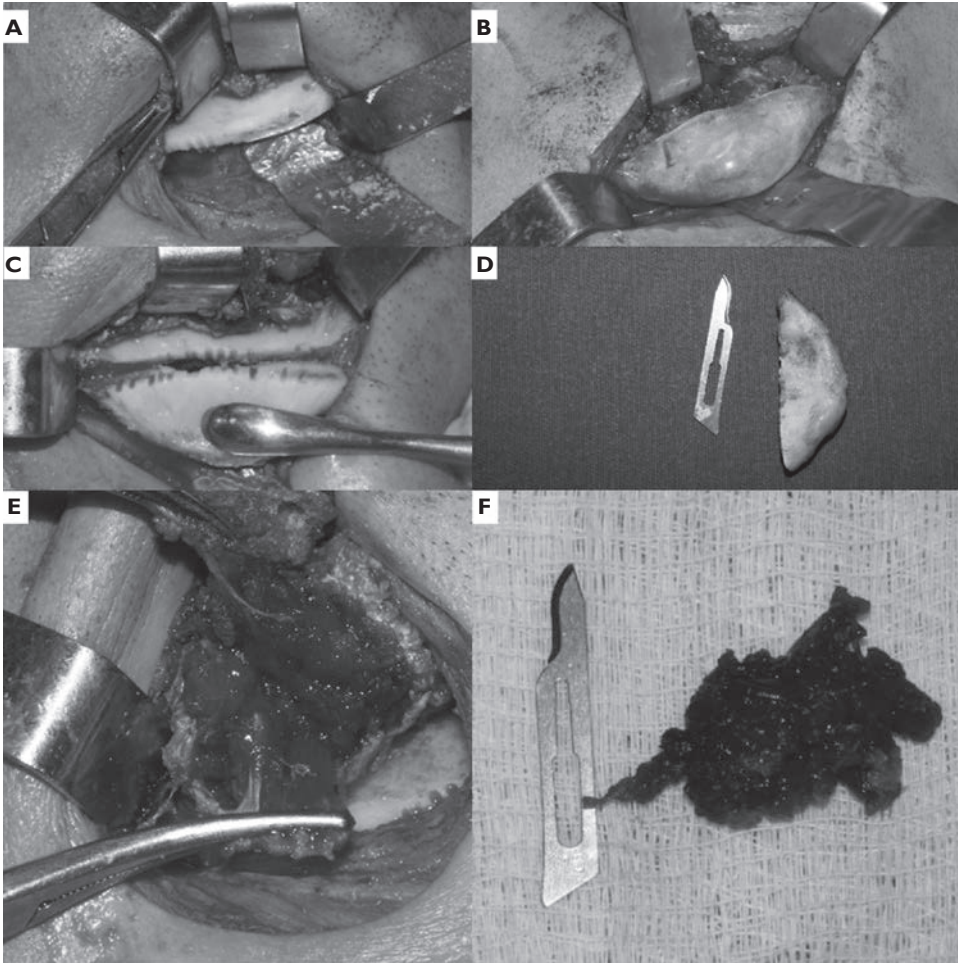


Figure 5 – Trans-operative: A) left mandibular angle exposed; B) left cutting guide positioned in the mandibular angle; C) osteotomy of the mandibular angle and subsequent osteoplasty; D) mandibular angle removed; E) myotomy of the masseter muscle; F) masseter muscle removed.

No complications occurred in the postoperative period. No damage to the marginal nerve of the mandible was seen. After 1 year of surgery, he declares to be satisfied with the result (Figure 1D–G). The satisfaction questionnaire was applied again, and the result was $16/16 \times 100 = 100$. The post operative computed tomography was taken (Figure 3D–F).

All procedures performed in studies involving human participants were in accordance with the ethical standards of the institutional and/or national research committee and with the 1964 Helsinki Declaration and its later amendments or comparable ethical standards.

Discussion

There are 10 types of face according to Poch's classification, with the masseter muscle representing a relevant structure in facial aesthetics. For that reason, masseter hypertrophy leads to an unsightly shape, the so-called square face (Andreishchev et al., 2014; Bocchialini et al., 2017). Clinical evaluation is important for diagnosis, as well as panoramic radiography and photographs, to determine the amount of bone to be resected (Kim and Kameyama, 1992). Computed tomography is an excellent tool for more information regarding anatomical structures, but it is not ideal for defining the limits between the buccal and lingual bone wall, which can be achieved via magnetic resonance imaging (MRI) (Kim and Kameyama, 1992). Ultrasonography is able to meet the needs of MRI, being a cheap and quick exam to be performed (Kim and Kameyama, 1992). In the present case, a clinical evaluation was carried out, with photographic documentation, evaluation of panoramic radiography, and computed tomography scan, which was used for three-dimensional printing, impression of the stereolithographic model, and preparation of surgical guides.

The use of imaging mainly helps to exclude pathologies directing the treatment (Pereira et al., 2006; Rispoli et al., 2008; Özkan et al., 2012; Simão et al., 2014; Ayhan et al., 2018). The panoramic view shows the main contraindication for a surgical procedure, which would be the inferior position of the mandibular canal (Andreishchev et al., 2014). Thus, after clinical and imaging evaluation, it was found that, in the present case, the patient did not present bone pathologies, besides that he presented excessive bone structure in the mandibular angles, allowing the surgical procedure. Furthermore, the literature states that, to achieve an ideal aesthetic outcome, partial resection of the masseter muscle and the mandibular angle provides ideal aesthetic results (Ayhan et al., 2018). Thus, as the patient's main complaint was aesthetics, and botulinum toxin A infiltration requires periodic procedures, the patient opted for a definitive treatment.

Given that there is no consensus as to the ideal option for the treatment of MH, the patient's expectations must be considered, in addition to the clinical and imaging assessment (Oliveira et al., 2004; Pary and Pary, 2011; Ayhan et al., 2018). The indication for the use of botulinum toxin as an exclusive treatment involves conditions in which the masseter muscle is well developed, but without bone protrusion, or when there is a large amount of adipose tissue around the chin or zygomatic region (Kim et al., 2005). After complete evaluation, excess bone tissue was observed in the region of the mandibular angle bilaterally, not resulting in the exclusive indication of infiltrating botulinum toxin into the muscle. Another point considered in the choice of treatment was the patient's socioeconomic issue, given that the application of botulinum toxin is necessary at intervals of 6 months, resulting in a high cost for the patient's financial situation.

The number of alternatives for surgical treatment is wide, and the option of resection of the mandibular angle and the lower portion of the masseter with

intraoral access is widespread (Tabrizi et al., 2010; Pary and Pary, 2011; Ayhan et al., 2018). Nevertheless, muscle traction makes visualization for the surgeon, limited access to perform a resection of the ideal amount of the mandibular angle. In such a case, extraoral access would be a more advisable procedure, despite the risk of scarring and nerve injury (Pereira et al., 2006; Pary and Pary, 2011; Ayhan et al., 2018). Other side effects of surgical management would be hemorrhage, hematoma, asymmetric resection (Kim et al., 2005; Xu and Yu, 2013), infection, limitation of mouth opening, and sequelae from general anesthesia (Özkan et al., 2012; Xu and Yu, 2013). Thus, an important step in the resection of the mandibular angle by extraoral access is the correct and symmetrical design of the reference lines for access, as it can guarantee postoperative symmetry (Andreishchev et al., 2014; Ayhan et al., 2018). In the present case, extraoral access was chosen, with demarcations made along Langer's lines, and no trans- or postoperative hemorrhage was observed. The function of the facial expression muscles was maintained, as shown in Figure 1D–G, and facial symmetry was clinically observed (Figure 1D–G). Furthermore, the surgeon's experience is essential for the performance of the surgical procedure (Rispoli et al., 2008; Xu and Yu, 2013), and part of the success of the present case can be attributed to the 20 years of experience of the oral and maxillofacial surgeon who performed the procedure.

Many techniques have been used for the resection of the mandibular angle (Oliveira et al., 2004; Pereira et al., 2006; Andreishchev et al., 2014). It is suggested that osteotomy should be performed with a saw (Andreishchev et al., 2014). In some cases, the use of surgical burrs decreases the precision of the cut due to its lower stability, causing damage to the surrounding soft tissues and leading to an increased chance of bleeding in the trans- and postsurgical period (Andreishchev et al., 2014). Resection of the lingual bone plate from the mandibular angle gives a more delicate result during masticatory movements (Andreishchev et al., 2014). The surgical guide is predictable to the treatment and make the osteotomy as symmetrical as possible in cases of bilateral masseter hypertrophy. It is manufactured through 3D biomodels obtained from computed tomography scan which may have titanium or acrylic resin as its material (Bocchialini et al., 2017; Trento et al., 2017). The use of this artifice is valuable, considering that the main complaint of patients in masseter hypertrophy involves facial aesthetics, as in the present case. The guide material used in the report was acrylic resin, aiming to reduce cost to the patient, maintaining the treatment.

Satisfactory aesthetic results require additional surgical procedures such as the resection of the buccal fat pad to emphasize the narrowing of the lower third of the face, as its location contributes to the contour of the lower third of the face (Oliveira et al., 2004; Xu and Yu, 2013; Andreishchev et al., 2014). In this case the most conservative treatment possible was chosen, and thus, the buccal fat pad was maintained.

After osteotomy, muscle volume decreases with time, due to the decrease in muscle tone (Kim et al., 2005; Pary and Pary, 2011). The masseter volume can be estimated

by the muscle thickness in several CT slices (Yu et al., 2007; Andreishchev et al., 2014; Almukhtar and Fabi, 2019). The literature shows that this measurement was performed in patients who received botulinum toxin application (Almukhtar and Fabi, 2019). Despite being an exam indicated for the evaluation, we did not find articles that compared the volume of the masseter muscle in a quantitative way. Thus, it is suggested that studies be carried out to develop protocols for measuring muscle volume and to offer an even more thorough assessment for cases of masseter muscle hypertrophy.

The masseter muscle plays a key role in aesthetics and facial shape (Xu and Yu, 2013), and the shape of the face can influence judgments, made in a brief time of personal contact, influencing attitudes and quality of life (Yu et al., 2014; Todorov et al., 2015). Physical characteristics are part of what the human being observes in the other person to form and maintain their social relationships (Yu et al., 2014; Todorov et al., 2015). The literature shows that facial features can influence the interpretation and reaction that people have towards someone, as well as influencing decisions and social behavior (May, 1996; Yu et al., 2014; Todorov et al., 2015). A crucial point is the confidence that facial expression can convey (May, 1996; Yu et al., 2014; Todorov et al., 2015), which may even influence necessary characteristics at work, such as leadership skills or how competent an employee is (Yu et al., 2014). When a patient is bullied for their appearance, they may show nervous and angry expressions, which, in particular, negatively influences social relationships (May, 1996). It is already demonstrated in the literature that feedback from the environment influences the success of an individual's actions, and research has deepened the studies in relation to this topic (Hajcak et al., 2006), as well as in relation to facial expression and how it influences the trust of social interactions (Yu et al., 2014; Todorov et al., 2015). Therefore, with the awareness of the patient's initial complaint of being a victim of bullying in his job, the fact of a positive result in the treatment, with an adequate aesthetic appearance, directed the patient to the normal return of his daily activities, which we can consider a success in the treatment.

There is no specific questionnaire for surgical treatment in MH, so the choice of the Facelift Outcome Evaluation questionnaire was based on the fact that, according to the literature, it has already been tested in relation to its validity, reliability, and response capacity, being a reliable quantitative tool for measuring results (Furlani, 2015). This questionnaire was translated from English into Portuguese and adapted by Furlani (2015) for the evaluation of rhytidoplasty, its application taking about 1 minute. Because it is a questionnaire aimed at facial aesthetics in general, small adaptations were necessary to make it viable for its application with MH patients. Two questions were excluded, as they referred solely to wrinkles, and the formula required a few adjustments. We observed that the response evolved from 12.5 in the preoperative period to 100 in the postoperative period, which is the maximum satisfaction value. This demonstrates the positive result of the procedure. There are other questionnaires aimed at assessing facial aesthetics, including more complete

ones, such as the Face-Q (Furlani, 2015), but the only complaint of the patient was in relation to the lower third of the face, which led us to apply the FOE. We suggest, however, that a questionnaire be developed exclusively for application to masseter hypertrophy.

Conclusion

Finally, it is important to consider the patient opinion when performing aesthetic procedures. The application of the adapted Facelift Outcome Evaluation questionnaire subjectively showed the positive result of the treatment. We suggest that a questionnaire applied exclusively to masseter hypertrophy should be developed, in addition to studies to develop muscle volume measurement protocols, for a more specific evaluation of the surgical result.

Acknowledgements: The authors would like to acknowledge each professional of the medical team, laboratory, and imaging center, which was involved in each phase of the treatment of the patient but do not fulfil the authorship criteria.

References

- Almukhtar, R. M., Fabi, S. G. (2019) The masseter muscle and its role in facial contouring, aging, and quality of life: A literature review. *Plast. Reconstr. Surg.* **143(1)**, 39E–48E.
- Andreishchev, A. R., Nicot, R., Ferri, J. (2014) Mandibular angle resection and masticatory muscle hypertrophy – A technical note and morphological optimization. *Rev. Stomatol. Chir. Maxillofac. Chir. Orale* **115(5)**, 301–307.
- Anehosur, V., Mehra, A., Kumar, N. (2020) Management of masseter muscle hypertrophy and role of adjunctive surgical procedures. *Craniomaxillofacial Trauma Reconstruction Open* **5**, 247275122091314.
- Ayhan, M., İşler, S. C., Kasapoglu, C. (2018) Combination of medical and surgical treatments for masseter hypertrophy. *Case Rep. Dent.* **2018**, 7168472.
- Bocchialini, G., Castellani, A., Negrini, S., Rossi, A. (2017) New management in bilateral masseter muscle hypertrophy. *Craniomaxillofac. Trauma Reconstr.* **10(4)**, 325–328.
- Bravo, B. S. F., Balassiano, L. K. de A., da Rocha, C. R. M., de Bastos, J. T., Chaves e Silva, P. M., de Freitas, B. M. P. (2016) Afinamento do terço inferior da face com uso de toxina botulínica no músculo masseter. *Surg. Cosmet. Dermatol.* **8(1)**, 55–60. (in Portuguese)
- Furlani, E. A. T. (2015) Cultural adaptation of rhytidectomy outcome evaluation questionnaire: Facial outcome evaluation. *Revista Brasileira de Cirurgia Plástica – Brazilian Journal of Plastic Surgery* **30(3)**, 501–505.
- Hajcak, G., Moser, J. S., Holroyd, C. B., Simons, R. F. (2006) The feedback-related negativity reflects the binary evaluation of good versus bad outcomes. *Biol. Psychol.* **71(2)**, 148–154.
- Kim, H. C., Kameyama, T. (1992) Mandibular anguloplasty. *Kurume Med. J.* **39(3)**, 147–151.
- Kim, N. H., Chung, J. H., Park, R. H., Park, J. B. (2005) The use of botulinum toxin type A in aesthetic mandibular contouring. *Plast. Reconstr. Surg.* **115(3)**, 919–930.
- Kühl, S., Brochhausen, C., Götz, H., Filippi, A., Payer, M., d’Hoedt, B., Kreisler, M. (2013) The influence of bone substitute materials on the bone volume after maxillary sinus augmentation: A microcomputerized tomography study. *Clin. Oral Investig.* **17(2)**, 543–551.
- May, B. J. (1996) On decision making. *Phys. Ther.* **76(11)**, 1232–1241.

- Oliveira, D. M., Nogueira, R. V. B., Vasconcelos, R. J. de H., Vasconcelos, B. C. do E. (2004) Hipertrofia do masseter: Relato de caso. *Revista de Cirurgia e Traumatologia Buco-Maxilo-Facial* **4(1)**, 31–38. (in Portuguese)
- Özkan, B. T., Tabrizi, R., Cigerim, L. (2012) Management of bilateral masseter muscle hypertrophy. *J. Craniofac. Surg.* **23(1)**, 14–16.
- Pary, A., Pary, K. (2011) Masseteric hypertrophy: Considerations regarding treatment planning decisions and introduction of a novel surgical technique. *J. Oral Maxillofac. Surg.* **69(3)**, 944–949.
- Pereira, A. M., Gôndola, A. O., da Silva, J. J., Valente, R. O. de H., de Medeiros, M. F., Dourado Júnior, E. (2006) Hipertrofia do músculo masseter: Relato de caso clínico utilizando técnica alternativa. *RGO* **54(4)**, 369–373. (in Portuguese)
- Rispoli, D. Z., Camargo, P. M., Pires, J. L., Fonseca, V. R., Mandelli, K. K., Pereira, M. A. C. (2008) Hipertrofia benigna do músculo masseter. *Braz. J. Otorhinolaryngol.* **74(5)**, 790–793. (in Portuguese)
- Simão, N. R., Borba, A. M., da Silva, A. L. F., de Almeida, N. S. (2014) Hipertrofia benigna do músculo masseter – relato de caso. *Rev. Assoc. Paul. Cir. Dent.* **68(4)**, 351–355. (in Portuguese)
- Tabrizi, R., Ozkan, B. T., Zare, S. (2010) Correction of lower facial wideness due to masseter hypertrophy. *J. Craniofac. Surg.* **21(4)**, 1096–1097.
- Todorov, A., Olivola, C. Y., Dotsch, R., Mende-Siedlecki, P. (2015) Social attributions from faces: Determinants, consequences, accuracy, and functional significance. *Annu. Rev. Psychol.* **66**, 519–545.
- Trento, G. D. S., Benato, L. S., Rebellato, N. L. B., Klüppel, L. E. (2017) Surgical resolution of bilateral hypertrophy of masseter muscle through intraoral approach. *J. Craniofac. Surg.* **28(4)**, e400–e402.
- Xu, J., Yu, Y. (2013) A modified surgical method of lower-face recontouring. *Aesthetic Plast. Surg.* **37(2)**, 216–221.
- Yu, C. C., Chen, P. K. T., Chen, Y. R. (2007) Botulinum toxin A for lower facial contouring: A prospective study. *Aesthetic Plast. Surg.* **31(5)**, 445–451.
- Yu, M., Saleem, M., Gonzalez, C. (2014) Developing trust: First impressions and experience. *J. Econ. Psychol.* **43**, 16–29.

Instructions to Authors

Prague Medical Report is an English multidisciplinary biomedical journal published quarterly by the First Faculty of Medicine of the Charles University. Prague Medical Report (Prague Med Rep) is indexed and abstracted by Index-medicus, MEDLINE, PubMed, EuroPub, CNKI, DOAJ, EBSCO, and Scopus.

Articles issued in the journal

- a) Primary scientific studies on the medical topics (not exceeding 30 pages in standardized A4 format – i.e. 30 lines and 60–65 characters per line – including tables, graphs or illustrations)
- b) Short communications
- c) Case reports
- d) Reviews
- e) Lectures or discourses of great interest
- f) Information about activities of the First Faculty of Medicine and other associated medical or biological organizations

Layout of the manuscript

- a) Title of the study (brief and concise, without abbreviations)
- b) Information about the author(s) in the following form:
 - first name and surname of the author(s) (without scientific titles)
 - institution(s) represented by the author(s)
 - full corresponding (mailing) author's reference address (including first name, surname and scientific titles, postal code, phone/fax number and e-mail)
- c) Abstract (maximum 250 words)
- d) Key words (4–6 terms)
- e) Running title (reduced title of the article that will appear at the footer (page break), not more than 50 typewritten characters including spaces)
- f) Introduction
 - The use of abbreviations should be restricted to SI symbols and those recommended by the IUPAC-IUB. Abbreviations should be defined in brackets on first appearance in the text. Standard units of measurements and chemical symbols of elements may be used without definition.
- g) Material and Methods
- h) Results
- i) Discussion

j) Conclusion

k) References

- All the sources of relevant information for the study should be cited in the text (citations such as “personal communication” or “confidential data” are not accepted).
- It is not permitted to cite any abstract in the References list.
- References should be listed alphabetically at the end of the paper and typed double-spaced on separate pages. First and last page numbers must be given. Journal names should be abbreviated according to the Chemical Abstract Service Source Index. All co-authors should be listed in each reference (et al. cannot be used).
- Examples of the style to be used are:
Yokoyama, K., Gachelin, G. (1991) An Abnormal signal transduction pathway in CD4–CD8– double-negative lymph node cells of MRL *lpr/lpr* mice. *Eur. J. Immunol.* **21**, 2987–2992.
Loyd, D., Poole, R. K., Edwards, S. W. (1992) *The Cell Division Cycle. Temporal Organization and Control of Cellular Growth and Reproduction.* Academic Press, London.
Teich, N. (1984) Taxonomy of retroviruses. In: *RNA Tumor Viruses*, eds. Weiss, R., Teich, N., Varmus, H., Coffin, J., pp. 25–207, Cold Spring Harbor Laboratory, Cold Spring Harbor, New York.

l) tables, figures, illustrations, graphs, diagrams, photographs, etc. (incl. legends)

Technical instructions

- a) Manuscripts (in UK English only) must be delivered in the electronic form via Online Manuscript Submission and Tracking system (<http://www.praguemedicalreport.org/>). In case of problems, contact the Prague Medical Report Office (medical.report@lf1.cuni.cz). The online submission has to include the complete version of the article in PDF format, separately the manuscript as a MS Word file and a cover letter. The detailed version of the Instructions to Authors can be found at: http://www.praguemedicalreport.org/download/instructions_to_authors.pdf.
- b) Text should be written in MS WORD only. We accept only documents that have been spell-checked with UK English as a default language.
- c) Please, write your text in Times New Roman script, size 12, and line spacing 1.5.
- d) Text should be justified to the left, with no paragraph indent (use Enter key only); do not centre any headings or subheadings.

- e) Document must be paginated-numbered beginning with the title page.
- f) Tables and graphs should represent extra files, and must be paginated too.
- g) Edit tables in the following way: Make a plain text, indent by Tab (arrow key) all the data belonging to a line and finish the line by Enter key. For all the notes in table, use letter x, not *.
- h) Make your graphs only in black-and-white. Deliver them in electronic form in TIFF or JPG format only.
- i) Deliver illustrations and pictures (in black-and-white) in TIFF or JPG format only. The coloured print is possible and paid after agreement with the Prague Medical Report Office.
- j) Mark all the pictures with numbers; corresponding legend(s) should be delivered in an extra file. Mark the position of every picture (photo) in the manuscript by the corresponding number; keep the order 1, 2, 3...

Authors' Declaration

The corresponding (or first author) of the manuscript must print, fill and sign by his/her own hand the Authors Declaration and fax it (or send by post) to the Prague Medical Report Office. Manuscript without this Declaration cannot be published. The Authors' Declaration can be found by visiting our web pages: <http://pmr.lf1.cuni.cz> or web pages of Prague Medical Report Online Manuscript Submission and Tracking system: <http://www.praguemedicalreport.org/>.

Editorial procedure

Each manuscript is evaluated by the editorial board and by a standard referee (at least two expert reviews are required). After the assessment the author is informed about the result. In the case the referee requires major revision of the manuscript, it will be sent back to the author to make the changes. The final version of the manuscript undergoes language revision and together with other manuscripts, it is processed for printing.

Concurrently, proofs are electronically sent (in PDF format) to the corresponding (mailing) author. Author is to make the proofs in PDF paper copy and deliver it back to the editorial office by fax or as a scanned file by e-mail. Everything should be done in the required time. Only corrections of serious errors, grammatical mistakes and misprints can be accepted. More extensive changes of the manuscript, inscriptions or overwriting cannot be accepted and will be disregarded. Proofs that are not delivered back in time cannot be accepted.

Article processing charge

Authors do not pay any article processing charge.

Open Access Statement

This is an open access journal which means that all content is freely available without charge to the user or his/her institution. Users are allowed to read, download, copy,

distribute, print, search, or link to the full texts of the articles, or use them for any other lawful purpose, without asking prior permission from the publisher or the author. This is in accordance with the BOAI definition of open access.

Copyright Statement

The journal applies the Creative Commons Attribution 4.0 International License to articles and other works we publish. If you submit your paper for publication by Prague Medical Report, you agree to have the CC BY license applied to your work. The journal allows the author(s) to hold the copyright without restrictions.

Editorial Office

Prague Medical Report

Kateřinská 32, 121 08 Prague 2, Czech Republic

e-mail: medical.report@lf1.cuni.cz

Phone: +420 224 964 570. Fax: +420 224 964 574

Prague Medical REPORT

(Sborník lékařský)

Published by the First Faculty of Medicine, Charles University, Karolinum Press,
Ovocný trh 560/5, 116 36 Praha 1 – Staré Město, Czech Republic, www.karolinum.cz

Editorial Office: Prague Medical Report, Kateřinská 32, 121 08 Prague 2, Czech Republic,
Phone: +420 224 964 570, Fax: +420 224 964 574,

e-mail: medical.report@lf1.cuni.cz

Editor in Chief: Kateřina Jandová, MD., PhD.

Foreign Language Editor: Prof. Jaroslav Pokorný, MD., DSc.

Executive Editor: Mgr. Lucie Šulcová

Editorial Board: Prof. Jan Betka, MD., DSc.; Zdeněk Kostrouch, MD., PhD.;

Prof. Emanuel Nečas, MD., DSc.; Prof. Karel Smetana, MD., DSc.;

Prof. Karel Šonka, MD., DSc.; Assoc. Prof. Jan Tošovský, MD., PhD.;

Prof. Jiří Zeman, MD., DSc.

Published as quarterly journal. Typeset and printed by Karolinum Press.

Annual subscription (4 issues) EUR 60,–. Single copy EUR 20,–.

Distribution: Karolinum Press, Ovocný trh 560/5,

116 36 Praha 1, Czech Republic, e-mail: journals@karolinum.cz

ISSN 1214-6994 (Print)

ISSN 2336-2936 (Online)

Reg. No. MK ČR E 796